Elucidation of Relationship between Glutathione and Plant Defense in *Arabidopsis thaliana*

Thesis submitted for the degree of

Doctor of Philosophy (Science)

in

Biotechnology

by

Priyanka Boro

Department of Biotechnology

University of Calcutta

2022

In fond Memories of
My Grandma

Dedication

This thesis is proudly dedicated to my country, India. I consider this as my small contribution to the scientific community which will hopefully be helpful for the betterment of our society.

ACKNOWLEDGEMENT

Pursuing PhD was like a dream come true. From the last 5 years of research experience I have learned a lot and I have realized that it's much more than just getting your work published and receiving the degree certificate. The happiness of a successful experiment after days and months of hard work is incomparable.

Though the journey was full of ups and downs but the ride was joyful and memorable. From parents to supervisor, to lab mates and circle of friends who have helped me in the midst of problems while doing this whole work, I would like to acknowledge all of them.

Above all, I am grateful to the Almighty, for the guidance, strength, power of mind, protection and ability to giving us a healthy life. My deep gratitude goes first to my Ph.D. supervisor, ***Dr. Sharmila Chattopadhyay****, Emeritus Scientist, CSIR-Indian Institute of Chemical Biology, Kolkata, for giving me the opportunity to do research and providing invaluable guidance throughout this journey. She has expertly guided me all through my PhD tenure and always reminded me not to lose focus from my final goal in these 5 years of research experience. Her unwavering enthusiasm to do good science kept me going and her constant encouraging words has helped me give a moral boost to continue my research work. It was a great pleasure and privilege for me to work with her.*

I would like to express my gratitude to ***Dr. Arun Bandopadhyay****, Director, CSIR-Indian Institute of Chemical Biology, Kolkata, for providing me the necessary facilities and kind permission to carry out my research work.*

I would also like to acknowledge ***Dr. Sucheta Tripathy****,* ***Dr. Smruti Behera*** *and* ***Dr. Deepak Kumar*** *of CSIR-IICB for extending their generous hand by providing some instruments and reagents for completing some crucial experiments.*

*I would also like to thank the **Central Instrumentation Facility (CIF)** section of CSIR-IICB, for providing me instruments like confocal microscope, ChemiDocto to carry out my experiments efficiently.*

*I wish to express my warm and sincere thanks to all the greenhouse **staff members** of **West Bengal State Council of Science and Technology (WBSCST)**, Salt Lake, Kolkata, India, for sharing their expertise in raising of Arabidopsis plants in greenhouse conditions. I would also hereby acknowledge **Sandor Speciality Diagnostics Pvt. Ltd**., Hyderabad, India for LC-QTOF-MSMS service.*

Furthermore, I would like to acknowledge Council of Scientific & Industrial Research (CSIR), New Delhi for my fellowship.

*My appreciation extends out to my lab mates **Asma di, Soumi di, Kajal**, and my seniors **Riddhi di, Saptarshi da and Deepak da.** Special thanks to **Rabin da,** for helping me throughout my research work for maintaining Arabidopsis plants.*

*In addition, I am thankful to all my friends (**Punam, Riyanka, Ranjini, Madhu, Labani, Sandipa, Shouvik, Yajnasheni, Roop, Sonali, Aleepta, Moumita, Varsha, Priya, Sukanya, Dipayan, Debanjan**) from the bottom of my heart, for their immense motivation throughout these years of my research.*

*Last but not the least, I am indebted to my parents, **Bishnu Boro** and **Anjana Boro**; my brother, **Suman Boro**; and my grandparents for their unconditional love and support throughout my life. They are the reason of my existence and this thesis is the result of countless and arduous sacrifices of them. I would like to give special thanks to my husband, **Debajyoti Das**, for having all the stimulating scientific discussions that has helped me to overcome the experimental hurdles. It's their constant love and faith in me that kept me going in this whole journey. Thank you all for being my strength and source of inspiration.*

Priyanka Boro

CONTENTS

LIST OF FIGURES

LIST OF TABLES

Page No.

CHAPTER 1

CHAPTER 2

LIST OF ABBREVIATIONS

AAL: *Alternaria alternata* f.sp. *lycopersici*

ABA: Abscisic acid

ABC: ATP-binding cassette

ACD: Accelerated cell death

ACN: Acetonitrle

ADC2: Arginine decarboxylase 2

APCB1: Aspartyl protease 1

ARF: ADP ribosylation factor

ATP: Adenosine triphosphate

As: Arsenic

AsA: Ascorbate

BR: Brassinosteroid

BSA: Bovine serum albumin

Cd: Cadmium

cDNA: complementary DNA

CLT1: CRT-like transporter

CO: Carbon monoxide

Cr: Chromium

CTAB: Cetyl trimethyl aminobromide

DHAR: Dehydroascorbate reductase

DNA: Deoxyribonucleic acid

DTT: Dithiothreitol

EDTA: Ethylenediamine tetraacetic acid

EGF: Epidermal growth factor

ESI: Electrospray ionization

ET: Ethylene

EtBr: Ethylene bromide

FGF: Fibroblast growth factor

FLD: Flowering locus D

GAPC2: Glyceraldehyde-3-phosphate dehydrogenase

GLK1: Glucokinase 1

GPX: Glutathione peroxidase

GR: Glutathione reductase

GS: Glutathione synthase

GSH: Glutathione

GSL: Glucosinolate

GSSG: Glutathione disulphide

GST: Glutathione S-transferase

(h)GSH: Homo glutathione

H_2O_2: Hydrogen peroxide

H_2S: Hydrogen sulfide

Hg: Mercury

HPLC: High Performance Liquid Chromatography

HR: Hypersensitive response

HSPs: Heat shock proteins

IAO_X: Indol-3-aldoxime

iGSL: indole GSL

INA: 2,6-dichloroisonicotinc acid

JA: Jasmonic acid

KEGG: Kyoto encyclopaedia of genes and genomes

LB: Luria Bertani

LC-MS/MS-QTOF: Liquid chromatography- Mass spectrometry/ Mass spectrometry-Quadrupole- time of flight

MACPF1: Membrane attack complex/perforin

MBP: Myelin basic protein

MBBR: Monobromobimane

MeJA: Methyl jasmonate

MOPS: 3-(N-morpholino) propanesulfonic acid

MPK: Mitogen activated protein kinase

MS: Murashige and Skoog

NO: Nitric oxide

NPR1: Non-expresser of pathogenesis-related 1

OD: Optical Density

PANTHER: Protein analysis through evolutionary relationships

pCaMV35S: promoter CaMV35S

PCs: Phytochelatins

PCS: Phytochelatin synthase

PEG: Polyethylene glycol

PLGS: Protein lynx global server

PMSF: Phenylmethylsulfonyl fluoride

PP2C: Phisphatase 2C

PR1: Pathogenesis-related 1

PSM: Plant secondary metabolite

PTI: PAMP-triggered immunity

RH: Relative humidity

RLK: Receptor-like kinase

RNA: Ribonucleic acid

ROS: Reactive oxygen species

RT-PCR: Real time-polymerase chain reaction

SA: Salicylic acid

SAR: Systemic acquired resistance

SDS: Sodium dodecyl sulfate

SE: Standard error

SERK3: Somatic embryogenesis receptor kinase 3

SIPK: Salicylic acid- induced protein kinase

TF: Transcription factor

TOR: Target of rapamycin

TSS: Transcription Start Site

U: Uranium

UPLC: Ultra-performance liquid chromatography

WIPK: Wound-induced protein kinase

β-ME: β-mercaptoethanol

γ-EC: γ-glutamylcysteine

γ-ECS: γ-glutamylcysteine synthetase

PREFACE

1. **Introduction**

In nature, plants live in intricate surroundings where they are constantly facing numerous environmental stresses, which involve multiple abiotic as well as biotic factors that hamper the growth, development and productivity of plants considerably. Plants being sessile in nature cannot avoid such unfavourable situations. To overcome and survive in this ever-changing environment, they have developed complicated mechanisms and strategies to perceive signals that allow them to respond to environmental changes and endure the consequent calamities thereby inducing immediate and acclamatory defense responses. Such defense response comprises of a set of signal transduction pathways and its rapid deployment. The discrete components of this defense machinery includes various structural barriers viz. cell walls, waxy cuticular layers as well as chemical weapons like phytoalexins, different hydrolytic enzymes etc. The defense mechanism may be triggered specifically or non-specifically by a range of abiotic and biotic factors where the transcriptional activation of various plant genes is also considered as an early and determinative event. Recent research works are primarily focusing on the understanding of plant responses to multiple stresses at a time that is responsible for much more complex networking scenario. Moreover, whether multiple stresses work in synergistic, antagonistic or additive way, that is still left to be explored. One probable effect of exposure to multiple stresses is that plants facing one stress can become further resistant to other stresses. This phenomenon is known as cross-tolerance.

Under stress, generation of reactive oxygen species (ROS) viz. hydrogen peroxide (H_2O_2), superoxide anion (O_2^-), hydroxyl radicals (OH^-) etc. [1-3], nitric oxide (NO) [4,5], accumulation of phytohormones viz. salicylic acid (SA), abscisic acid (ABA), ethylene (ET), jasmonic acid (JA) etc. [6-12], as well as alteration in ions fluxes and callose accumulation [13-17] are part of the first and immediate responses where resulting signal transduction activate the defense metabolic reprogramming thereby making the plant tolerant to stress (**Fig. 1**). Some other plant defense responses include induction of mitogen-activated protein kinase (MPK) cascade [18-20], activation of defense-related gene and regulatory elements [21-28] etc.

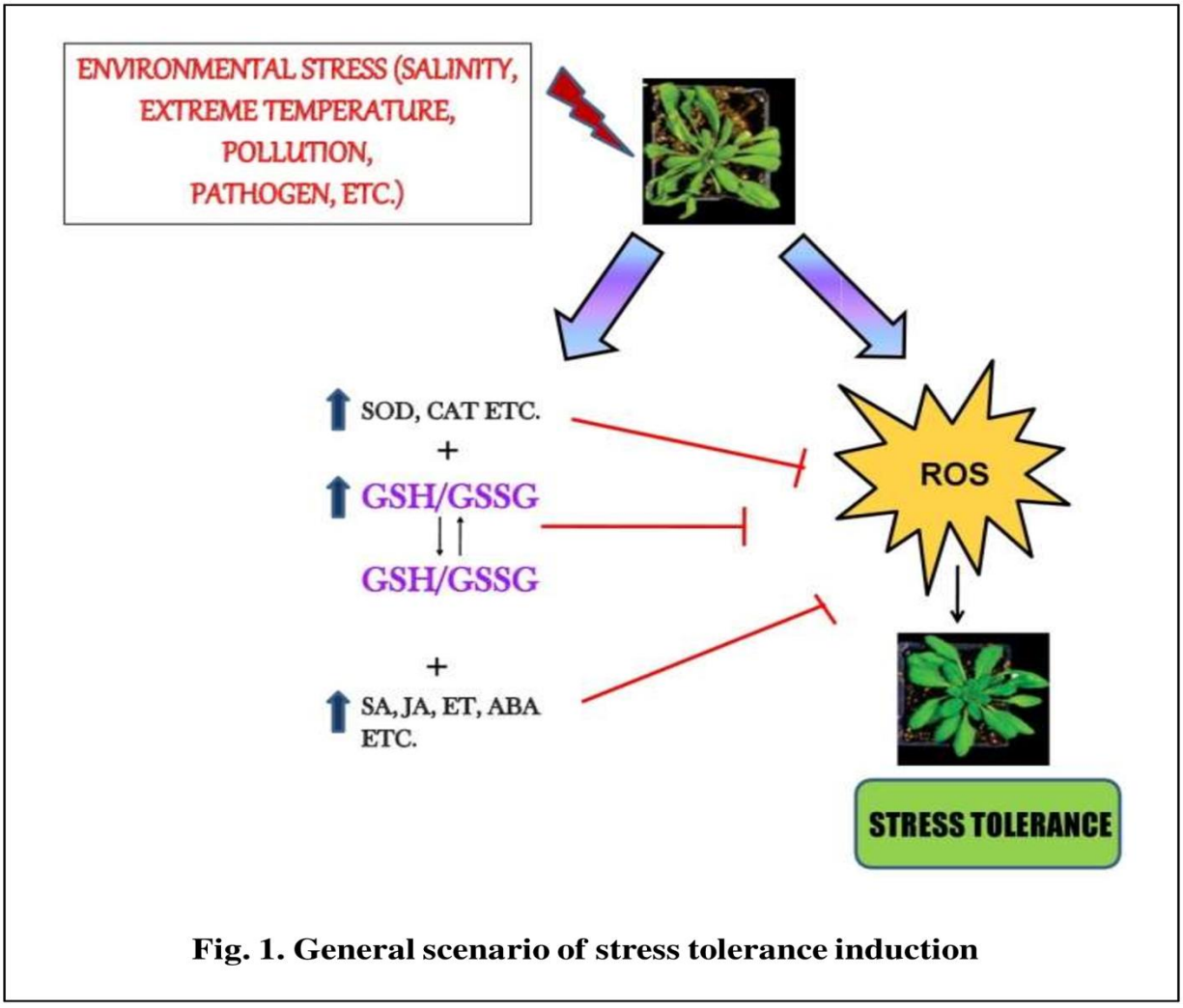

Fig. 1. General scenario of stress tolerance induction

The emerging role of brassinosteroids (BR), which are polyhydroxysteroids also plays a vital role in conferring stress tolerance to a varied range of abiotic factors, is also worth mentioning in this context [29-34]. In addition, calcium signaling [35-38] have important functions to play in integrating and coordinating the entire plant stress responses. Additionally, the amount of ROS production is very finely regulated by the plant system i.e. while higher levels of ROS is known to cause cell death, in general, lower levels are mainly known to regulate plant stress responses [39,40] as shown in **Fig. 2**.

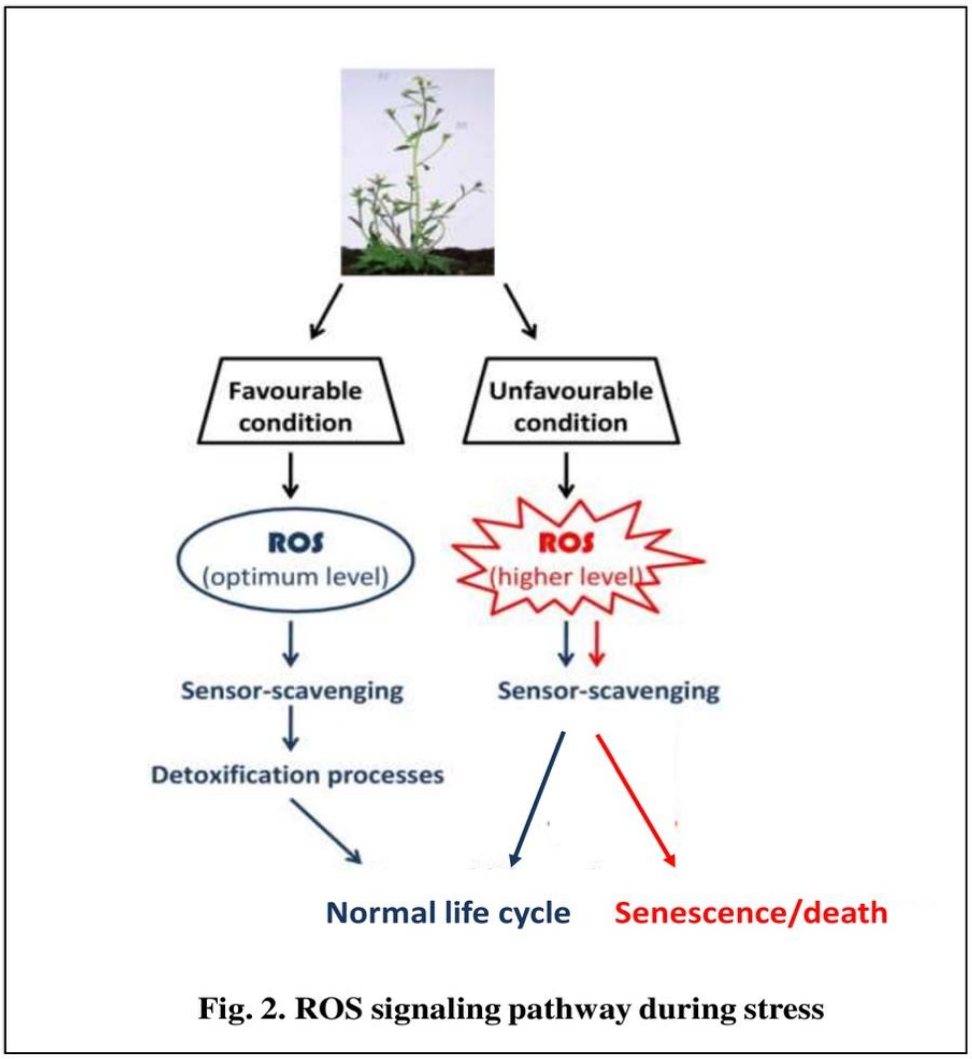

Fig. 2. ROS signaling pathway during stress

Investigations have shown diverse biological roles of the plant secondary metabolites (PSM) in mitigating environmental stresses as well. This has helped in improving metabolite production in plant cells by manipulating the *in-vivo* and *in-vitro* growth environment. The plant metabolites that helps in stress mitigation are the flavonoids, terpenoids, phenolic compounds, aliphatic polyamines like spermidine, putrescine and spermine, terpenes, phytoalexins, lignin and many more (**Fig. 3**). Further, enzymatic (catalases, peroxidases, dismutases etc.) and non-enzymatic [ascorbic acid, lipoic acid, glutathione (GSH), flavonoids like arylamines, carotenoids, quercetin etc.] antioxidants help in scavenging the ROS molecules which eventually help to cope during unfavourable conditions. Accumulation of few osmo-protectants acting as biochemical markers for stress tolerance includes proline, glycine betaine, soluble sugars etc. which help in maintaining the balance inside membranes and other cellular structures (**Fig. 3**).

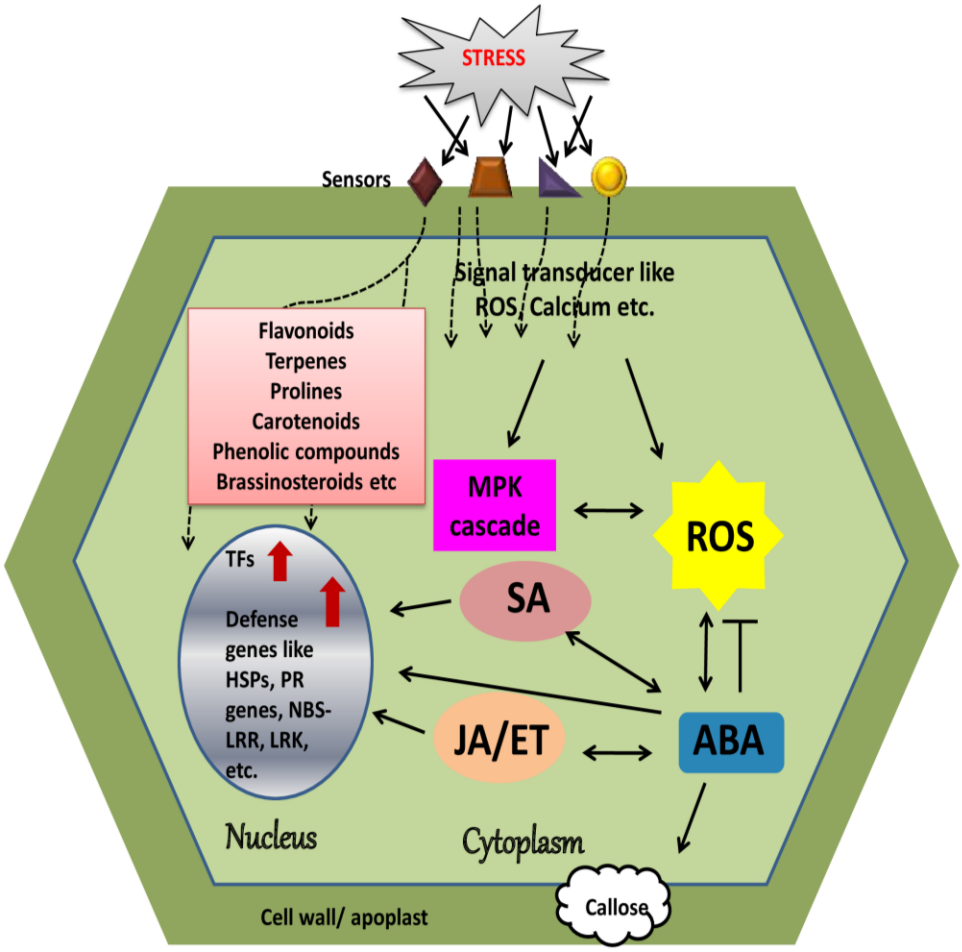

Fig. 3. Complex networking among phytohormones, ROS, MPK cascade, PSMs and various defense modulators during environmental stress

2. Glutathione: An overview

Glutathione (GSH) is a non-protein, water soluble metabolite that is found in majority of the plant species [41] and plays key role in cell function and metabolism. GSH is also progressively acquiring significance as a fundamental modulator in defense networking [42-44] performing various significant functions in plant system which makes it a multifunctional metabolite [45]. However, Li et al. in the year 2003 [46], reported that some organisms have other thiol factors in

their system. Interestingly, the thiol group in the cysteine moiety of GSH makes it an antioxidant molecule [47-49]. Mostly, GSH occur in its reduced form. This reduced form is maintained by glutathione reductase (GR) enzyme in cells. Apart from being master antioxidant molecule, GSH has been involved in various essential functions viz. cell division, protein synthesis, DNA repair etc. (**Fig. 4**).

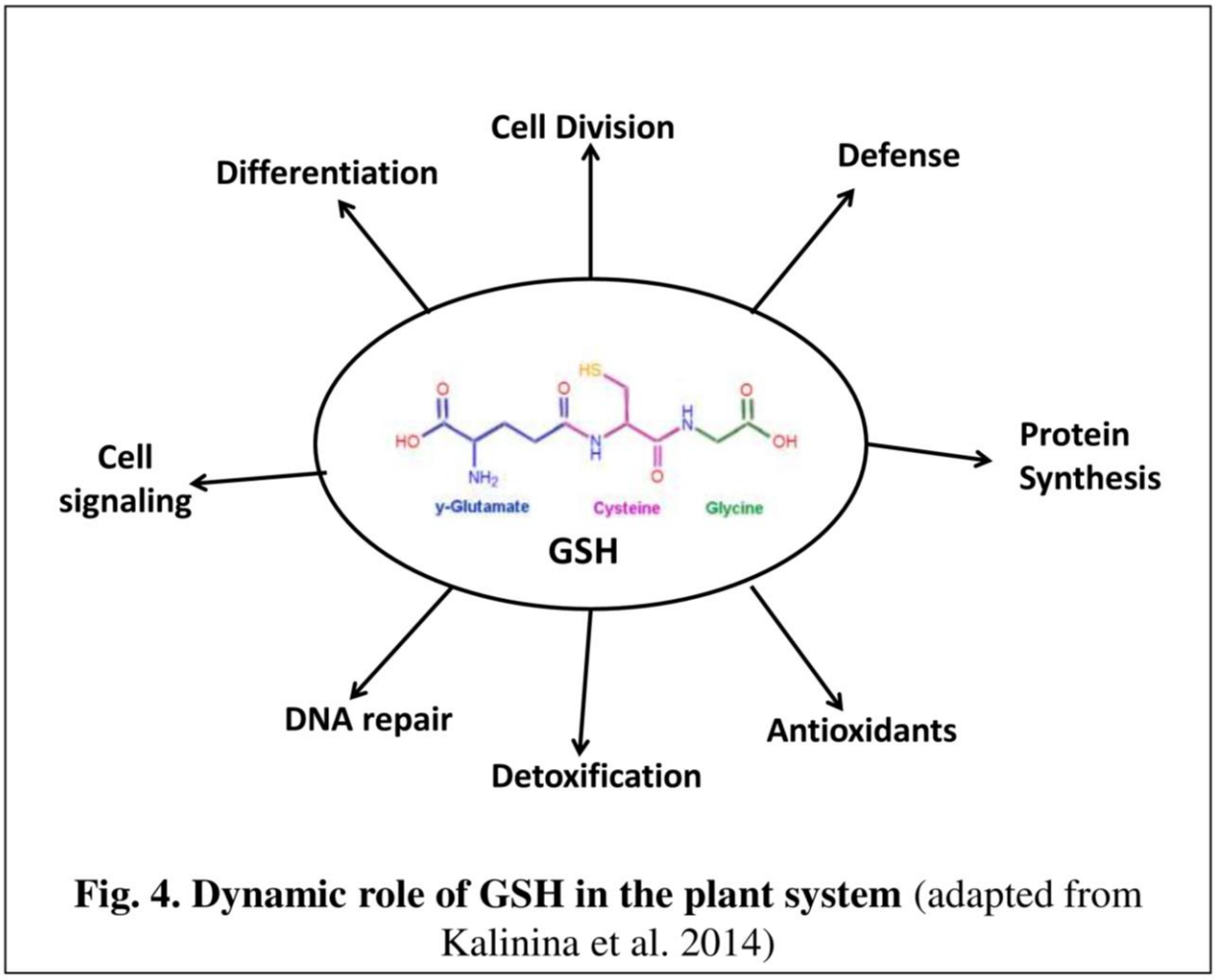

Fig. 4. Dynamic role of GSH in the plant system (adapted from Kalinina et al. 2014)

The cellular GSH content are influenced by diverse processes like amino acid synthesis, detoxification of ROS, role in DNA repair, acting as substrate in phytochelatins synthesis and so on [50]. GSH's position in maintaining balance between cellular reductants and oxidants makes it a suitable signaling molecule [49]. In recent years, substantial breakthrough in the perception of GSH biosynthesis, its transport, degradation, particularly in the context of maintaining cellular redox homeostasis under optimal and stress conditions have been deciphered. In addition, the crucial role of GSH in antioxidant signaling pathway has also been decoded [51,52].

3. Biosynthesis of GSH

Since GSH is a pseudo peptide, its biosynthesis does not follow the classical protein synthesis pathway. It is called a pseudo peptide as glutamine in its structure forms bond with cysteine moiety by carboxyl group side-chain and not through α-carbon carboxyl group. The GSH biosynthetic pathway is a two-step process involving two enzymes which requires ATP as shown in **Fig. 5**. The initial step includes conjugation of L-cysteine and L-glutamate to form γ-glutamylcysteine (γ-EC). γ-glutamylcysteine synthetase (γ-ECS; EC 6.3.2.2) enzyme catalyses the first step. Lastly, GSH synthetase (GS) catalyses the incorporation of glycine to the C-terminal ends of *y*-EC (GS; EC 6.3.2.3) [53]. Exception is there in *Streptococcus agalactiae* where GSH is biosynthesized in one step.

GSH biosynthesis is known to be regulated at two levels. Firstly, the feed-back inhibition of GSH to γ-ECS [54,55]. According to another study, GSH competes with glutamate to inhibit γ-ECS [55]. Second factor is concentration of cysteine [56,57].

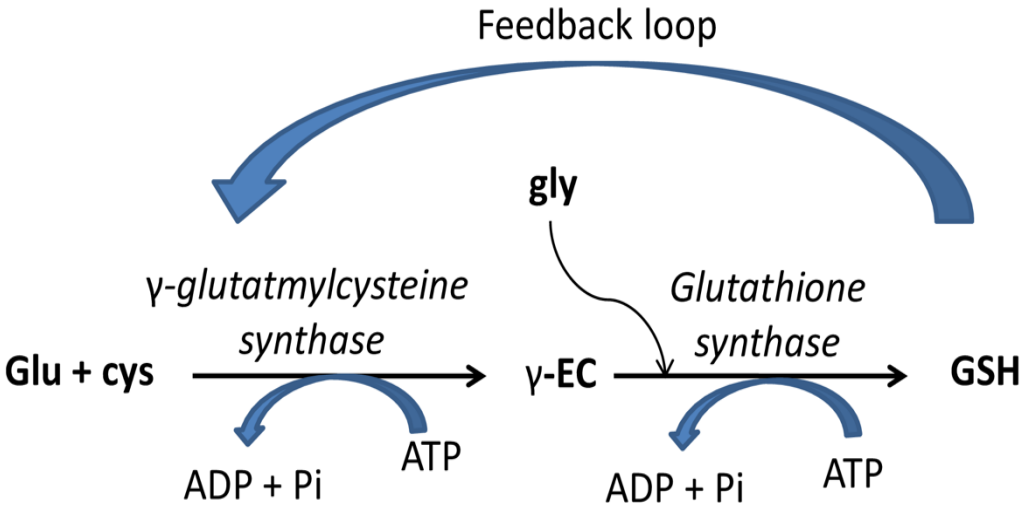

Fig. 5. Biosynthesis of GSH (adapted from Meister, 1988). In plants, GSH is synthesized in a two-step process. The first step is catalysed by the enzyme γ-glutatmylcysteine synthase (γ-ECS) while the final step is catalysed by the enzyme glutathione synthase (GS).

4. Compartmentalization of GSH biosynthesis in plants

Compartmentalization of GSH biosynthesis is unique to plants. Studies demonstrated that γ-ECS is localised in chloroplasts exclusively while GS having 2 distinct transcript types which results in chloroplastic or cytosolic GS protein synthesis [54,58] as shown in **Fig. 6**. Consequently chloroplastic GSH synthesis occurs by the plastidal GS while cytoplasmic GSH synthesis requires transport of peptide to the cytoplasm [59,60].

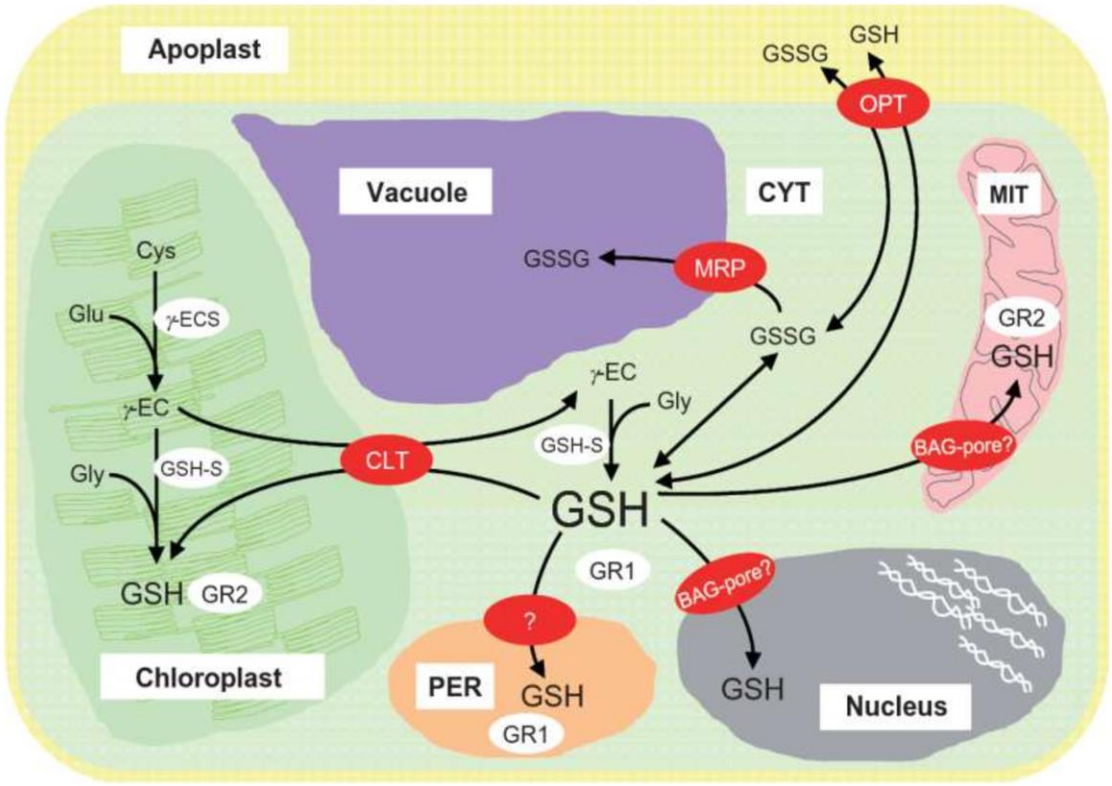

Fig. 6. Compartmentalization of GSH biosynthesis in plants (adapted from Noctor et al. 2012)

5. Distribution of GSH in plants

GSH is a nearly ubiquitous molecule and is present in almost all forms of life including plants, animals and some prokaryotes. The range of GSH concentration is 0.5−10 mM in all mammalian tissues especially in liver. 85−90 % of the GSH content is found in cytosol, while mitochondria,

nuclear matrix, and peroxisomes have the remaining content of it [61]. In plant cells, GSH is present at a concentration of 2−5 mM, compared to GSSG (oxidised form of GSH) which is present at a concentration of 10−200 μM [62]. However, GSH concentration inside chloroplast also ranges between 1−4.5 mM [63]. In plant cells, GSH is virtually present in all sub-cellular compartments. The concentration of GSH inside cytosol was reported to be about 3 mM in *Arabidopsis thaliana* cells [64]. While the amount of GSH inside chloroplast was 1–2 mM in *Pisum sativum* [65].

GSH levels have been found to be in the range of 2–3 mM in many plant tissues [66]. According to Hartmann et al. 2004 [67], in poplar, the mesophyll cells and epidermal cells of leaves contain GSH in the range of 0.2–0.3 mM. On the other hand, in *Arabidopsis*, various leaf cells had different GSH contents [68]. In the developing root hair cells of *Arabidopsis*, the cytosolic GSH content was around 2.7 mM and non-root hair cells it was 5.5 mM. Similar concentrations were also noted in cell suspension cultures of *Arabidopsis* [69,64].

6. Functions of GSH in plants

In plants, a broad range of function is performed by GSH, including redox buffer [70] , detoxification of heavy metals and xenobiotics, synthesizing sulfur-containing glucosinolates and alkaloid compounds like camalexin etc. [71], reduced sulphur transportation, induction of various defense gene expression, posttranslational modifications of proteins by glutathionylating the thiol residues [72,73], cross-talking with phytohormones and so on. Role of GSH in cell cycle regulation in alfalfa [74] and somatic embryogenesis in wheat [75] have also been reported. Also AsA-GSH cycle was found to be related to the aging of soybean seeds [76]. Association of GSH with secondary metabolites like tryptophan, lignin and glucosinolates has been reported in *A. thaliana* when exposed to exogenous GSH [77].

The critical role of GSH in plant growth and development has also been well documented. Vernoux et al. in the year 2000 [78], reported a developmental pathway via GSH which is vital for cell division during post-embryonic root development. Cairns et al. 2006 [79], have indicated towards the key role of GSH in embryo development. Speiser et al. 2018 [80], studied the synchronization of sulfur flux between GSH biosynthesis and protein translation controlling the growth by modulating Target of Rapamycin (TOR). It was also observed that GSH conjugates

transfer via ABC transporter augments the quality and yield of chickpea seeds [81]. GSH pool also has a crucial role to play in flower development and improving pollen vigour [82].

Other than these, involvement of GSH with various phytohormones and effective stress modulators to mitigate stress has been widely investigated in the last couple of decades. Details of these have been discussed below.

7. Role of GSH in stress tolerance

7.1. In abiotic stress

Abiotic stress affects agriculture and crop production immensely. Understanding the mechanism of plant stress tolerance holds the key for successful selection of stress tolerant crops to combat environmental pollution and changing climate [83]. Plants' responses to abiotic stresses have been found to be similar, if not identical, regardless of the nature of the stress factor. ROS formation is a normal phenomenon in the chloroplast, mitochondrion and peroxisome under ambient growth condition. However, their production increases dramatically under abiotic stress [1,84,85]. AsA-GSH redox cycle has also been studied against various abiotic stresses [86]. A triad of GSH, ascorbic acid and α-tocopherol interacting with one another during abiotic stress was deciphered [87]. Role of GSH homeostasis inside cells in regulating plant growth under control and stress conditions, particularly drought and salinity, has also been studied [88]. Increase in AsA and GSH pools in plastids, peroxisomes and cytosol has been demonstrated as a part of plants' response to short term high light treatment [89]. Again, an alteration of GSH metabolism by over-expressing *NAC* transcription factors (TFs) improved stress tolerance [90]. Hasanuzzaman et al. 2019 [91], further elucidated the recent progress on the role of AsA-GSH cycle with reference to oxidative stress tolerance.

7.1.1. GSH against salinity stress

The simplest way of getting an idea about GSH's role in plant defense is to quantify the total GSH content under stressed condition. Almost 3-fold rise in GSH accumulation was noted in salt stress treated wild-type of *Brassica napus.* However, there was no change in GSH content in the transgenic plants over-expressing a Na+/H+ antiporter [92]. GSH content was found to be less by 50-70 % in mitochondria of *Lycopersicon esculentum* when treated with salinity stress whereas

in *L. pennellii* the GSH content remained unchanged [93]. It was also suggested that GSH recycling could be one of the reason of conferring salinity stress tolerance to *glyoxalase I* and *II* genes over-expression lines of rice and tobacco [94,95]. Chen et al. 2012 [96] demonstrated that the combined effect of AsA and GSH under salt stress in *A. thaliana* knock out mutants of *GSTU17*. Additionally, it was reported that the amalgamated effect of metal (loid) and salinity stress was mitigated jointly by proline and GSH [97]. The potential role of exogenously applied GSH, sulphur and proline has been established in mitigating salt stress [98,99]. Similarly, GST was reported to improve the stress tolerance level in tomato and *A. thaliana* under salinity stress [100-102]. In another study, gene knockout of *GR3* in rice showed increased susceptibility towards salt stress [103]. Interestingly, exogenous application of GSH resulted in reduced susceptibility to salinity stress in rice root apices [99] and in tomato seedlings by modulating ions homeostasis and polyamine metabolism [104]. Besides, SA-induced enhancement of GSH metabolism helped in reducing the effect of salinity stress in *Vigna angularis* [105]. Lastly, the indirect role of GSH regulated by thymol (a naturally found medicine) in combating salinity stress was also reported [106,107].

7.1.2. GSH against temperature stress

As far as previous reports are concerned, GSH has a major role to play in chilling stress. Elevated GSH level and increase in GR activity were noted in eastern white pine needles under cold stress [108]. Leipner et al. 1999 [109] showed lower GSH content in sensitive lines of maize than chilling-tolerant lines in cool spring periods. Following studies showed identical results under controlled environmental conditions in wheat and rice [110,111]. In maize, cold stress treatment resulted in increased expression of *γ-ECS* gene [112]. The significance of GSH in the context of photo-protection at different temperatures in *Soldanella alpina* and *Ranunculus glacialis* was also studied [113]. Interplay between GSH and other factors like NO, CO, ROS in recalcitrant seeds of *Baccaurea ramiflora* has been shown [114]. GPX's role in mitigating salt and chilling stress has also been documented [115]. AsA-GSH cycle regulated by melatonin was reported to alleviate oxidative stress induced by cold treatment [116]. The role played by GSH as a result of plant tolerance to chilling stress induced by treating H_2S in cucumber seedlings has been well studied [117]. In addition, GSH application attenuated chilling injury in pepper fruits by regulating the AsA-GSH cycle and improving antioxidant capacity [118]. In a recent

investigation, under combined cold and osmotic stress, the role of GSH in the context of regulating MPK3 has also been noted [119].

Interestingly, upon heat treatment, increased accumulation of total GSH was reported in *Triticum aestivum* and *Zea mays* [120,121]. Ma et al. 2008 [122] showed the consequence of high temperature on enzymes related to AsA-GSH cycle in apple leaves. Similarly, effect of heat stress on the anti-oxidative system of rice was also reported [123]. GSH feeding was also observed to confer stress tolerance to mung bean seedlings upon short-term heat treatment by regulating the antioxidant and glyoxalase systems and by enhancing physiological conditions [124]. The importance of AsA-GSH cycle against heat stress in *Brassica campestris L.* was reported by Zou et al. 2016 [125]. In kiwifruit, melatonin induced regulation of AsA-GSH cycle which exerted a protective effect against heat-related damage has been noted [126]. The key role of the AsA-GSH system in maintaining the redox homeostasis under heat stress in maize has been shown as well [127]. NO and H_2S was found to reduce the harmful effects of heat stress in wheat via AsA-GSH detoxification cycle [128].

7.1.3. GSH in water and drought

Under water stress, the content of GSH and its association with protein biosynthesis was reported in the drought-tolerant variety of *Tortula* sp. [129]. Higher GSH concentration was also noticed in presence of inadequate water in zucchini squash and poplar [130,131]. Again, water stress-induced effect on AsA-GSH metabolism in *Andropyron cristatum* leaves has been reported [132]. Under water stress, the result of H_2S treatment on metabolic processes related to GSH was studied by Shan et al. 2011 [133]. ABA regulated GSH metabolism in soybean leaves under water stress which was also well explained well by Xing et al. 2016 [134].

Likewise, during drought stress in *A. thaliana* guard cells, regulation of GSH-mediated ABA signaling have also been demonstrated [135]. Transgenic tobacco plants with enhanced GSH levels also exhibited tolerance to drought stress in a number of studies. GSH-induced drought tolerance through up-regulation of glyoxalase system has been reported in mung bean [136]. AsA-GSH biosynthesis regulated by ABA was found to enhance the tolerance of wheat seedlings to drought [137]. Additionally, over-expression of the glutathione peroxidase 5 from *Rhodiola* increased drought tolerance in *Salvia miltiorrhiza* [138]. Enhanced drought tolerance in *Arabidopsis* was observed by over-expressing *NAC085* which thereby regulated

GSH biosynthesis, GSH-dependent ROS detoxification, redox balance and methylglyoxal [139]. Raja et al. 2021 [140], again deciphered AsA-GSH cycle's importance in alleviating the effect of drought stress in *L. esculentum*. A new approach was used to silence a *GST* gene in grape which helped the plant to recover from the effect of drought stress [141].

7.1.4. GSH in light stress

Transgenic *Nicotiana tabacum* revealed enhanced tolerance to photo-oxidative stress with high chloroplastic GR activity [142]. *GR* over-expression in wheat protoplast led to photo-oxidative stress tolerance in wheat [143]. According to another report, chloroplastic GPX plays a prominent role in the crosstalk between immune responses and photo-oxidative stress [144]. Besides, DHAR 1 and 2 are known to modulate the levels of GSH and ascorbate in *Arabidopsis* under higher light stress [145]. Additionally, GSH-dependent processes were reported to take part in light-induced gene regulation in *Arabidopsis* leaves by König et al. 2018 [146]. Terai et al. 2020 [147], suggested that GSH content set a threshold for high light-induced AsA accumulation in *Arabidopsis*.

7.1.5. GSH in metal detoxification

Phytochelatins (PCs) help in metal detoxification process within plants in which it chelates to the toxic metals like cadmium (Cd) by their sulfhydryl residues and then the complex is transported into vacuoles. GSH is the precursor of PCs catalyzed by the enzyme phytochelatin synthase (PCS; EC 2.3.2.15) [148-151]. Involvement of GSH under heavy metal stress in plants has been discussed by Schützendüble and Polle, 2002 [152]. Upon Cd stress, enhanced expression of *γ-ECS*, *GS* and *GR* transcripts were observed. Exposing the plant to H_2O_2 or metals whose detoxification doesn't involve PCs did not exhibit similar effect. The *γ-ECS* and *GS* genes also responded to drought, light and certain pathogen stresses [153]. We have also demonstrated that the transgenic mint over-expressing *GS* has been reported to exhibit tolerance to heavy metal stress [154]. Similar effect of exogenous GSH application in barley genotype differing in Cd tolerance was also reported [155]. The effect on GSH homeostasis in calcium-deficient tomato root has also been studied [156]. Utilisation of GSH during nitrogen deficiency in *Colletotrichum graminicola* was reported too [157]. Role of GSH in metal toxicity in response to various other metals like arsenic (As) toxicity [158], Cd toxicity [159] and chromium (Cr) toxicity [160] were

documented. GSH's role as metal chelator and its relevance in toxic metals phytoextraction has also been reported [161]. *A. thaliana* mutants, *pad2-1* and *vtc2-1* were reported to be sensitive to Cd owing to the low GSH level [162]. Effect of GSH level by Cd treatment in citrus fruits has also been studied [163]. AsA-GSH redox cycle has also been studied against iron (Fe) deficiency has also reported [164]. Involvement of γ-glutamyl cyclotransferase in maintaining GSH homeostasis has been shown [165]. Inhibition of Cd transport by GSH was also reported [166]. Role of GSH against uranium (U) toxicity in *A. thaliana* was unravelled [167].

Next, effect of Cd and mercury (Hg) in mutant of *A. thaliana* viz. *rax1-1*, *cad2-1* and *pad2-1* has also been investigated [168]. The AsA-GSH cycle regulated by NO alleviated oxidative damage in roots of wheat after treating with aluminium [169]. It was found that sulfur and selenium control the formation of ET and improve oxidative stress induced by Cd stress thereby increasing the production of proline and GSH [170]. Intriguingly, ZAT6 transcription factor was reported to directly target *GSH1* and positively modulate Cd-induced stress tolerance in *Arabidopsis* [171]. It was also reported that CRT-like transporter (*CLT1)* is essential in GSH homeostasis, facilitating the transport of γ-EC and GSH from chloroplasts to cytoplasm, that further led to Cd and As detoxification in rice [172]. Recently, it was documented that exogenous silicon resulted in correlative actions of AsA-GSH and glyoxalase pathway thereby maintaining the redox state of AsA and GSH and minimizing the Cd-induced oxidative damage [173]. GSH is also reported to confer Hg tolerance in plants [174]. It was further shown that the double mutant *14-3-3κλ* exhibited enhanced Cd tolerance with higher Cd accumulation, while *14-3-3κ* or *14-3-3λ* double mutants revealed elevated Cd sensitivity under Cd toxicity [175]. The function of GSH antioxidant defense system in mitigating As stress in fungus *Hebeloma cylindrosporum* has been well studied by Khullar and Reddy, 2020 [176]. Recently, a new finding suggested GSH-mediated regulation of auxin pathway to take place under nutrient (phosphate)-deprived condition [177]. Most recently, cytokinins were reported to regulate GSH level under Cd stress in *Trigonella foenum-graecum* seedlings [178]. GSH was also found to mitigate Cd toxicity by inducing GSH-related gene expression and suppressing Cd transporter gene expression [179]. In soyabean, GSH was reported to mitigate the effect of Cr stress [180].

7.2. Role of GSH in biotic stress

Plants faces a varied range of environmental stresses on a regular basis that include biotic stresses generated by a plethora of plant pathogens against which plants set up a series of defense response. Activation of inducible defenses may be very specific to the type of invader encountered. GSH feeding was found to trigger several genes encoding enzymes related to biosynthesis of phytoalexins and lignin in cell culture of bean plants [181]. It was also reported that expression of chalcone synthase was induced upon elicitor stimulation upon GSH feeding [182]. Treating soybean cells with fungal elicitor or GSH resulted in fast solubilization of cell wall components which are hydroxyproline-rich structural proteins [183]. Previous investigations revealed that herbicides application resulted in significant increase of GSH levels in roots of tomato and melon along with enhanced resistance against *Fusarium oxysporum* [184].

Alteration in cellular GSH levels surrounding the site of pathogen ingression was observed together with higher expression of GSTs, GPX [185-187] that also helped in decreasing lipid peroxidation. In tomato cells, a significantly higher GSH along with GSSG accumulation have been observed after *Cladosporium fulvum* treatment [188]. Tobacco mosaic virus infected tobacco leaves showed higher GSH accumulation than SA treated leaves [189].

Xiang and Oliver in the year 1998 [190], portrayed JA's significance under abiotic stresses in terms of higher expression of GSH metabolic genes. Glucosinolate (GSL) is a class of sulphur containing compounds found in Brassicaceae family. Upon tissue injury, GSL react with myrosinase enzyme which generates toxic compounds essential for defense response against herbivores [191]. In plants, GSL production is usually constitutive in nature [192], however according to few reports, their production is triggered by wounding as well [193,194]. Treatment with an active SA analogue viz. 2, 6-dichloroisonicotinic acid (INA) leads to reduction of NPR1 thereby increasing the GSH level and resulting in increased expression of the pathogenesis-related (*PR1*) gene [70].

About 32 stress-related genes were altered as a result of alteration in GSH metabolism in *A. thaliana* mutants like *rax1-1* and *cad2-1* [66]. In Brassicaceae, camalexin that acts as phytoalexin has antimicrobial and anti-fungal properties [195]. In another study by Freeman et al. in the year 2005 [196], GSH-mediated tolerance to nickel was exhibited from over-expression of SA in *Thlaspi,* which is a hyper-accumulator of nickel. The *pad2.1* mutant (GSH deficient) of

A. thaliana also showed increased susceptibility towards pathogens like *Alternaria brassicicola* [197], *Pseudomonas syringae* [198], and insects like *Spodoptera littoralis* [199].

It was also documented by Mhamdi et al. in the year 2010 [200], that GSH level modulates and interacts with SA along with other phytohormone signaling pathways involved in pathogen response, resulting in accumulation of SA, increased JA-related gene expressions in *A. thaliana*. A previous study showed that cyp79B2 cyp79B3 which is a double mutant fails to produce indol-3-aldoxime (IAOx), which is a common precursor of camalexin and iGSL biosynthesis and had susceptibility to *P. brassicae* [201]. *A. thaliana* upon infection with *P. brassicae* showed up-regulation of gene expression related to camalexin and iGSL biosynthesis [202]. Low GSH level effected the accumulation of camalexin and glucosinolates (antimicrobial compounds) in *pad2-1* mutants [203]. Fascinatingly, GSH has been reported to be a sulfur source in their biosynthesis [71]. Role of GSH in SA-deficient plants against RNA viruses has been documented [204]. Impact on AsA and GSH level in Eucalyptus trees infected with *Phytophthora cinnamomi* was also reported [205]. Effect on GSH metabolism during hypersensitive response (HR) has also been shown by Király et al. 2012 [206]. Importance of GSH status in activating pathogenesis-related phytohormone signaling pathways via NPR1 was reported [207]. *A. thaliana* redox status in response to caterpillar herbivores also suggested GSH-dependent suppression of plant induced defense [208]. A combined role of tryptophan and GSH for defense against hemibiotrophs was also shown [209]. Involvement of glutamate receptor like channel 3.3 in triggering cytosolic calcium through GSH under *P. syringae* infection has also been reported in *A. thaliana* [210]. GSH's involvement in plants-microbe interaction has also been reported [211]. Interestingly, reduced redox potential of GSH was observed in rice blast fungus *Magnaporthe oryzae* against host oxidative stress [212]. The effect of GSH depletion on root development of *A. thaliana* mutants has also been studied in relation to auxin and strigolactone signaling [213]. Datta et al. 2015 [214], developed a transgenic line over-expressing γ-*ECS* gene showed increased tolerance to fungus *B. cinerea*. Matern et al. in the year 2015 [215], suggested a crosstalk between GSH and tobacco wound-induced protein kinase (WIPK), salicylic acid induced protein kinase (SIPK) during *P. syringae* infection. In the year 2018, Banday and Nandi [216], suggested GSTT2 to be an interactor of FLD, which is essential for systemic acquired resistance (SAR) and SAR-associated epigenetic modifications. *In-vivo* analysis GSH redox status in *Arabidopsis* infected with *P. syringae* pv. tomato *AvrB* has been noted recently [217]. Chen et al. in the year

2020 [218], reported that (h) GSH metabolism plays a key role in conferring resistance against nematodes in resistant soybeans. Elevated GSH content in tobacco resulted in reduced susceptibility to powdery mildew pathogen *Euoidium longipes* [219]. Exogenous GSH was found to reduce the effect of bacterial spot disease in *Capsicum annum* by regulating photosystem II and H_2O_2 scavenging antioxidant enzyme system [220]. The critical role of GSTs against aphid attacks was very recently reported by Zhang et al. 2022a [221].

8. Cross-talk of GSH and diverse signaling pathways to combat stress

Antioxidants like GSH and AsA, function together with ROS that forms an integral part of cellular networking system perceiving signal from the environment and controlling plant growth, development, and stress tolerance/mitigation. The differential redox potential throughout the cellular membranes, initiates a cascade of signaling pathways, including downstream adjustments in hormone metabolism and turnover. Phytohormones are well-established cellular signaling molecules which has vital role to play in immune responses during pathogen attack as well as for beneficial microbes' intervention, besides abiotic stress conditions [222-225]. Redox signaling pathway is triggered by environmental factors which activates the oxidative burst-generating enzymes. Besides ROS, the level of GSH, AsA, tocopherols and carotenoids, and other antioxidant enzymes are also altered during environmental stress. They are also known to be a part of a large stress signaling network those crosstalks among one another to regulate plant growth and defense responses. The established phytohormones SA, ET, JA, ABA and it's their respective derivatives also play pivotal roles in the regulation of induced defenses [21,226,227,27,228-231,8,232].

Noctor et al. 2012 [49], further reported GSH's role in shielding cells from unfavourable stress factors by activating various defense machinery. Furthermore, GSH's function in phytohormones-mediated signaling pathways has also been discussed by Foyer and Noctor, 2011 [48]. Investigations on defense-signaling pathways revealed that phytohormones like SA, ET, JA and ABA form an interconnecting complicated network [8]. This complex network allows the plant system to modify its defense response to the invaders encountered [233-235]. In recent times, a mechanism for regulation of signaling through GSH-dependent system has been proposed by Noctor et al. in the year 2013 [236], which says that sequestration of GSSG may be

necessary to clear the cytosol in order to dodge enormous oxidative stimulation during stressed conditions.

The crosstalk between GSH and other established signaling molecules in the regulation of plant defense response are also being studied. GSH is known to crosstalk with SA and JA pathways via NPR1, which acts to transfer part of the JA-mediated negative control by SA [237]. Further, GSH was reported to regulate methyl jasmonate (MeJA) signaling cascade and stomatal closure in guard cell of *Arabidopsis* [238-241]. Previous investigation also revealed that ET and SA protect plants against ozone exposure by increasing GSH biosynthesis *de-novo* [242]. GSH was reported to help in enduring biotic stress in NPR1-dependent SA-mediated pathway in *N. tabacum* [243,244]. The correlation between JA and GSH was well deciphered by Spoel and Loake, 2011 [245], where it was suggested that JA regulated the GSH pool. Han et al. 2013a [246], pointed out towards the NPR1-independent regulation of SA signaling by GSH in *Arabidopsis thaliana*. Similarly, the involvement of GSH in the regulation of JA signaling in response to intracellular oxidation has also been postulated [247]. It has also been reported that SA temporally regulates the genes encoding the enzymes of AsA-GSH cycle, during salt stress resulting in increased amount of GSH and AsA in cells of wheat [248]. Additionally, it was suggested by Dai et al. 2015 [249], that exogenous JA application which induced H_2O_2 would trigger MEK1/2 phosphorylation thereby activating the AsA and GSH metabolic enzymes. Datta et al. (2015) [214] reported that modulation of ET by GSH takes place via transcription factor WRKY33. Moreover, ET formation was studied to be influenced by sulfur and selenium, resulting in improved proline and GSH production and thus alleviating Cd-induced oxidative stress in wheat [170]. Kovacs et al. 2015 [250], implied the crosstalk between NO and GSH, which is integral to the NPR1-dependent defense signaling pathway, and demonstrated that GSH helps in maintaining redox homeostasis and has function in signaling pathways in the defense machinery. Liting et al. in the year 2015 [137], unravelled the molecular mechanism of ABA-induced drought tolerance by increasing GSH biosynthesis in common wheat. Exogenous JA was noted to activate the AsA-GSH cycle, which conferred drought tolerance [251]. The relationship of GSH with lignin, tryptophan and GLS along with SA and ET was reported by Sinha et al. 2015 [77]. Alongside, microarray data revealed that an ABA mutant of *A. thaliana* viz. *aba1.6* when treated with combined osmotic and cold stress was found to have low GSH content denoting the GSH-ABA crosstalk [252]. Exogenous JA-induced H_2S production

activated the AsA and GSH metabolism [253]. GSH is also known to compensate for SA deficiency in tobacco to maintain resistance to *Tobacco Mosaic Virus* [254]. SA was reported to be involved in up-regulating AsA-GSH cycle against salinity stress in *Capsicum annuum* [255]. In a recent report, results revealed that GSH-mediated SA and ET regulation helps in mitigating AAL-toxin-induced stress in *A. thaliana* [256]. Subsequently, the role of GSH in different cellular organelles under biotic stress has been very well deciphered [257]. Most recently, SA was reported to alleviate vanadium stress in a GSH-dependant manner by regulating AsA-GSH cycle [258].

Thus extensive literature survey suggests that the master antioxidant, GSH, plays a significant role in biotic and abiotic stress tolerance through its crosstalk with various phytohormones as well as through ROS detoxification.

9. Genetic manipulation of the GSH biosynthetic pathway gene/s in stress tolerance

In spite of various regulations over GSH biosynthesis, plant cells put up considerable increase in total amount of GSH. Initial studies of several independent lines of poplar over-expressing *γ-ECS*, the key enzyme of GSH biosynthesis showed no effect on phenotype [259]. Similarly, any marked phenotypic effects were absent in poplar and *Brassica juncea* having high levels of GSH [259,260].

Studies showing over-expression of *γ-ECS* gene in *E. coli* cytoplasm and chloroplast produced 3 to 10-fold increase in GSH in poplar leaves [261,259]. However, over-expression of γ-ECS resulted in elevated GSH content and increased oxidative stress in the chloroplast of transgenic tobacco [262]. Compared to *γ-ECS*, over-expression of *GS* had considerably less effects on GSH contents. No significant gain in enzyme activity of GS was found [51,259]. Nevertheless, remarkable increase in GSH synthesis was noted when γ-EC was over-expressed in the leaf tissue of transgenic poplar [57]. Over-expression of *γ-ECS* in *A. thaliana* also accentuated GSH level, though the increase was not so significant [263]. Herschbach et al. 2010 [264], demonstrated that changes in chloroplastic and cytosolic GSH contents would eventually affect photosynthetic rate, growth and the whole plant sulphur nutrition. Expression of a bi-functional γ-ECS/GS enzyme in tobacco has shown that the GSH pool can be enhanced upto 20-

fold having no prominent effect on the growth and development of plants [265,243]. Further study of a single cytosolic over-expressor of GS was reported to improve the biomass and photosynthesis performance of transgenic poplars [266]. According to studies, *γ-ECS* gene over-expression emulates transcriptional response under low temperature stress when the *A. thaliana* seeds are vernalized [267]. A transgenic approach was also used to complement the GSH null mutants of *A. thaliana* by bacterial and *A. thaliana* GS respectively and it was demonstrated that redirecting γ-ECS activity particularly in cytoplasm or constricting GSH accumulation in chloroplasts had least impact on plant development, indicating smooth intra-cellular exchange of γ-EC and GSH between the plastid and cytosol compartments [268]. Over-expression of *AtGSTU19* was reported to confer tolerance to salt, drought and methyl viologen stresses in *Arabidopsis* [269]. Over-expression of GS in rice plants showed improved stress tolerance and productivity under paddy field conditions [270]. Martin et al. 2018 [271], showed over-expression of *E. coli GSH1* induces GSH accumulation and changes somatic embryogenesis and plant development in *Hevea brasiliensis.* Over-expression of *GS* in paddy fields resulted in increased lateral root development and productivity in terms of grain yield in rice [272]. Lastly, over-expressing protein phosphatises (PP2C) resulted in improved tolerance capacity of *Triticum aestivum* under drought conditions [273]. Together, here in the write up we have provided a glimpse of the significant contribution of GSH in imparting stress tolerance to the plants under stress.

SCOPE OF THE STUDY

Plant defense response is regulated by a network of signal transduction pathways in which GSH is one of the vital players. In the context of mitigating stress, GSH's role in multistep interplay with known and established signaling factors has also been studied extensively till date. Investigations revealed the dynamic role of GSH in plant immunity, as an intracellular redox buffer, its involvement in biosynthesis of plant defence compounds etc. Besides that, lowering the cellular GSH content had an insightful effect on plant defence against environmental stress. Interestingly, the crosstalk of GSH with SIPK and WIPK to combat biotic stress has been noted in the recent year [215]. Furthermore, study also indicated enhanced expression of *N. tabacum* MPKK (NtMPKK) in transgenic *N. tabacum* (*NtGB* line) with higher GSH content [243]. On top, up-regulation of *Arabidopsis MP3K19* gene in GSH fed *A. thaliana* wild type, Col-0 plants was also noticed [77]. Together, previous studies point towards that there might be interplay between GSH and MPK cascade that takes place as a result of defense response *in planta*. However, the molecular mechanism of GSH-MPK interplay in combating stress is yet to be understood in depth. With this background, present study aims to explore the role of GSH in plant defense and dissect the molecular mechanism of GSH-MPK interplay.

The objectives of the research work has been summarised below:

- ✓ Comparative proteomic analysis of combined osmotic and cold stress treated *A. thaliana* under altered GSH level.
- ✓ Study the effect of combined abiotic stress (osmotic + cold) on the expression of the MPKs in *A. thaliana* exhibiting altered GSH content.
- ✓ Development of transgenic *A. thaliana* overexpressing *MPK* gene and its molecular analysis.

CHAPTER 1

Chapter 1: Comparative proteomic analysis of combined osmotic and cold stress treated *A. thaliana* under altered GSH level

1. Introduction

Proteomic study is one of the important high-throughput technologies for the analysis of proteins on a genome-wide scale. This study helps us to gain deeper insight regarding protein abundance, protein-protein interactions, and protein modifications in order to maintain a well-organized plant system and to communicate with its surroundings [274]. The advantage of proteomics approach is to examine the differential expression of proteins during the action of a range of stress factors [275-277].

Plant stress proteomics is a dynamic discipline which is used to investigate plant proteome system and biological functions of proteins under stress [278,279]. Documentary evidences on plant proteome under stress have risen exponentially in the few decades. The reason behind this sudden craze of plant proteomics studies are the advancements in high-throughput instrumentation techniques that helps in separating mixture of complex protein and identification of the individual protein species as well as by advancements in genomics like availability of complete genomic sequence information of different plant species.

Both abiotic and biotic stress factors generate notable changes in plant proteome system that results in metabolic changes to altered condition and an enrichment of plant stress tolerance. There are numerous reports on responses of plant proteome against abiotic stresses [277,280] as well as pathogen attack [281,282] which provide important overviews of differential expression patterns of proteins under stress. However, there is very few information about plant stress proteomic study under altered GSH level. Comparative proteomic profiling of differentially expressed proteins in rice roots revealed GSH playing a central role during As stress [283]. Proteomic profiling analysis revealed that GSH has important roles to play responding to osmotic stress in wheat [284]. In our laboratory, there are few documentary evidences that focused on studying the proteome profiling under varied GSH conditions [285,286,214,77,256]. Besides, present study deals with a comparative proteomic profiling of combined stress treated *Arabidopsis* under varied GSH conditions.

Arabidopsis thaliana, Thale cress or mouse-ear cress is a tiny, annual weed; having fairly shorter lifecycle and it is native to Eurasia. It is a widely used as a model organism in plant biology.

The taxonomic classification of *A. thaliana* is as follows:

Kingdom: Plantae

Clade: Tracheophytes

Clade: Eudicots

Clade: Eudicots

Clade: Rosids

Order: Brassicales

Family: Brassicaceae

Genus: *Arabidopsis*

Species: *Arabidopsis thaliana L.*

Arabidopsis are multicellular eukaryotes of approximately 120 Mbp of genome size, organised into five chromosomes [287]. It is the first seed plant whose complete genome had been sequenced in the year 2000. In the days of genomics, this mega-data caught attention of every researcher to characterise the function of approximately 28,000 genes in *Arabidopsis* genome. Mutant screens played a very significant role in this journey of establishing *Arabidopsis* as a model plant system. Columbia (Col) and Landsberg erecta (Ler) are commonly used wild-type lines for scientific studies. However, due to the vast number of mutant availability, good quality genome sequence and microarray data [288,289], and many other physio-biochemical reasons, Col-0 is chosen over Ler type. The mutants in *Arabidopsis* are known to have low GSH content than wild-types and the gene that codes for γ-ECS, the first enzyme of GSH biosynthetic pathway is mutated. These mutants show a varied range of phenotypes which are as follows:

a) *rml1*: 3 % of wild-type GSH; termination in plant development [49].

b) *rax1-1*: 40 % of wild-type GSH; susceptibility to photo-oxidative stress [66].

c) *cad2-1*: 30 % of wild-type GSH; susceptibility to metal toxicity and biotic stress [290,198].

d) *pad2-1*: 20 % of wild-type GSH; sensitive to biotic stress [198] and reduction in iron (Fe)-dependent zinc tolerance [291].

These mutant lines are readily available in well-known *Arabidopsis* stock centres like Nottingham Arabidopsis Stock Centre, UK (NASC) and Arabidopsis Biological Resource Centre, USA (ABRC).

Taken together, *Arabidopsis* will hold back its place in plant biology for the next couple of years. Nevertheless, this is to remember that the objective to study *Arabidopsis* genome is to further explore the deeper insight of other plants, particularly the target ones in general from biological and physiological aspect.

2. Materials & Methods

2.1. Plant materials and their growth conditions, GSH feeding

All *Arabidopsis thaliana* seeds were procured from NASC. Col-0 (NASC ID: N1092; ABRC stock number: CS1092) used as wild-type. All seeds were surface sterilized and germinated in Murashige and Skoog (MS) media [292]. The seeds were grown inside growth chamber at 22±1°C having16 hours of 150 µE m^{-2} sec^{-1} light and 8 hours dark cycles [293].

Three week old seedlings of Col-0 were transferred to MS medium containing 100 µM GSH, which was maintained under same growth condition for 72 hours [77,214].

2.2. Combined osmotic and cold stress treatment

For treating plants with combined osmotic and cold stress, 3 week old seedlings of *Arabidopsis* were placed in wet filter papers at 4°C for 5 minutes and then moved to MS media containing 30 % PEG solution and maintained at 4°C for an additional 6 hours as standardized before [214,294].

2.3. RNA isolation and semi quantitative RT-PCR analysis

The expression of few selected genes was checked by semi-quantitative RT-PCR. All material (pipette tips, 1.5 mL, and 2 mL tubes) used for the extraction of RNA were autoclaved and wiped with RNAse OFF (Takara BIO Inc., Japan). Total RNA isolation carried out from *A. thaliana* leaves by using TRIzol@ reagent (Invitrogen, India). 100 mg of leaf tissues were crushed in liquid nitrogen and then homogenised in 1 mL of TRIzol@. The collected sample was centrifuged at 4ºC, 12000 × g for 15 minutes. 0.5 mL of iso-propanol (Merck, India) was mixed to the upper clear phase of the centrifuged solution and incubated for 10 minutes. Next, centrifugation was done at 4ºC, 12000 × g for 15 minutes. White pellet of RNA was washed with

70 % ethanol (Merck, India), air dried and dissolved in RNAse free water. RNA quality was checked on 1.2 % formaldehyde agarose gel. Formaldehyde gel preparation was done as per standard protocol [295]. The RNA sample was denatured in denaturing solution [295] for 1 hour at 55^{o}C, quick chilled in ice for 10 minutes and then checked on 1.2 % agarose gel with 2.2 M formaldehyde. The denatured RNA samples were run on the gel with 1 X MOPS buffer, at 35 V. The RNA samples were quantified using a nano-drop spectrophotometer (Sigma-svi, Germany).

From 1 µg of RNA, complementary DNA (cDNA) was synthesised by using RevertAidH Minus First Strand cDNA synthesis kit (ThermoScientific, Lithuania) as per manufacturer's guidelines. 1 µg of RNA was quantified and to it 1 µL of oligo dT primer (100 µM) was added. To this solution, RNAse free water was added to make up the volume till 12 µL. This solution was then incubated at 70^{o}C for 5 minutes. In the next step, 4 µL, 2 µL and 1 µL of 5 X reaction buffer, 10 mM dNTP and RiboLock RNase inhibitor were mixed respectively. This solution was incubated for 5 minutes at 37^{o}C. Finally, 1 µL of RevertAid Reverse Transcriptase (200 u μL^{-1}) was mixed and incubated for 1 hour at 42^{o}C. The reaction was then terminated by incubating it for 10 minutes at 70^{o}C.

cDNA synthesised was utilized in semi-quantitative RT-PCR analysis for the expression check of few stress marker genes like *OSMOTIN*, *Hsp70*, *APX1*, *ADC2* and *Hsp18.2*. Along with this, expression analysis of *PR1* was also checked in GSH-fed Col-0 samples. The sample mix [295] was prepared in 0.2 mL tubes and PCR was performed in Thermo cycler. The sequence of the primer pairs is listed in **Table 1**. *Tubulin* expression was used for normalization. All experiments were performed in three biological plants samples which were grown independently. The PCR conditions used is as follows:-

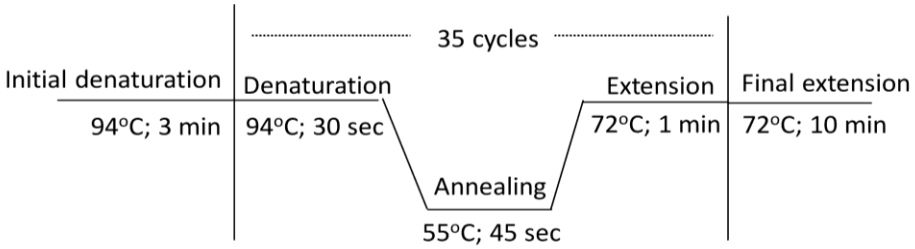

Table 1: List of primer sequences used in semi quantitative RT-PCR analysis

Genes	Forward Primer (5'-3')	Reverse Primer (5'-3')
OSMOTIN	CCTCTTGGTCTCTACTTT	ATTCTCCTCGGTGAC
HSP70	CTGTTCAAGCGGATAAG	CTCCATACACTTCCTAAAC
APX	AAGCTCAGAGGTTTGAT	CAGAAAGCTTCATGTGG
ADC2	GCTTGAGCAAGAAGAAG	CAGCTGATCGACATAAAG
HSP18.2	GTCTTTGATCCGTTCTC	GATATCGATGGACTTGAC
Tubulin	CACCATCTACCCTTCTC	CATACCCTCTCCTACATAC

2.4. Agarose gel electrophoresis for PCR products

1 % agarose gel was used for all semi-quantitative PCR products to analyze their expression pattern. The agarose gel was prepared by adding 0.4 g of agarose in 1 X TE buffer composing of 40 mM Tris-HCl, 1 mM EDTA, and 0.1 % glacial acetic acid. The mixture was heated at 450 W for 2 minutes in a microwave oven. 2 µL of ethidium bromide (EtBr; 0.5 µg mL^{-1}) was added to the mixture and then the solution was poured in the gel casting tray. All samples were mixed with 10 X DNA loading buffer and then loaded inside the gel wells. A suitable DNA ladder was used in one lane. After loading the DNA samples, gel was run in 1 X TE buffer at 75 V for 45 – 60 minutes.

2.5. Estimation of total GSH content

GSH was extracted from Col-0 and GSH-fed Col-0 samples. GSH was quantified by HPLC analysis as standardized before [243,214] following the protocol of Tsakraklides et al. 2002 [296] with minor modifications. For that, frozen leaves tissues were extracted with 10 µL mg^{-1} extraction buffer (0.1 M HCl, 1 mM EDTA). Samples were centrifuged at 13,000 × g for 10 minutes having temperature of 4°C. The pH of the supernatant was adjusted to 8.0 with 0.5 M sodium borate. To 80 µL of the pH adjusted supernatant, 5µL of 30 mM DTT was mixed and maintained at room temperature for 10 minutes for the reduction of all thiol groups**.** To this, 5 µL of 60 mM monobromobimane (MBBR) was mixed and maintained in dark for 20 minutes. Next, 100 µL of 20 % acetic acid was added to lower the pH for stabilisation of the MBBR adducts.

HPLC was performed following a standardized protocol [243], using a 515 HPLC pump and AccQTag (3.9 × 150 mm) column. GSH was quantified using a fluorescence detector whose wavelength of excitation was 360 nm and wavelength of emission was 450 nm. The compositions of solvents used were:

i. Solvent A: Triethylamine (TEA), pH 5.05 and sodium acetate
ii. Solvent B: Acetonitrile: water = 30: 70

The conditions for elution were 94 % A: 0–9 minutes; 94 %–91.5 % A: 9–16 minutes; linear gradient of 75 % A: 16–22 minutes; linear decrease to 0 %: 22–30 minutes. GSH solution was used as standard. All experiments were performed in three biological plants samples which were grown independently.

2.6. Estimation of GSH:GSSG ratio

GSH:GSSG ratio was measured according to Ishikawa et al. 2010 [297]. Briefly, leaf tissues were grounded in liquid N_2 and homogenized in 100 mM potassium phosphate buffer (pH 7.4). Total GSH was measured by GR recycling system coupled with 5, 5′-dithiobis (2-nitrobenzoic acid) (DTNB) by measuring 5′-thio- 2-nitrobenzoic acid (TNB) formation at 412 nm. Each reaction mixture contained 5 mM phosphate buffer (pH 7.4), 1 mM EDTA, 0.2 mM GSSG, 0.6 mM DTNB and the cell extract. The reaction mixture was incubated for 5 minutes and then 2 units of GSH reductase were added and absorption was measured after 3 minutes at 412 nm. GSSG was measured by pre-treating the samples with 2-vinylpyridine to mask GSH and assayed in the presence of GR and DTNB as above. GSH content was calculated by subtracting the GSSG content from the total GSH content and GSH:GSSG ratio was determined as well. All experiments were performed thrice with plants grown independently.

2.7. Protein isolation

1 g of leaf tissues were used for protein isolation. Grounded tissues were then suspended in 3 mL of extraction buffer (0.7 M sucrose, 0.05 M EDTA, 0.5 M Tris-HCl, 0.1 M KCl, 0.001 M PMSF, 2 % β-mercaptoethanol) and rest of the procedure was performed following the standard protocol [298,299]. Next, equal volume of Tris-saturated phenol was mixed to it. The mixture was shaken at 4°C for 30 minutes and spinned at a speed of 5,000 × g for 30 minutes at 4°C. The supernatant

was separated and equal portion of extraction buffer was added again. Resultant mixture was shaken for 30 minutes at 4°C and centrifuged at a condition mentioned previously. Again, to the supernatant, 5 volumes of 0.1 M ammonium acetate were added. The mixture was then maintained overnight at -20°C. The solution was centrifuged for 30 minutes and the pellet was washed with ice cold methanol twice. This was followed by another two washes with ice cold acetone. The pellet was collected by centrifugation for 10 minutes. The pellet was allowed to air dry and was further dissolved in 50 mM ammonium bicarbonate solution for LC-MS/MS-QTOF analysis.

2.8. In-gel digestion and LC-MS/MS-QTOF analysis

100 µg of isolated protein was used for digestion. 100 mM DTT was added to the protein samples and kept at 95°C for 1 hour. Next, 250 mM iodoacetamide was added to the samples and placed in dark for 45 minutes. For digesting the samples, trypsin enzyme was used and maintained overnight at 37°C. For sample extraction, 0.1 % formic acid was added to the samples and placed at 37°C for 45 minutes. The soup was dried using a speed vacuum centrifuge machine and the pellet was dissolved in 20 µL of formic acid.

For liquid chromatography (LC), one biological sample was chosen consisting of three technical replicas. 10 µL of sample was injected on C18 UPLC column (Waters, UK). The elution system comprised of:

i) Phase A (0.1 % of formic acid in water)
ii) Phase B (0.1 % of formic acid in ACN).

The separated peptides were detected by Synapt G2 QTOF instrument (Waters, UK) supplemented with electrospray ionization (ESI) source. All data was analysed by MassLynx 4.1 WATERS. For identifying proteins, MS/MS spectra of each and every peptide were tallied with the sequence database available on PLGS software (Protein Lynx Global Server), WATERS. The details of the program setup for LC and parameters used in Synapt G2 QTOF instrument are mentioned in **Table 2** and **Table 3**.

Table 2: Program set-up for LC

S.No	Time	Flow	% A	% B	Curve
1	Initial	0.300	98.0	2.0	Initial
2	1.00	0.300	98.0	2.0	6
3	30.00	0.300	50.0	50.0	6
4	32.00	0.300	50.0	50.0	6
5	40.00	0.300	20.0	80.0	6
6	45.00	0.300	20.0	80.0	6
7	50.00	0.300	98.0	2.0	6
8	55.00	0.300	98.0	2.0	6
9	60.00	0.300	98.0	2.0	6

Table 3: Parameters used in Synapt G2 QTOF instrument

Polarity	ES+
Analyser	Resolution Mode
Capillary (kV)	3.5000
Source Temperature (°C)	150
Sampling Cone	45
Extraction Cone	4.5
Source Gas Flow (mL/min)	30
Desolvation Temperature (°C)	350
Cone Gas Flow (L/h)	30
Desolvation Gas Flow (L/h)	800
Acquisition Time : Start time (min)	0
End Time (min)	60
Source	ES
Acquisition Mode: Polarity	Positive
Analyzer Mode	Resolution
TOF MS: Start range	50Da
End range	1500Da
Scanning time	0.5 sec
Data Format	Continuum
Collision Energy: Function-1 Low Energy: Trap Collision Energy	On – 6V
Transfer Collision Energy	On – 6V
Function-2 High Energy: Ramp Trap Collision Energy	On – 20V to 45V
Ramp Transfer Collision Energy	Off
Cone Voltage	40V

2.9. Raw data analysis

The raw data was processed and analysed using PLGS software 3.0.2. The FASTA sequences of proteins were used for searching the peptides present in the processed data. The protein identification was reviewed for each sample which was followed by expression analysis on the PLGS software. The details of parameters used for analysis of raw data of LC-MS/MS-QTOF are mentioned in **Table 4**.

Table 4: Parameters used for analysis of raw data of LC-MS/MS-QTOF

Peptide tolerance (ppm)	50
Fragment tolerance (ppm)	100
Minimum number of fragment matches for peptides	2
Minimum number of fragment matches for proteins	5
Minimum number of peptide matches for proteins	2
Missed Cleavages	1
Modification	Carbamidomethyl_c, Oxidation_m
Database	Viridiplantae (swiss prot)

2.10. Statistical analysis

Semi-quantitative RT-PCR analysis, HPLC and GSH:GSSG ratio determination assay were performed in triplicate, and the data are presented as the mean ± standard error (SE). For statistical analysis, a multiple t-test followed by the two-stage step-up method of Benjamini, Kreiger, and Yekutieli was used (GraphPad InStat software, v. 8). $P<0.332$, 0.002, 0.001 were considered to be statistically significant.

3. Results

3.1. Elevated GSH content and increased expression of PR1 transcript in GSH-fed Col-0 samples

Previous studies have demonstrated higher GSH level in exogenously fed Col-0 plants with 100 µM GSH for 72 hours [214,77]. To validate this, GSH content and GSH:GSSG ratio were determined in GSH-fed Col-0 plants. Results revealed almost 2-fold increase in GSH content in GSH-fed Col-0 plants (**Fig. 1A**). Similarly, significantly higher GSH:GSSG ratio was also noted in GSH-fed Col-0 plants (**Fig. 1B)**. In earlier studies, it was demonstrated that *PR1* can be used as a marker for enhanced GSH condition [300,246]. The expression analysis of *PR1* in Col-0 samples treated with GSH revealed remarkable increase in *PR1* expression (**Fig. 1C**).

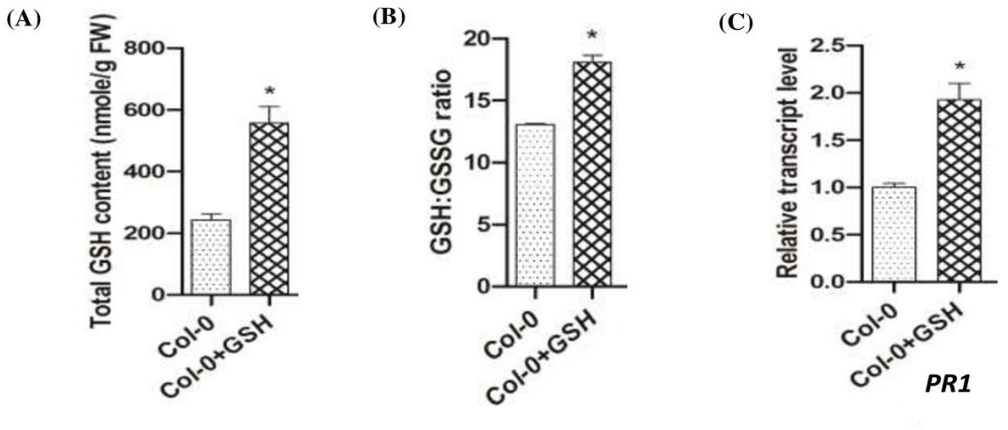

Fig. 1. Establishment of GSH-fed conditions. **(A)** Estimation of GSH content by HPLC. **(B)** Determination of GSH:GSSG ratio. **(C)** *PR1* expression analysis in Col-0 (control) and GSH-fed Col-0 plants. Experiments were repeated with three biological samples. *P<0.332.

3.2. Up-regulated expression of stress marker genes revealed establishment of stressed conditions in Arabidopsis

To understand the establishment of the stress treated condition (combined osmotic + cold), the expression profile of selected stress marker genes viz. *OSMOTIN*, *Hsp70*, *APX1*, *ADC2* and *Hsp18.2* were checked. The samples used here were control Col-0, control GSH-fed Col-0, treated Col-0 and treated GSH-fed Col-0 plants. Results revealed up-regulated expression of the

above mentioned genes in treated samples of Col-0 and GSH-fed Col-0 samples in comparison to control samples of Col-0 and GSH-fed Col-0 (**Fig. 2**). Therefore, it was revealed that the stress treated condition had been properly established.

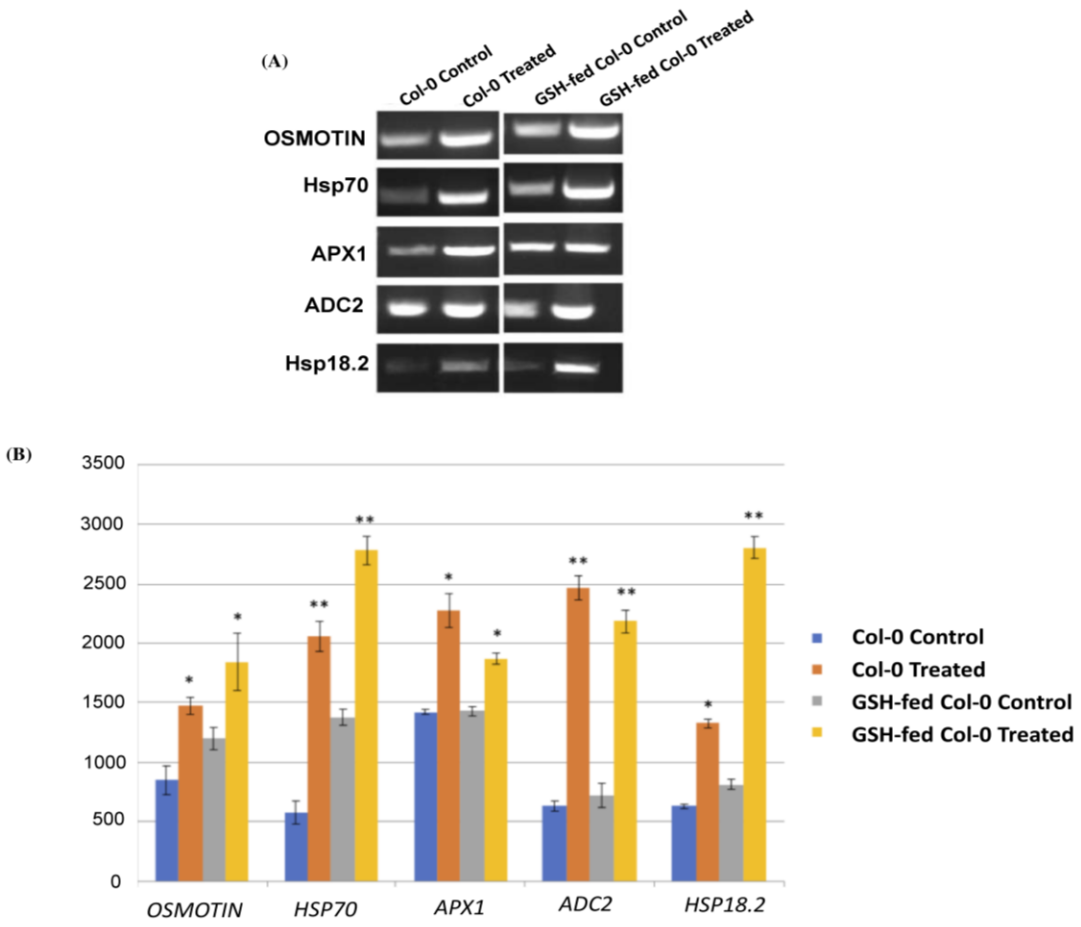

Fig. 2. Physiological responses of Col-0 and GSH-fed Col-0 under combine osmotic and stress treatment. **(A)** Gel images **(B)** Graphical representation showing up-regulation of *OSMOTIN, Hsp70, APX1, ADC2, Hsp18.2* in treated Col-0 and GSH-fed Col-0 plants compared to samples without any stress treatment viz. control Col-0 and GSH-fed Col-0. Experiments were repeated with three biological samples. *P<0.332, **P<0.002.

3.3. KEGG and PANTHER classification of differentially accumulated proteins

In order to attain a deeper insight into the differential protein accumulation in presence and absence of exogenous GSH during combined osmotic and cold stress treated condition in *Arabidopsis*, we had performed comparative proteomic profiling using LC-MS/MS-QTOF. Under combined osmotic and cold stress, Col-0 plants (without GSH feeding) served as control

of the experiment against GSH-fed Col-0 samples. Numerous proteins were identified which revealed some interesting data. Results of proteomic study revealed that in Col-0 (without GSH feeding), 978 proteins were identified. Whereas, 972 proteins were identified in GSH-fed Col-0 samples, out of which, 136 and 104 proteins were noted down-accumulated and up-accumulated respectively. List of all differentially expressed proteins are provided in **Table 4.** The KEGG classification of differentially expressed proteins was performed. KEGG classification of proteins revealed that among all the 136 down-accumulated proteins, 61.9 % proteins were associated with stress and defense category, 9 % of the proteins belonged to carbon and energy metabolism group (**Fig. 3**). From the up-accumulated proteins, 42 % of the proteins were related to stress and defense group, 8.6 % belonged to carbon and energy metabolism group (**Fig. 3**).

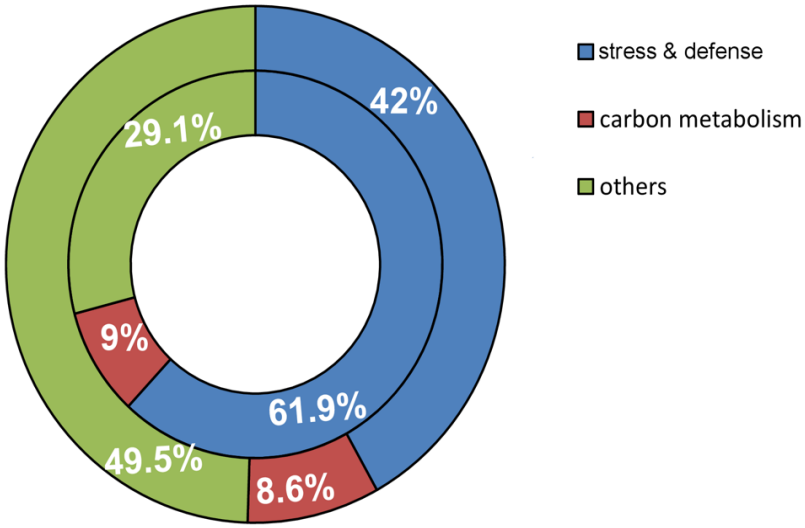

Fig. 3. Functional classification of differentially accumulated proteins in LC-QTOF-MS/MS by KEGG software. The outer circles showing the classification of up-accumulated proteins whereas the inner circle showing the classification of down-accumulated proteins. Data presented here is of one biological sample consisting of three technical replicas.

Analysis by PANTHER, categorized both down and up-accumulated proteins on the basis of molecular function, biological process, cellular component, protein classes and metabolic pathways. The list of all down and up-accumulated proteins is mentioned in **Table 5**. Based on molecular function of down-accumulated proteins, 64.7 % of the proteins belonged to category showing catalytic activity (**Fig. 4A**). In this category proteins like RuvB-like protein 1

(Q9FMR9), Methylesterase 9 (O23171) and serine/threonine protein phosphatase 2A (Q9LVE2) were noted to have hydrolase activity. Cytosolic form of glucose-6-phosphate isomerase (P34795) was noted to have intramolecular transferase activity, oxalate-CoA ligase (Q9SMT7) was noted to have ligase activity, Betaine aldehyde dehydrogenase 2, mitochondria (Q9STS1), DMR6-like oxygenase 2 (Q9ZSA7), L-ascorbate peroxidase 3 (Q42564) and alcohol dehydrogenase class-3 (Q96533) were noted to have oxido-reductase activity. L-type lectin-domain containing receptor kinase (Q9LSR9) and Histidine kinase 5 (Q3S4A7) were noted to have transferase activity. Apart from proteins showing catalytic activity, 23.5 % belonged to protein having binding activity, 5.9 % belonged to proteins that acts as molecular function regulator, 2.9 % each belonged to proteins having molecular transducer activity and transporter activity respectively (**Fig. 4A**). The proteins under binding activity category comprised of ACD11 homolog protein (Q8L7U7), transcription factor MYB108 (Q9LDE1), GLABROUS1 enhancer-binding protein (Q9ASZ1), alcohol dehydrogenase class-3 (Q96533) and ribosome-recycling factor (Q9M1X0). Dirigent protein 23 (Q84TH6) and serine/threonine protein phosphatase 2A (Q9LVE2) belonged to molecular function regulator category. Histidine kinase 5 (Q3S4A7) and ACD11 homolog protein (Q8L7U7) belonged to molecular transducer activity and transporter activity respectively.

Based on different biological processes of down-regulated proteins, 31 % were known to possess different cellular functions which includes ribosome-recycling factor (Q9M1X0), oxalate-CoA ligase (Q9SMT7), L-ascorbate peroxidase 3 (Q42564) (**Fig. 4B**). 28.6 % belonged to the proteins involved in different metabolic processes (**Fig. 10B**), like (S)-2-hydroxy-acid oxidase GLO2 (Q9LRS0), beta carbonic anhydrase 1, chloroplastic (P27140), methylesterase 9 (O23171). As shown in **Fig. 4B,** 21.4 % proteins were expressed in response to stimulus like biotic stress, chemical stress viz. L-type lectin-domain containing receptor kinase I.8 (Q9LSR9), L-ascorbate peroxidase 3 (Q42564), alcohol dehydrogenase class-3 (Q96533), 11.9 % were responsible for biological regulation like Dirigent protein 23 (Q84TH6), protein SGT1 homolog B (Q9SUT5), 4.8 % belonged to protein group responsible for cellular component organization or biogenesis like RuvB-like protein 1 (Q9FMR9), pre-mRNA-processing factor 19 homolog 2 (O22785) and 2.4 % belonged to the proteins that determines localization of other proteins like ACD11 homolog protein (Q8L7U7).

Based on cellular compartmentalization classification of down-regulated proteins (**Fig. 4C**), 56.3 % of the proteins were noted to be cellular proteins like glucan endo-1, 3-beta-glucosidase 13 (Q9FJU9), (S)-2-hydroxy-acid oxidase GLO2 (Q9LRS0). 28.1 % were organellar proteins like phytochrome B (P14713), ribosome-recycling factor (Q9M1X0). 12.5 % were protein-containing complex like pre-mRNA-processing factor 19 homolog 2 (O22785) and 3.1 % were membrane proteins like histidine kinase 5 (Q3S4A7) (**Fig. 4C**).

Based on protein classes the PANTHER classification (**Fig. 4D**)**,** revealed 28.6 % belonged to oxidoreductase group like betaine aldehyde dehydrogenase 2 (Q9STS1), alcohol dehydrogenase class-3 (Q96533), oxalate-CoA ligase (Q9SMT7). 23.8 % belonged to transferase group like phosphoribulokinase (P25697), polyamine oxidase 5 (Q9SU79). 19 % belonged to hydrolase group like methylesterase 9 (O23171), serine/threonine protein phosphatase 2A (Q9LVE2).

As shown in **Fig. 4E,** classification based on protein involved in various metabolic pathways 20 % of the proteins belonged to each of the following group viz. EGF receptor signaling pathway, FGF receptor signaling pathway, glycolysis, pentose phosphate pathway and salvage pathway. The protein involved in both EGF and FGF receptor signaling pathway was serine/threonine protein phosphatase 2A (Q9LVE2), protein involved in glycolysis and pentose phosphate pathway was glucose-6-phosphate isomerise (P34795) and the protein involved in salvage pathway was phosphoribulokinase / uridine kinase family (Q9C664).

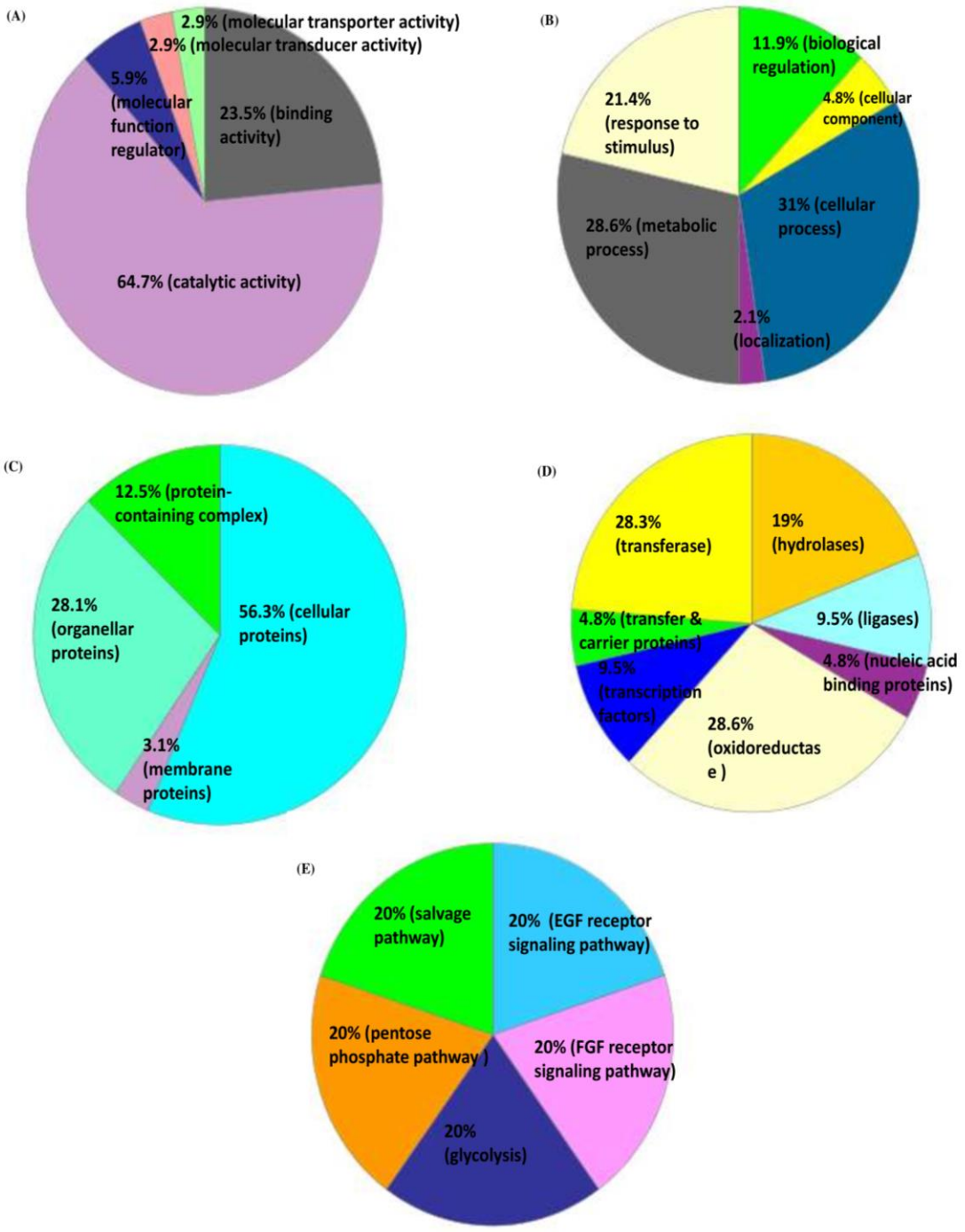

Fig. 4. Functional classification of down-accumulated proteins by PANTHER software based on (A) Molecular function **(B)** Biological process **(C)** Cellular compartmentalization **(D)** Protein class **(E)** Metabolic pathways.

Based on molecular function classification of up-regulated proteins (**Fig. 5A**), revealed that 65.4 % of the proteins belonged to category showing catalytic activity viz. tryptophan synthase (Q42529), cold-responsive protein kinase 1 (Q93YN1), glyceraldehyde-3-phosphate dehydrogenase (Q9FX54), porphobilinogen deaminase (Q43316), polyamine oxidase 1 (Q9FNA2), cinnamyl alcohol dehydrogenase 8 (Q02972), 3-ketoacyl-CoA thiolase 5 (Q570C8), β-glucosidase 26 (O64883), malate dehydrogenase 1 (O82399), aspartate-tRNA ligase 2 (Q9M084), poly(ADP-ribose) glycohydrolase 1 (Q9SKB3), NADPH-quinone oxidoreductase (Q9LK88) and aspartyl protease APCB1 (Q9M9A8). 19.2 % were noted to have binding activity viz. calreticulin-3 **(**O041530), transcription activator GLK1 (Q9SIV3), aspartate-tRNA ligase 2 (Q9M084), NADPH-quinone oxidoreductase (Q9LK88). 11.5 % of the proteins were noted to have transporter activity viz. sugar transport protein 4 (Q39228), protein detoxification 51 (Q9SZE2) and bidirectional sugar transporter SWEET15 (Q9FY94). 3.8 % were noted to have transcription regulator activity viz. transcription activator GLK1 (Q9SIV3).

Based on different biological processes of up-regulated proteins (**Fig. 5B**), 31.1 % were noted to be involved in metabolic processes viz. tryptophan synthase (Q42529), mitogen-activated protein kinase 3 (Q39023), HSP20-like chaperones (Q9S732), glyceraldehyde-3-phosphate dehydrogenase GAPC2 (Q9FX54), porphobilinogen deaminase (Q43316), cinnamyl alcohol dehydrogenase 8 (Q02972) and aspartyl protease APCB1 (Q9M9A8). 27.1 % of them had cellular functions viz. tryptophan synthase alpha chain (Q42529), cold-responsive protein kinase 1 (Q93YN1), mitogen-activated protein kinase 3 (Q39023), MACPF domain-containing protein (Q8L612) (**Fig. 5B**). 25 % were proteins that are expressed in response to stimulus biotic, abiotic, chemical factors which include proteins like TIFY 6A (Q58G47), TIFY 3B (Q9C5K8), regulatory protein NPR1 (P93002), zinc finger protein ZAT12 (Q42410). 14.6 % of the proteins were noted to be involved in biological regulation viz. poly (ADP-ribose) glycohydrolase 1 (Q9SKB3), TIFY 10A (Q9LMA8), mitogen-activated protein kinase 3 (Q39023). 2.1 % belonged to the protein group that determines localization of other proteins like exocyst complex component EXO70B1 (Q9FGH9),

Based on cellular compartmentalization classification of up-regulated proteins (**Fig. 5C**), 63 % of them were noted to be cellular proteins like poly (ADP-ribose) glycohydrolase 1 (Q9SKB3), non-functional pseudokinase ZED1 (Q8LGB6), GAPC2 (Q9FX54), 3-ketoacyl-CoA thiolase 5 (Q570C8), glucan endo-1,3-beta-glucosidase 6 (Q93Z08). 29.6 % were organellar

proteins which include proteins like tryptophan synthase (Q42529), transcription activator GLK1 (Q9SIV3), NPR1 (P93002). 3.7 % belonged to each group of proteins viz. membrane proteins and protein forming complex. The membrane proteins included sugar transport protein 4 (Q39228) and protein forming complex included aspartate-tRNA ligase 2 (Q9M084).

Based on different protein classes of up-regulated proteins, 20 % of the proteins belonged to the oxidoreductase group (**Fig. 5D**), which include proteins like GAPC2 (Q9FX54), NADPH quinine oxidoreductase (Q9LK88), malate dehydrogenase 1 (O82399), polyamine oxidase 1 (Q9FNA2). 16 % of the proteins belonged to each of the group viz. transferase and hydrolase. The transferase group of proteins included mitogen-activated protein kinase 3 (Q39023), polyamine oxidase 1 (Q9FNA2), 3-ketoacyl-CoA thiolase 5 (Q570C8). The hydrolase group of proteins included tryptophan synthase (Q42529), poly (ADP-ribose) glycohydrolase 1 (Q9SKB3), porphobilinogen deaminase (Q43316), aspartyl protease APCB1 (Q9M9A8). 8 % of the proteins belonged to each of the group viz. cytoskeletal and transporter group. The cytoskeletal group of proteins included SUPPRESSOR OF K (+) TRANSPORT GROWTH DEFECT 1 (Q9ZNT0). The transporter group of proteins included DETOXIFICATION 51 (Q9SZE2), sugar transport protein 4 (Q39228). 4 % of the proteins belonged to each of the group viz. calcium binding proteins and nucleic acid binding proteins respectively (**Fig. 5D**). The calcium binding proteins includes calreticulin-3 chaperone proteins viz. HSP20 like chaperones superfamily (Q9S732), isomerise like tryptophan synthase (Q42529), ligases like aspastate-tRNA ligase 2 (Q9M084), lyases like tryptophan synthase (Q42529), membrane traffic proteins like exocyst complex component EXO70B1 (Q9FGH9). The nucleic acid binding proteins includes aspartate-tRNA ligase (Q9M084).

Based on proteins involved in various metabolic pathways of up-regulated proteins (**Fig. 5E**), 6.3 % of the proteins belonged to each of the different categories. Some of the categories include apoptosis signaling pathways, proteins involved in glycolysis viz. GAPC2 (Q9FX54), heme biosynthesis pathway, pyruvate metabolism pathway like malate dehydrogenase 1 (O82399) and tryptophan biosynthesis pathway proteins like tryptophan synthase TRA1 (Q42529).

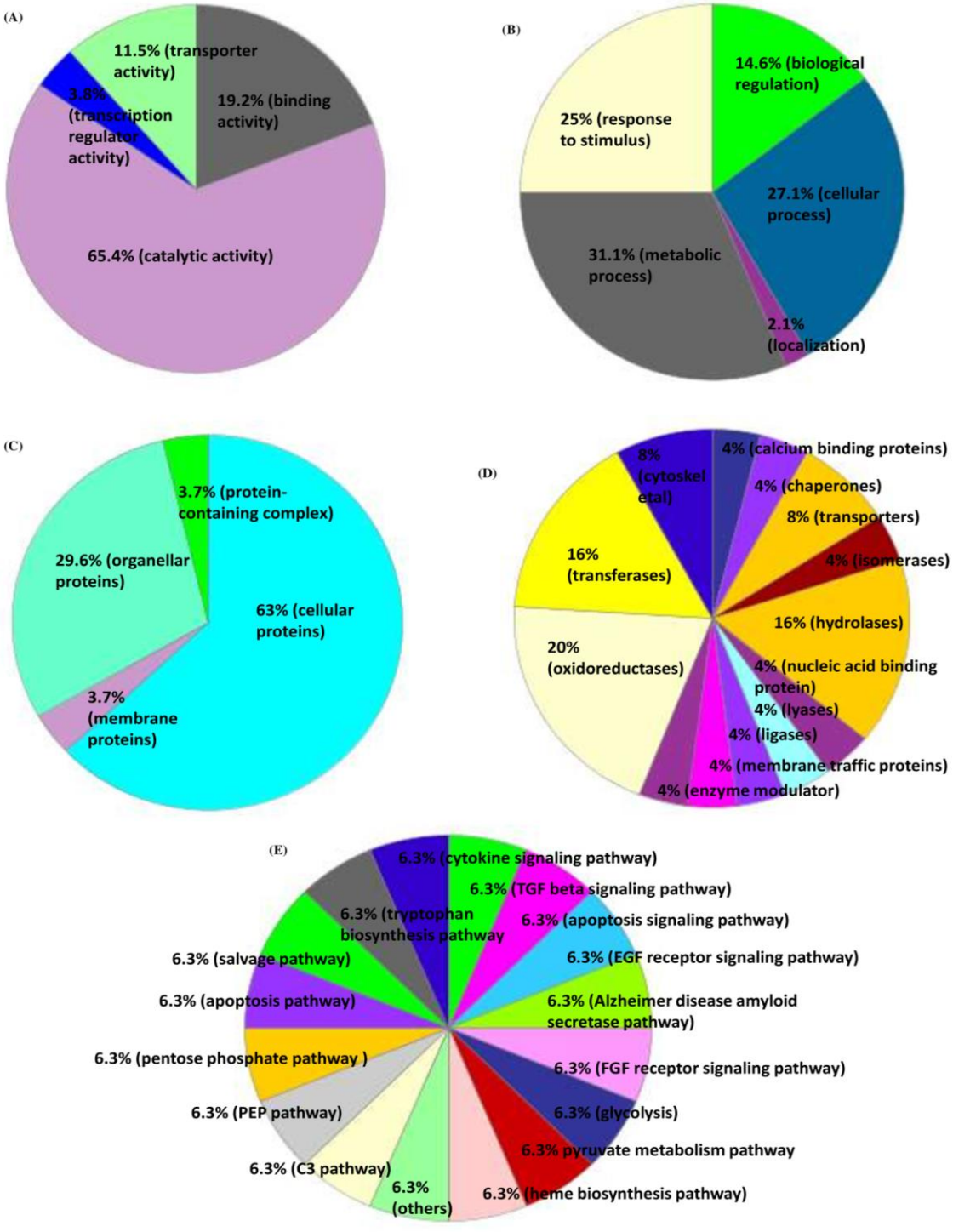

Fig. 5. Functional classification of up-accumulated proteins by PANTHER software based on (A) Molecular function **(B)** Biological process **(C)** Cellular compartmentalization **(D)** Protein class **(E)** Metabolic pathways.

Table 5: List of differentially expressed proteins in GSH-fed Col-0 identified by LC-MS/MS-QTOF

SRL. NO.	ACCESSION NUMBER	PROTEIN [ORGANISM]	SCORE	FOLD CHANGE
	LIST OF PROTEINS DOWN ACCUMULATED IN TREATED GSH-FED COL-0			
1	Q9C7I7	MLP-like protein 165 [*A. thaliana*]	116.68	0.035084
2	Q541X8	Uncharacterized protein At1g35260/ T9I1_17 [*A. thaliana*]	116.68	0.036516
3	A0A178WLG3	MLP165 [*A. thaliana*]	116.68	0.037628
4	A0A178WJG1	Uncharacterized protein At1g36040 [*A. thaliana*]	92.78	0.038006
5	Q9SUT5	Protein SGT1 homolog B [*A.thaliana*]	173.28	0.046888
6	F4JN35	Protein NTM1-like 9 [*A.thaliana*]	130.64	0.06457
7	Q9FXA9	Putative pentatricopeptide repeat-containing protein At1g56570 [*A.thaliana*]	207.54	0.076536
8	Q8W4D4	BAG-associated GRAM protein 1 [*A.thaliana*]	112.56	0.089815
9	A0A178VP38	diacylglycerol kinase At2g16350 [*A.thaliana*]	137.65	0.116484
10	Q9LVE2	Serine/threonine protein phosphatase 2A 59 kDa regulatory subunit B' zeta isoform [*A.thaliana*]	95.16	0.126186
11	Q9STS1	Betaine aldehyde dehydrogenase 2, mitochondrial [*A.thaliana*]	66.81	0.133989
12	A0A384LE60	Uncharacterized protein At3g28710 [*A.thaliana*]	6.07	0.145148
13	Q8LDJ8	Major latex protein, putative [*A.thaliana*]	67.12	0.145148
14	Q9FGZ4	Probable WRKY transcription factor	65.55	0.158817

		48 [*A.thaliana*]		
15	Q9LZV6	Probable WRKY transcription factor 62 [*A.thaliana*]	216.99	0.160414
16	Q8W493	Ferredoxin--NADP reductase, leaf isozyme 2, chloroplastic [*A.thaliana*]	171.65	0.180866
17	A0A178W801	MLO4 OS=Arabidopsis thaliana At1g11240 [*A.thaliana*]	24.28	0.182684
18	Q9LDE1	Transcription factor MYB108 [*A.thaliana*]	115.92	0.182684
19	Q9FJU9	Glucan endo-1,3-beta-glucosidase 13 [*A.thaliana*]	498.86	0.197899
20	B2BDD7	Enhanced disease susceptibility 1 [*A.thaliana*]	253.14	0.214381
21	Q9FGC7	Zeaxanthin epoxidase, chloroplastic[*A.thaliana*]	109.27	0.218712
22	Q9LDZ5	Probable serine/threonine-protein kinase PBL21 [*A.thaliana*]	121.65	0.218712
23	F4I7Y4	Serine/threonine-protein kinase BSK11 [*A.thaliana*]	47.35	0.22091
24	Q9SU72	Protein EDS1 OS=Arabidopsis thaliana [*A.thaliana*]	342.65	0.227638
25	Q9SY91	Probable serine/threonine-protein kinase PBL15 [*A.thaliana*]	48.85	0.246597
26	D9IX20	Accelerated cell death 6 (Fragment) At4g14400 [*A.thaliana*]	108.32	0.249075
27	Q6XMI3	Salicylate/benzoate carboxyl methyltransferase [*A.thaliana*]	133.93	0.251579
28	P25697	Phospho ribulokinase, chloroplastic [*A.thaliana*]	189.51	0.254107

29	D9IX21	Accelerated cell death 6 [*A.thaliana*]	108.32	0.264477
30	Q9FMR9	RuvB-like protein 1 [*A.thaliana*]	150.67	0.26982
31	F4I2N7	Receptor-like protein kinase 7 [*A.thaliana*]	80.47	0.272532
32	F4I924	Transmembrane protein At1g17780 [*A.thaliana*]	460.9	0.275271
33	Q9SU79	Probable polyamine oxidase 5 [*A.thaliana*]	171.9	0.275271
34	R9YWT5	Accelerated cell death 6 (Fragment) [*A.thaliana*]	176.94	0.280832
35	R9YY22	Accelerated cell death 6 (Fragment) [*A.thaliana*]	108.32	0.280832
36	Q8LLD0	Nuclear pore complex protein NUP96 [*A.thaliana*]	150.05	0.283654
37	Q42564	L-ascorbate peroxidase 3 [*A.thaliana*]	123.13	0.286505
38	R9YWV7	Accelerated cell death 6 (Fragment) [*A.thaliana*]	110.2	0.289384
39	A0A178V6E6	ACD6 At4g16620 [*A.thaliana*]	108.32	0.29523
40	R9YXU1	Accelerated cell death 6 (Fragment)	108.32	0.29523
41	Q9M1G4	Probable L-type lectin-domain containing receptor kinase I.5 [*A.thaliana*]	105.1	0.298197
42	R9YWU4	Accelerated cell death 6 (Fragment) [*A.thaliana*]	108.32	0.304221
43	B0ZU76	Enhanced disease susceptibility 1 protein (Fragment) [*A.thaliana*]	83.04	0.323033
44	B0ZU51	Enhanced disease susceptibility 1 protein (Fragment)	64.25	0.323033
45	F4HP45	Brassinosteroid signaling positive	247.59	0.329559

		regulator (BZR1) family protein [*A.thaliana*]		
46	P27140	Beta carbonic anhydrase 1, chloroplastic [*A.thaliana*]	150.63	0.336216
47	B2BDD1	Enhanced disease susceptibility 1 [*A.thaliana*]	168.22	0.336216
48	Q9LSR9	L-type lectin-domain containing receptor kinase I.8 [*A.thaliana*]	169.09	0.336216
49	D9IX18	Accelerated cell death 6 At4g14400 [*A.thaliana*]	150.65	0.343008
50	B0ZU49	Enhanced disease susceptibility 1 protein (Fragment) [*A.thaliana*]	83.04	0.343008
51	Q8VYE5	Glucan endo-1,3-beta-glucosidase 12 [*A.thaliana*]	112.86	0.346456
52	Q9LUZ6	Protein PMR5 [*A.thaliana*]	357.71	0.353455
53	B0ZU44	Enhanced disease susceptibility 1 protein (Fragment) [*A.thaliana*]	83.04	0.353455
54	Q9SR87	Probable L-type lectin-domain containing receptor kinase VI.1 [*A.thaliana*]	169.54	0.353455
55	Q2V4D5	Putative defensin-like protein 36 At1g69828 [*A.thaliana*]	788.87	0.353455
56	Q96533	Alcohol dehydrogenase class-3 [*A.thaliana*]	135.22	0.357007
57	Q9ASZ1	GLABROUS1 enhancer-binding protein [*A.thaliana*]	337.84	0.357007
58	Q8L9T5	RING-H2 finger protein ATL2 [*A.thaliana*]	101.99	0.357007
59	R9YXL9	Accelerated cell death 6 [*A.thaliana*]	150.65	0.357007

60	O82484	Putative disease resistance protein At4g10780 At4g10780 [*A.thaliana*]	171.91	0.360595
61	Q9LS26	Serine/threonine-protein kinase BSK2 [*A.thaliana*]	220.38	0.364219
62	P48578	Serine/threonine-protein phosphatase PP2A-4 catalytic subunit [*A.thaliana*]	113.66	0.367879
63	D9IWY6	Accelerated cell death 6 (Fragment) At4g14400 [*A.thaliana*]	146.22	0.367879
64	B2BDC6	Enhanced disease susceptibility 1 [*A.thaliana*]	168.22	0.371577
65	Q9LW57	Plastid-lipid-associated protein 6, chloroplastic [*A.thaliana*]	198.01	0.375311
66	Q3S4A7	Histidine kinase 5 [*A.thaliana*]	142.02	0.379083
67	Q9ZSA7	Protein DMR6-LIKE OXYGENASE 2 [*A.thaliana*]	65.24	0.386741
68	Q9SI85	Probable disease resistance protein At1g62630 At1g62630 [*A.thaliana*]	31.96	0.390628
69	B2BDM2	Phytoalexin deficient 4 [*A.thaliana*]	90.05	0.390628
70	Q9ZT75	Uncharacterized protein F9H3.10 [*A.thaliana*]	82.65	0.394554
71	F4JFV6	Aldolase-type TIM barrel family protein [*A.thaliana*]	71.79	0.394554
72	B0ZX36	Ethylene receptor 1 (Fragment) [*A.thaliana*]	67.31	0.398519
73	F4I5D5	WAT1-related protein At1g70260 At1g70260 [*A.thaliana*]	129.73	0.398519
74	P34795	Glucose-6-phosphate isomerase, cytosolic [*A.thaliana*]	51.46	0.398519
75	D9IWY2	Accelerated cell death 6 (Fragment)	146.22	0.398519

		At4g14400 [*A.thaliana*]		
76	D9IWW8	Accelerated cell death 6 At4g14400 [*A.thaliana*]	167.44	0.398519
77	B0ZUH7	Phytoalexin-deficient 4 protein (Fragment) [*A.thaliana*]	131.83	0.402524
78	Q9M109	Ankyrin repeat family protein At4g03470 [*A.thaliana*]	82.65	0.402524
79	Q39241	Thioredoxin H5 [*A.thaliana*]	219.23	0.402524
80	A0A1P8BGG0	Emsy N Terminus (ENT)/ plant Tudor-like domains-containing protein [*A.thaliana*]	124.4	0.402524
81	R9YUX0	Accelerated cell death 6 (Fragment) [*A.thaliana*]	125.12	0.402524
82	D9IWY7	Accelerated cell death 6 (Fragment) At4g14400 [*A.thaliana*]	146.22	0.402524
83	D9IWX8	Accelerated cell death 6 At4g14400 [*A.thaliana*]	125.12	0.402524
84	R9YXX6	Accelerated cell death 6 (Fragment) [*A.thaliana*]	150.65	0.40657
85	D9IWY1	Accelerated cell death 6 (Fragment) [*A.thaliana*]	103.9	0.40657
86	D9IWW5	Accelerated cell death 6 (Fragment) At4g14400 [*A.thaliana*]	177.73	0.414783
87	R9YWT8	Accelerated cell death 6 [*A.thaliana*]	125.12	0.418952
88	B0ZXA2	Ethylene receptor 1 (Fragment) [*A.thaliana*]	281.22	0.418952
89	B2BDL0	Phytoalexin deficient 4 [*A.thaliana*]	90.05	0.418952
90	D9IWY0	Accelerated cell death 6 (Fragment) At4g14400 [*A.thaliana*]	103.9	0.418952

91	D9IX17	Accelerated cell death 6 At4g14400 [*A.thaliana*]	176.94	0.423162
92	Q9M2R1	Protein GIGAS CELL1 [*A.thaliana*]	134.52	0.423162
93	Q9M1X0	Ribosome-recycling factor, chloroplastic [*A.thaliana*]	72.01	0.423162
94	Q9C7C4	Protein EMSY-LIKE 1 [*A.thaliana*]	246.92	0.427415
95	Q9LRS0	(S)-2-hydroxy-acid oxidase GLO2 [*A.thaliana*]	71.79	0.427415
96	Q84TH6	Dirigent protein 23 [*A.thaliana*]	87.52	0.427415
97	O23171	Methylesterase 9 [*A.thaliana*]	12.46	0.427415
98	P14713	Phytochrome B [*A.thaliana*]	175.87	0.431711
99	B0ZXB6	Ethylene receptor 1 (Fragment) [*A.thaliana*]	281.22	0.431711
100	B0ZX93	Ethylene receptor 1 (Fragment) [*A.thaliana*]	281.22	0.431711
101	A0A178VB56	EML1 At3g12140 [*A.thaliana*]	347.27	0.436049
102	A0A178V9V5	EML1 At3g12140 [*A.thaliana*]	246.92	0.440432
103	A0A178V8U6	EML1 At3g12140 [*A.thaliana*]	246.92	0.440432
104	O65670	At4g39830 At4g39830 [*A.thaliana*]	110.55	0.440432
105	A9QM73	Protein SMG7 [*A.thaliana*]	102.18	0.444858
106	Q9LIM9	Major latex protein-like At3g26460 [*A.thaliana*]	6.07	0.444858
107	Q9LII8	Protein KINESIN LIGHT CHAIN-RELATED 2 [*A.thaliana*]	124.78	0.444858
108	B0ZXB7	Ethylene receptor 1 (Fragment) [*A.thaliana*]	281.22	0.444858
109	Q8L7U7	ACD11 homolog protein At4g39670 [*A.thaliana*]	268.6	0.444858

110	Q38862	Inositol-3-phosphate synthase isozyme 2 [*A.thaliana*]	180.54	0.449329
111	F4JT78	Disease resistance protein RPP2A [*A.thaliana*]	138.75	0.449329
112	A0A178VS35	diacylglycerol kinase At2g16350 [*A.thaliana*]	137.65	0.449329
113	B0ZX92	Ethylene receptor 1 (Fragment) [*A.thaliana*]	281.22	0.453845
114	Q8W1D5	CBL-interacting serine/threonine-protein kinase 25 [*A.thaliana*]	67.47	0.453845
115	R9YXL5	Accelerated cell death 6 [*A.thaliana*]	150.65	0.453845
116	Q7X6T3	Defensin-like protein 99 [*A.thaliana*]	16.13	0.458406
117	A0A384KEZ4	Uncharacterized protein At3g28720 [*A.thaliana*]	150.03	0.458406
118	R9YY54	Accelerated cell death 6 [*A.thaliana*]	139.01	0.458406
119	Q9SMT7	Oxalate--CoA ligase [*A.thaliana*]	64.17	0.458406
120	B0ZX58	Ethylene receptor 1 (Fragment) [*A.thaliana*]	292.25	0.463013
121	Q9LDT0	Putative cysteine-rich receptor-like protein kinase 30 [*A.thaliana*]	34.2	0.463013
122	B2BDL7	Phytoalexin deficient 4 [*A.thaliana*]	99.62	0.467666
123	Q9C664	Inorganic pyrophosphatase TTM2 [*A.thaliana*]	158.87	0.472367
124	F4HVY0	Very-long-chain aldehyde decarbonylase CER1 [*A.thaliana*]	40.34	0.472367
125	B0ZX26	Ethylene receptor 1 (Fragment) [*A.thaliana*]	296.44	0.477114
126	B0ZXB9	Ethylene receptor 1 (Fragment) [*A.thaliana*]	292.25	0.481909

127	Q66GR6	Single-stranded DNA-binding protein WHY3, chloroplastic [*A.thaliana*]	104	0.481909
128	D9IWY4	Accelerated cell death 6 At4g14400 [*A.thaliana*]	162.54	0.481909
129	O22785	Pre-mRNA-processing factor 19 homolog 2 [*A.thaliana*]	64.47	0.486752
130	Q8GZ74	At3g26470 [*A.thaliana*]	115.13	0.486752
131	Q9LIM8	Powdery mildew resistance protein, RPW8 domain-containing protein At3g26470 [*A.thaliana*]	150.03	0.491644
132	D9IWY5	Accelerated cell death 6 At4g14400 [*A.thaliana*]	162.54	0.491644
133	B0ZXB5	Ethylene receptor 1 (Fragment) [*A.thaliana*]	292.25	0.496585
134	Q9SAV1	Myrosinase-binding protein 2 [*A.thaliana*]	344.53	0.496585
135	Q9SU71	Protein EDS1B [*A.thaliana*]	229.86	0.496585
136	Q8L9S5	Uncharacterized protein [*A.thaliana*]	150.03	0.496585
	LIST OF PROTEINS UP ACCUMULATED IN TREATED GSH-FED COL-0			
137	Q8L612	MACPF domain-containing protein At1g14780 [*A.thaliana*]	173.06	2.013753
138	Q9FL69	ADP-ribosylation factor GTPase-activating protein AGD5 [*A.thaliana*]	124.54	2.033991
139	Q9LQ54	Probable disease resistance protein At1g59620 [*A.thaliana*]	61.34	2.033991
140	P0DI16	Probable disease resistance protein RDL5 [*A.thaliana*]	58.51	2.033991
141	F4JG88	Ankyrin repeat family protein	90.68	2.054433

		At4g03490 [*A.thaliana*]		
142	Q42410	Zinc finger protein ZAT12 [*A.thaliana*]	177.71	2.117
143	Q96262	Plasma membrane-associated cation-binding protein 1 [*A.thaliana*]	111.38	2.159766
144	Q39023	Mitogen-activated protein kinase 3 [*A.thaliana*]	323.29	2.161834
145	Q9SIP1	Stress-response A/B barrel domain-containing protein UP3 [*A.thaliana*]	79.92	2.181472
146	Q9STW5	MACPF domain-containing protein At4g24290 [*A.thaliana*]	27.67	2.181472
147	Q8W474	Probable disease resistance protein At1g58390 [*A.thaliana*]	67.44	2.181472
148	B0M006	Ethylene-insensitive3 (Fragment) [*A.thaliana*]	144.22	2.203396
149	B0M000	Ethylene-insensitive3 (Fragment) [*A.thaliana*]	144.22	2.203396
150	Q9LR59	F21B7.27 OS=Arabidopsis thaliana [*A.thaliana*]	95.81	2.203396
151	P59584	Disease resistance protein RPH8A [*A.thaliana*]	76	2.316367
152	Q93YN1	Cold-responsive protein kinase 1 [*A.thaliana*]	116.26	2.339647
153	B2BDJ6	Non-expressor of PR1 [*A.thaliana*]	160.4	2.339647
154	B0LZR6	Ethylene-insensitive3 (Fragment) [*A.thaliana*]	196.09	2.363161
155	Q9M9A8	Aspartyl protease APCB1 [*A.thaliana*]	53.97	2.386911
156	B0LZR7	Ethylene-insensitive3 (Fragment)	160.02	2.4109

		[*A.thaliana*]		
157	B0LZT0	Ethylene-insensitive3 (Fragment) [*A.thaliana*]	80.33	2.43513
158	P42737	Beta carbonic anhydrase 2, chloroplastic [*A.thaliana*]	206.13	2.50929
159	Q9LNV9	Receptor-like protein 1 [*A.thaliana*]	158.42	2.50929
160	B0LZZ5	Ethylene-insensitive3 (Fragment) [*A.thaliana*]	196.09	2.559981
161	B0LZW6	Ethylene-insensitive3 (Fragment) [*A.thaliana*]	133.84	2.559981
162	Q39228	Sugar transport protein 4 [*A.thaliana*]	61.85	2.58571
163	O04153	Calreticulin-3 [*A.thaliana*]	144.94	2.664456
164	Q9FNA2	Polyamine oxidase 1 [*A.thaliana*]	96.51	2.691234
165	B0LZT9	Ethylene-insensitive3 (Fragment) [*A.thaliana*]	133.84	2.718282
166	B0LZX6	Ethylene-insensitive3 (Fragment) [*A.thaliana*]	133.84	2.745601
167	B0LZT4	Ethylene-insensitive3 (Fragment) [*A.thaliana*]	196.09	2.745601
168	B0LZS0	Ethylene-insensitive3 (Fragment) [*A.thaliana*]	133.84	2.745601
169	Q9LFP7	Probable serine/threonine-protein kinase PIX7 [*A.thaliana*]	41.1	2.773195
170	E1A9B2	Ankyrin repeat family protein (Fragment) At4g0346 [*A.thaliana*]	695.12	2.857651
171	O64883	Beta-glucosidase 26, peroxisomal [*A.thaliana*]	193.29	2.857651
172	Q9LK88	NADPH:quinone oxidoreductase [*A.thaliana*]	206.36	2.886371

173	Q94F62	BRASSINOSTEROID INSENSITIVE 1-associated receptor kinase [*A.thaliana*]	74.21	2.91538
174	F4I902	Disease resistance protein CHS1 [*A.thaliana*]	127.61	2.91538
175	Q58G47	Protein TIFY 6A [*A.thaliana*]	526.68	2.91538
176	B0LZR9	Ethylene-insensitive3 (Fragment) [*A.thaliana*]	133.84	2.974274
177	Q9C9B9	Inorganic pyrophosphatase TTM1 [*A.thaliana*]	121.75	3.004166
178	B0M007	Ethylene-insensitive3 (Fragment) [*A.thaliana*]	202.51	3.034358
179	B0M003	Ethylene-insensitive3 (Fragment) [*A.thaliana*]	119.98	3.095656
180	B0LZS2	Ethylene-insensitive3 (Fragment) [*A.thaliana*]	133.84	3.095656
181	Q570C8	3-ketoacyl-CoA thiolase 5, peroxisomal [*A.thaliana*]	115.71	3.095656
182	B0LZX3	Ethylene-insensitive3 (Fragment) [*A.thaliana*]	196.09	3.158193
183	Q9M345	L-type lectin-domain containing receptor kinase IV.2 [*A.thaliana*]	124.24	3.158193
184	B9DI69	MLO-like protein (Fragment)	157.99	3.189933
185	B0LZZ4	Ethylene-insensitive3 (Fragment)	119.98	3.320117
186	Q9FX54	Glyceraldehyde-3-phosphate dehydrogenase GAPC2, cytosolic [*A.thaliana*]	134.78	3.353485
187	F4KJ05	Spermidine synthase 3 [*A.thaliana*]	58.41	3.632786
188	Q9FGH9	Exocyst complex component	247.83	3.669296

		EXO70B1 [*A.thaliana*]		
189	Q2V3H5	Putative defensin-like protein 307 At4g17718 [*A.thaliana*]	329.03	3.935351
190	F4K365	Defense protein-like protein At5g48657 [*A.thaliana*]	127.62	3.935351
191	Q9SK71	At2g20310 [*A.thaliana*]	116.03	4.13712
192	P93002	Regulatory protein NPR1 [*A.thaliana*]	164.13	4.392946
193	B0LZY5	Ethylene-insensitive3 (Fragment) [*A.thaliana*]	178.26	4.392946
193	B2BDI8	Non-expressor of PR1 [*A.thaliana*]	161.65	4.392946
194	B2BDJ4	Non-expressor of PR1 [*A.thaliana*]	164.13	4.437096
195	A0A178WHX4	SAI1 At1g57770 [*A.thaliana*]	161.65	4.481689
196	B2BDK4	Non-expressor of PR1 [*A.thaliana*]	141.15	4.526731
197	B2BDI7	Non-expressor of PR1 [*A.thaliana*]	161.65	4.526731
198	B2BDK0	Non-expressor of PR1 [*A.thaliana*]	143.63	4.572225
199	B2BDI5	Non-expressor of PR1 [*A.thaliana*]	161.65	4.572225
200	A0A1P8B6C4	Ankyrin repeat family protein At4g03440 [*A.thaliana*]	173.15	4.618177
201	Q9ZNT0	Protein SUPPRESSOR OF K(+) TRANSPORT GROWTH DEFECT 1 [*A.thaliana*]	111.27	4.618177
200	B2BDI6	Non-expressor of PR1 [*A.thaliana*]	164.13	4.71147
201	Q8L9W4	Non-expressor of PR1 [*A.thaliana*]	164.13	4.758821
202	O82399	Malate dehydrogenase 1, peroxisomal [*A.thaliana*]	230.19	4.806648
203	Q9ZT72	Ankyrin repeat family protein At4g03440 [*A.thaliana*]	173.15	4.854956

204	B2BDI9	Non-expressor of PR1 [*A.thaliana*]	161.65	4.903749
205	A0A178WD46	Uncharacterized protein At1g02930 [*A.thaliana*]	95.81	5.002811
206	Q9SKB3	Poly(ADP-ribose) glycohydrolase 1 [*A.thaliana*]	145.85	5.002811
207	Q9SIV3	Transcription activator GLK1 [*A.thaliana*]	192.19	5.155169
208	Q9C996	GDSL esterase/lipase 6 [*A.thaliana*]	44.3	5.20698
209	O24658	Endochitinase At2g43590 At2g43590[*A.thaliana*]	79.96	5.584529
210	Q9SRX9	E3 ubiquitin-protein ligase BAH1 [*A.thaliana*]	34.27	5.754603
211	O49621	MLO-like protein 1 [*A.thaliana*]	211.39	6.233887
212	A0A1P8B3N1	Ankyrin repeat family protein At4g03490 [*A.thaliana*]	41.44	6.685894
213	A0A1P8B3L8	Ankyrin repeat family protein At4g03490 [*A.thaliana*]	41.44	6.753089
214	Q0PW40	Cysteine-rich receptor-like protein kinase 13 [*A.thaliana*]	317.96	6.753089
215	Q43316	Porphobilinogen deaminase, chloroplastic[*A.thaliana*]	136.3	6.958751
216	Q9FY94	Bidirectional sugar transporter SWEET15 [*A.thaliana*]	131.88	7.242743
217	Q94FY7	Tocopherol cyclase, chloroplastic[*A.thaliana*]	115.98	7.538325
218	O80341	Ethylene-responsive transcription factor 5 [*A.thaliana*]	10.49	7.767901
219	Q7G1L2	Ethylene-responsive transcription factor RAP2-6 [*A.thaliana*]	127.7	8.331137

220	Q9FG33	Probable L-type lectin-domain containing receptor kinase S.5 [*A.thaliana*]	26.12	8.499439
221	Q9FK63	Calmodulin-binding receptor kinase CaMRLK[*A.thaliana*]	60.92	9.679401
222	Q9C5Z6	Protein RESISTANCE TO POWDERY MILDEW 8.2 [*A.thaliana*]	184.08	10.8049
223	P93037	Uncharacterized protein PK9 (Fragment) [*A.thaliana*]	109.47	12.55351
224	Q02972	Cinnamyl alcohol dehydrogenase 8 [*A.thaliana*]	120.84	13.32977
225	A8MRP4	Thionin-like protein 2 OS=Arabidopsis thaliana At1g12663 [*A.thaliana*]	390.99	13.73572
226	Q9SZE2	Protein DETOXIFICATION 51 [*A.thaliana*]	107.95	14.15404
227	Q8LGB6	Non-functional pseudokinase ZED1 [*A.thaliana*]	117.64	14.29629
228	Q1KPV0	Probable transmembrane GTPase FZO-like, chloroplastic [*A.thaliana*]	102.61	20.08554
229	Q9FGH4	Glucan endo-1,3-beta-glucosidase 9 At5g58480 [*A.thaliana*]	37.01	21.5419
230	Q9C5K8	Protein TIFY 3B [*A.thaliana*]	207.19	22.42104
231	Q42529	Tryptophan synthase alpha chain, chloroplastic[*A.thaliana*]	129.99	31.18696
232	Q93Z08	Glucan endo-1,3-beta-glucosidase 6 At5g58090 [*A.thaliana*]	111.55	34.46692
233	Q9S732	HSP20-like chaperones superfamily protein OS=*Arabidopsis thaliana*	84.01	36.23407

4. **Discussion**

Till date, proteomic analysis has been useful to investigate the cellular proteome profile under environmental stress [301-303]. However, to study the difference in protein accumulation under altered GSH content condition is still inadequate. Here, a quantitative comparative proteomic profiling was performed using LC-MS/MS-QTOF to divulge that area of studies. The present work was demonstrated in *A. thaliana* viz. Col-0 vs. exogenously GSH-fed Col-0 samples under combined stress condition (to mimic the environmental stressed condition), which was further classified depending on various criteria. As mentioned in result section, under stress treated condition, proteins related to diverse cellular functions were noted differentially accumulated in Col-0 samples exogenously fed with GSH with respect to Col-0. This revealed that GSH affects various metabolic and physiological processes in plants. The present discussion focuses on the differentially accumulated proteins grouped on the basis of their cellular functions. The ratio of protein abundance (GSH-fed Col-0:Col-0) below 0.5 was considered down-accumulated and the ratio above 2 was considered up-accumulated under stress.

4.1. Changes in proteins related to stress

Since decades GSH is known to have critical roles in plant defense system and differential accumulation of stress-induced proteins under altered GSH content can be substantiated with previous reports in our laboratory [243,304] where proteins related to stress were identified as differentially accumulated following GSH over-expression in *Nicotiana tabacum* and *Mentha arvensis*. One of the most prominent redox-regulated proteins in plant defense responses is non-expresser of PR genes1 (NPR1) which was noted up-accumulated in Col-0 samples exogenously fed with GSH [70,243,244,250]. Plant carbonic anhydrase is also a stress-induced protein that was up-accumulated in Col-0 samples exogenously fed with GSH [305]. MPK cascade is one of the major pathways that modulate innate immune responses in both plants and animals [19]. MPK3 being one of the key regulator of MPK cascade was also up-accumulated under enhanced GSH condition which corroborated with previous reports [243,77]. Interestingly, results revealed proteins related to HSPs family were also up-accumulated under GSH-fed condition. HSPs are involved in protein folding under normal as well as stressed conditions. Besides, disease resistance protein RPH8A was also up-accumulated in Col-0 samples exogenously fed with GSH.

4.2. Changes in proteins related to signaling

Earlier studies have indicated that alterations at GSH level might be as significant as elevated ROS level in redox signaling pathways [262,70,66,112]. ARF-GTPase activating proteins (ARF-GAP) were analyzed as up-accumulated, in Col-0 samples exogenously fed with GSH. These proteins belong to ADP ribosylation factor (ARF) GAPs superfamily. AGD5, a member of the class-2 GAP sub-family, is known to regulate membrane trafficking events [306]. BAK1, a receptor kinase related to BR signaling pathway [307], is a major player in plant immunity system and it is also known to remain associated with FLS2 and other immune sensors [308-310]. BAK1 is also known as SOMATIC EMBRYOGENESIS RECEPTOR KINASE 3 (SERK3), belonging to a subfamily of LRR-RLKs with five members [311]. Interestingly, BAK1 was up-accumulated in GSH-fed Col-0 samples.

A serine/threonine protein phosphatise 2A (PP2A) is a holoenzyme having two catalytic subunits. One of the subunit being β subunit determines the substrate specificity. This PP2A B' was reported to negatively regulate BR signaling pathways [312]. PP2A's role in the regulation of vesicle trafficking in the context of plant development was also studied [313] and noted down-accumulated in Col-0 samples exogenously fed with GSH.

4.3. Changes in proteins related to protein degradation

In ubiquitin proteosome system (UPS), ubiquitin ligase E3 was noted up-accumulated under enhanced GSH condition which again substantiated the established role of GSH in plant defense. UPS was also reported to modulate plant hormone signaling [314]. UPS can be a mode to counter the adverse effect of oxidative stress to protect the cell against oxidative damage [315]. Reports indicate towards the role of E3 in modulating signal responses triggered by biotic stress factors [316], in addition to its role in plant stress responses [317]. A novel E3 ligase was identified in *Ralstonia solanacearum* that causes full virulence suppressing plant's innate immunity [318]. Apart from E3, aspartyl protease (APCB1) which is involved in proteolytic processing of BAG6 and plant basal immunity [319] which was up-accumulated in Col-0 samples exogenously fed with GSH.

4.4. Changes in proteins related to redox

GSH is the master antioxidant of the cell and is responsible for maintaining cellular redox homeostasis. Therefore, any perturbation in GSH content will certainly alter the level of proteins related to redox. Cytosolic TRX in plants is essential for NPR1 reduction through SA-mediated pathway [300]. TRX5 was identified as up-accumulated in Col-0 samples exogenously fed with GSH, which plays an important role in de-nitrosylating SNO-NPR1 thereby promoting its nuclear translocation [320] and tolerance during salt stress [321]. TRX-dependent redox signalling in plant immunity was also reported by Mata-Pérez and Spoel, 2019 [322]. The role of TRX in light-dependent activation of photosynthetic reactions was also reported [323]. Most recently, role of TRX system under nitrate stress was very well documented [324].

4.5. Changes in proteins related to RNA synthesis and processing

Aspartate-tRNA ligase also known as aspartate-tRNA synthetase (AspRS) is an enzyme that takes part in biosynthesis of aminoacyl-tRNA required for transcription and was up-accumulated in Col-0 samples exogenously fed with GSH. AspRS has a role to play in defense activity against pathogen attack [325].

Various pre-mRNA processing factors are required for splicing of mRNA [326], miRNA biogenesis [327], defense response to bacterium [328], cell responses DNA damage [329], and many more. In this study, pre-mRNA-processing factor 19 (PRP19B) was down-accumulated in Col-0 samples exogenously fed with GSH.

4.6. Changes in proteins related to protein synthesis

Ribosome recycling mediated by ribosome recycling factor (RRF) is a very important part of translation process [330]. RRF recycles ribosome through disassembly of the post-termination complex. These RRFs are known to play a significant role in chloroplast formation and embryogenesis [331]. Over-expression of RRF improved toyocamycin production in *Streptomyces diastatochromogenes* [332]. Besides, shallomin in *Allium hirtifolium* Boiss showed more promising binding affinity with RRF and considered as lead molecule for future drug discovery [333]. The chloroplastic RRF was down-accumulated in Col-0 samples exogenously fed with GSH.

4.7. Changes in proteins related to energy metabolism

Carbonic anhydrase (CA) facilitates the reversible hydration of CO_2. It is majorly found in photosynthetic microorganisms and higher plants. CA has functional role in different biological processes including pH regulation, CO_2 transfer, ion exchange, respiration, and photosynthetic C_3 cycle [334-336]. β-carbonic anhydrase 2 (BCA2) was noted up-accumulated in Col-0 samples exogenously fed with GSH. Malate dehydrogenase (MDH) is an enzyme involved in TCA cycle. Peroxisomal MDH is essential for maintaining optimal rates of photorespiration in air. Over-expression of MDH helps in mitigating aluminium stress [337]. A comparative proteomics of isoenzymes of MDH from highly enriched plasma membrane preparations of maize and soluble isoenzymes revealed some interesting data [338]. The role of NAD-dependent MDH in chloroplast development was also studied [339]. Additionally, the role of MDH in common bean under salt stress treatment was reported by Yıldız et al. 2021 [340]. Besides, MDH1 is also known to have a major role in β-oxidation [341]. MDH1 was up-accumulated in Col-0 samples exogenously fed with GSH.

The chloroplastidal ferredoxin NADP reductase (FNR) is the enzyme that facilitates the electron transfer from photosystem I to NADPH during photosynthesis. Over-expressing FNR was reported to mitigate oxidative stress [342]. Presently, FNR was down-accumulated in GSH-fed Col-0. (S)-2-hydroxy-acid oxidase GLO2, involved in photorespiration, was down-accumulated in Col-0 samples exogenously fed with GSH.

4.8. Changes in proteins related to carbohydrate metabolism

Sugar transport protein 4 (STP4) helps in uptake of sugar to root tips, anthers and to cells that remain sugar-deprived under environmental stress [343]. STP4 was up-accumulated in Col-0 samples exogenously fed with GSH. The peroxisomal β-glucosidase 26 (BGLU26) helps in hydrolysis of non-reducing β-D-glucosyl residues yielding β-D-glucose. Besides, during pathogen-triggered resistance, it is required for both defense-related glucosinolate activation and callose deposition [344]. Glucan endo-1,3-β-glucosidase 9 helps in hydrolysis of β-D-glucosidic linkages which was up-accumulated in GSH-fed Col-0 samples. Glyceraldehyde-3-phosphate dehydrogenase (GAPC2) is a key enzyme in glycolysis which helps in carbohydrate metabolism and maintaining the cellular level of ATP [345]. It also helps in regulating heat stress [346]. The activity of GAPC2 has been reported to be inhibited by GSSG, H_2O_2 and S-nitrosoglutathione

(GSNO) [347]. Moreno et al. 2021 [348], reported the inhibition of GAPC by a di-peptide Tyr-Asp that affected plant redox metabolism. GAPC2 was up-accumulated in GSH-fed Col-0 plants.

However, glucan endo-1,3-β-glucosidase 13 was down-accumulated. Additionally, the cytosolic glucose-6-phosphate isomerase (PGIC) involved in glycolysis was down-accumulated in Col-0 samples exogenously fed with GSH.

4.9. Changes in proteins related to calcium signaling

Plasma membrane-associated cation-binding protein 1 (PCAP1) interacts with phosphatidylinositol phosphates (PtdInsPs) and calmodulin (CaM). It helps in intracellular signaling which allow PtdInsPs to remain attached to the plasma membrane till Ca^{2+}-CaM reaches at an adequate concentration, thereby facilitating the release of PtdInsPs followed by induction of InsPs-mediated signaling pathway [349]. PCAP1's role in stomatal closure and flagellin-induced immunity were also reported by Nagata et al. 2016 [350] and Giovannoni et al. 2021 [351] respectively. PCAP1 was noted up-accumulated in Col-0 samples exogenously fed with GSH. Additionally, calmodulin-binding receptor kinase (CaMRLK) was up-accumulated in Col-0 samples exogenously fed with GSH.

Nevertheless, NTM1-like 9 (NTL9) is a transcriptional regulator stimulated by proteolytic cleavage via regulated intra-membrane proteolysis (RIP). NTL9 was also known to regulate leaf senescence [352]**.** NTL9 was down-accumulated in Col-0 samples exogenously fed with GSH.

4.10. Changes in proteins related to ET, ABA and SA signaling

Exocyst complex component (EXO70B1) is known to be a positive regulator in ABA-dependent stomatal closure [353,354]**.** The significance of EXO70B1 in defense signaling pathway under biotic stress is very well elucidated [355,356]. EXO70B1 was noted up-accumulated in Col-0 samples exogenously fed with GSH.

Histidine kinase (HK) acts upstream of MPK cascade which phosphorylates its downstream target to an aspartate residue in the receiver domain. It is also a negative regulator of ABA and ET signaling pathway that inhibits the root elongation. It induces stomatal movement via H_2O_2 homeostasis in guard cells. It is also needed for acquiring immunity to bacterial and necrotrophic fungul attack [357-360]. HK5 was down-accumulated in Col-0 samples

exogenously fed with GSH. Inorganic pyrophosphatase (TTM) exhibits pyrophosphatase activity and it is a negative regulator of the SA-dependent augmentation of defense responses upon pathogen attack viz. *H. arabidopsidis* and *P. syringae* [361]. In this study, TTM2 was down-accumulated in GSH-fed Col-0.

4.11. Changes in proteins related to secondary metabolites biosynthesis pathways

Spermidine synthase 3 (SPD) takes part in polyamine biosynthesis pathway [362] and also known to mitigate biotic stress upon pathogen attack [363]**.** SPDS3 was up-accumulated in Col-0 samples exogenously fed with GSH. Polyamine oxidase (PAO) is a flavoenzyme involved in polyamine back-conversion [364]. PAO was also reported to be involved in wound healing [365]. Over-expression of PAO3 was also reported to confer salt tolerance in cucumber [366]. PAO1 was up-accumulated in GSH-fed Col-0. They help in acclimatizing to low-temperature and phloem loading [367]. VTE1, catalyzing the second last step of tocopherol synthesisalso helps in regulation of defense response [368]. VTE1 was up-accumulated in Col-0 samples exogenously fed with GSH.

4.12. Changes in proteins related to detoxification pathways

NADPH:quinone oxidoreductase (NQR) reduces quinone. NQR along with hydroquinone has a major role to play in detoxification pathways. It was up-accumulated in Col-0 samples exogenously fed with GSH.

Alcohol dehydrogenase (ADH) plays a central role in formaldehyde detoxification [369]**.** It was down-accumulated in Col-0 samples exogenously fed with GSH.

4.13. Changes in proteins related to regulation of genes via TFs

Zinc finger protein 12 (ZAT12) is a transcriptional regulator which is known to regulate a group of gene that functions in response to photo-oxidative, cold and oxidative stress [370-372]**.** Ethylene insensitive 3 (EIN3) is a key transcriptional regulator in ET signaling [373,374] and salt stress [375,376]**.** It is also reported to promote root hair growth [377]**.** Repression of EIN3 leads to suppressed apical hook formation [378]**.** Moreover, an interesting interplay between BR and ET via BZR1 and EIN3 was very well elucidated [379]. Both ZAT12 and EIN3 were up-accumulated in Col-0 samples exogenously fed with GSH.

MYB108 helps in regulation of stamen maturation, anther dehiscence, and in mitigating drought stress in herbaceous peony [380-382]. GLABROUS1 enhancer-binding protein (GEBP) specifically recognizes the GL1 enhancer sequence. GeBP together with GeBP-like proteins (GPL) play a significant role in cytokinine regulatory pathway [383]. Most recently, the GEBP family was very well studied in gramineae crops [384]. MYB108 and GEBP were down-accumulated in Col-0 samples exogenously fed with GSH.

4.14. Changes in proteins related to other functions

Ankyrin repeat family protein helps in protein-protein interactions. It regulates plant potassium channel [385], immune response [386], anti-oxidant metabolism [387]. It helps in mitigating abiotic stress [388] and biotic [389-390]. Additionally, tryptophan synthase (TSA1) is required for tryptophan biosynthesis. All the above mentioned proteins were up-accumulated in Col-0 samples exogenously fed with GSH.

On the other hand, oxalate-CoA ligase (AAE3) is required for oxalate catabolism [391,392]. Inositol-3-phosphate synthase isozyme 2 (IPS2) is involved in myo-inositol synthesis [393]. Both the above mentioned proteins were down-accumulated in Col-0 samples exogenously fed with GSH.

Together, comparative proteomic analysis of stress treated *Arabidopsis* under altered GSH level was noted to influence various proteins which are stress-responsive, involved in different signaling pathways (detoxification, phyto-hormone, metabolite synthesis pathways etc.) which in turn influenced the differential accumulation of many proteins. It is also worth mentioning that various noteworthy defense-related proteins like NPR1, MPK3, carbonic anhydrase (CA), HSPs, ankyrin repeat family proteins etc. were up-accumulated in GSH-fed Col-0 sample (**Table 5**). Nonetheless, till date, there are very few reports elucidating GSH-MPK3 interplay under stress. Considering the importance of this in stress mitigation and/or management, further investigation has been undertaken to obtain in depth insight into the GSH-MPK3 interplay and discussed in the next chapter.

CHAPTER 2

Chapter 2: Glutathione modulates MPK3 expression via transcription factor WRKY40 under combine osmotic and cold stress in *Arabidopsis thaliana*

1. Introduction

1.1. Mitogen-activated signaling cascade in plants

Signaling pathways in plants which are induced as a result of environmental stresses are very well established as well as complicated. The main reason behind such complication is its sessile nature that makes plants exposed to stress factors viz. biotic or abiotic. All such signaling pathways comprises of a diverse range of responses. Protein kinases have a pivotal role to play under such circumstances. Mitogen-activated protein kinase (MPK) pathway takes a central position in the whole plant defense machinery system in plants [394,395]. The cascade is comprised of kinase proteins of various types that help in transducing multiple external signals from extracellular area to intracellular region in plants. The external signal includes environmental stress factors viz. pathogen attack, temperature stress, water stress, radiation, heavy metal toxicity, photo-oxidative stress etc., developmental stimuli like cell division, differentiation and many more. Phosphorylation is one of the key features that keep the continuity of this pathway. The cascade is modulated by many other mechanisms which include modulation both at transcriptional and translational level as well as modulation at post-transcriptional level such as protein to protein interaction. The elaborate study of some particular MPK signaling pathways have demonstrated the specificity of the kinases in the pathways, signal transduction patterns, target identity and the complexity of the cascade.

Through phosphorylation relay mechanism, this cascade is minimally composed of MPKKKs (MPK kinase kinases), MPKKs (MPK kinases) and MPKs that link upstream receptors to downstream targets (**Fig. 1**). MPKKs phosphorylate the tyrosine and threonine residues of MPKs in the TXY motifs, subsequently the MPKKKs phosphorylate the serine-serine or threonine residues of MPKKs in the SXXXS/T motif. Many numbers of MPKs have been identified in plants and reports show that in presence of stress the kinase activity of MPK cascade proteins and transcript abundance of various *MPK* genes get increased (**Fig. 1**). The *Arabidopsis* genome contains about 110 genes coding for putative MPK pathway components: 20 MPKs, 10 MPKKs and more than 80 MPKKKs [396].

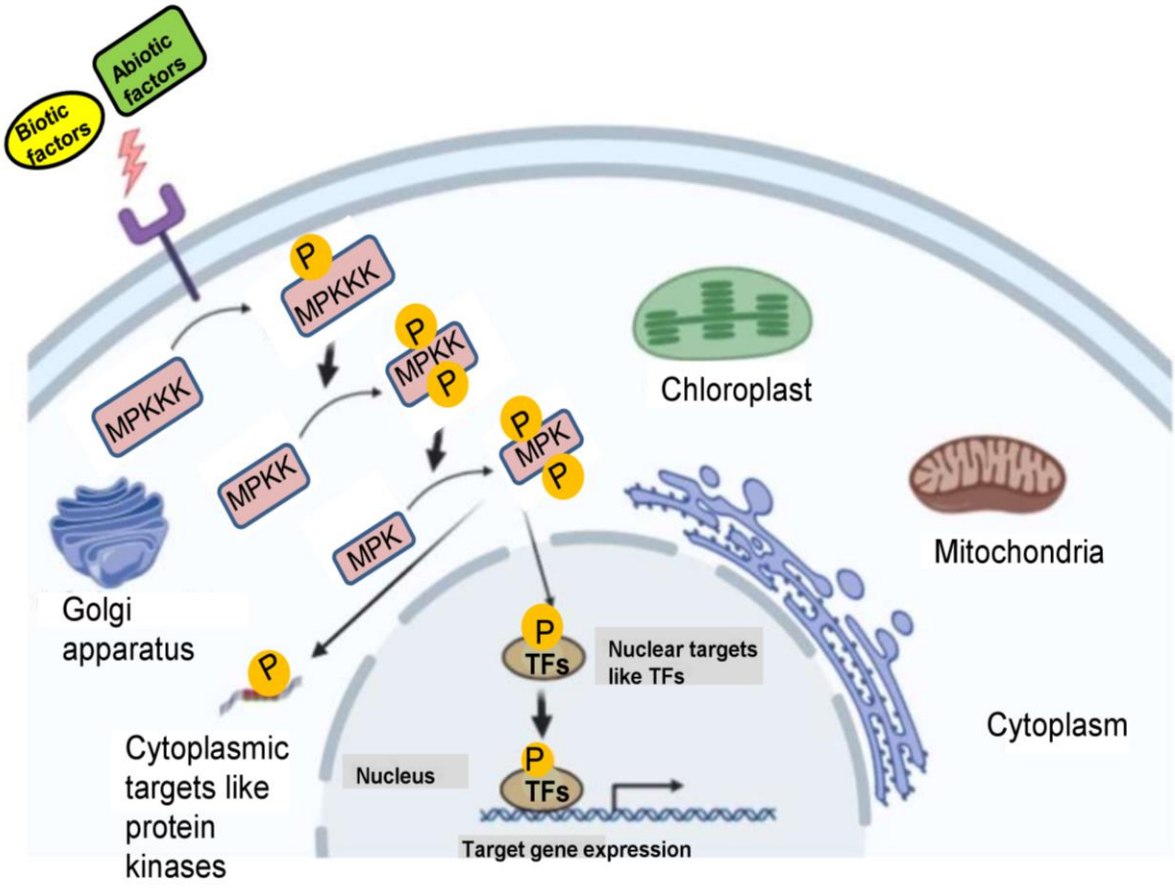

Fig. 1. MPK phosphorylation relay taking place under environmental stress

Based on phylogeny, plant MPKs are grouped into four classes viz. group A to D [396] and they have a conserved TXY consensus sequence in their activation site. Among them group A, B, and C possess the CD domain ([LH][LHY]DXX[DE]XX[DE]EPXC) in the C-terminal end , which is the docking site for their respective substrates and phosphatases [397]. The best-characterized MPKs in *Arabidopsis* are AtMPK3, AtMPK4 and AtMPK6 [398] while, salicylic acid-induced protein kinase (SIPK) and wounding-induced protein kinase (WIPK) in tobacco [399-401] and salt stress-induced MPK (SIMK) and stress-activated MPK (SAMK) in alfalfa [402,403]. Some phylogenetic studies have revealed that SIPK, AtMPK6, and SIMK are orthologs, whereas WIPK, AtMPK3, and SAMK are orthologs [404-406]. Various MPKKKs, MPKKs and MPKs identified in various plant species has been listed by **Nakagami et al.** in the year **2005** [407] as shown in **Fig. 2**.

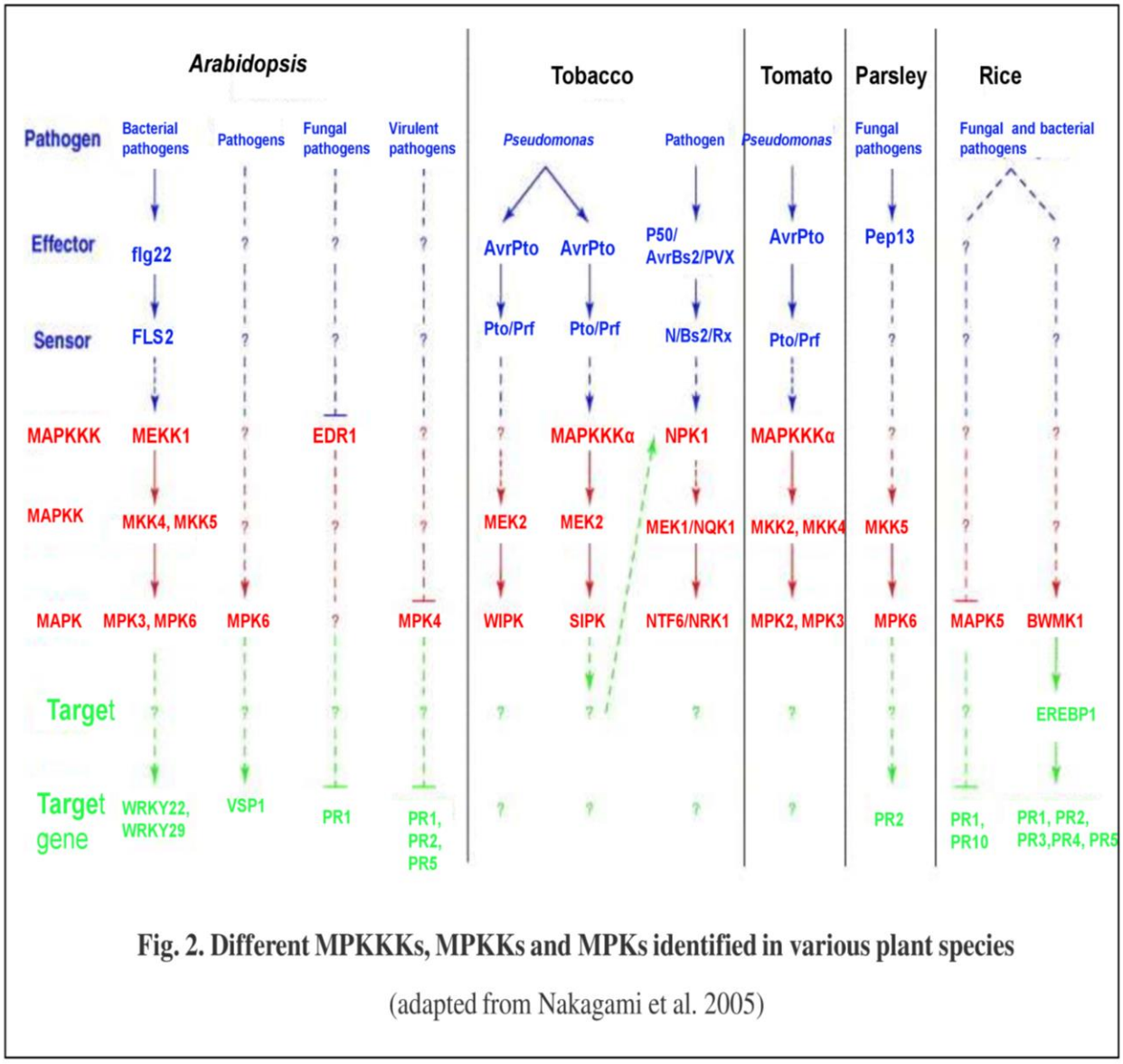

Fig. 2. Different MPKKKs, MPKKs and MPKs identified in various plant species

(adapted from Nakagami et al. 2005)

The role of MPK pathway is very well established in response to environmental stress in plants. Reports have documented MPKs beings activated upon exposure to heavy metals in higher plants [408]. MPK3 and MPK6 are activated due to Cd toxicity thereby leading to increased production of ROS in *A. thaliana* [409]. MPK4 as well as MPK6 are activated by chilling, salinity and drought stress [410]. Likewise, Kiegerl et al. 2000 [411] demonstrated alfalfa SIMKK-SIMK and tobacco NtMEK2 (MP2K)-SIPK/WIPK to play a major function during osmotic stress. Furthermore, **Takahashi et al. 2011** [412] studied the probable function of *Arabidopsis* MKK3 in maintaining ROS homeostasis. MEKK1 was also reported to negatively

control and activate MEKK2, thereby inducing the R protein SUMM2- mediated immune responses [413]. Furthermore, activated form of MPK4 was reportedly responsible to elevate the levels of *MEKK2* transcript that in turn triggered defense responses [414]. Some novel MPK, MPKK and MPKKK gene families were identified in cucumber during stress treatment [415]. Nonetheless, an early report demonstrated that the *mpkkk5* mutant exhibited increased flg22-induced MPK3-MPK6 activation but decreased chitin-induced MPK3-MPK6 activation [416]. Rice *MPKKK18* and *MPKKK24* were noted to function upstream of the MKK4-MPK3-MPK6 cascade in chitin signaling [417,418]. Lately, two different studies revealed that MPK3-MPK6 activation is induced by different types of elicitors which were greatly reduced in *mpkkk3-mpkkk5* double mutants [419,420]. In soybean, the MPK gene family was observed to function as a cohort during the defense response to *Heterodera glycines* [421].

MPK signaling cascade is not a simple linear cascade, but involves complicated cross-talks with other signaling pathways. MPK9 and MPK12 were observed to positively modulate ABA signaling in guard cells, and function upstream of ABA-mediated anion channel activation and downstream of ROS signaling pathway [422]. Biochemical studies have shown that MPK6 function downstream of MKK3, which pointed towards the JA signaling pathway via MKK3/MPK6 cascade [423]. MKK9 is mostly known to have a critical role in ET signaling because MPK3 and MPK6 (which function downstream of MKK9) control the genes related to ET biosynthetic pathway [424]. Earlier reports demonstrated that transient over-expression of the phospho-mimic mutant forms of MKK4/MKK5 (which function upstream of MPK3/MPK6) viz. $MKK4^{DD}$/$MKK5^{DD}$, induced transcription of *PAD2* and *PAD3* which are genes involved in GSH biosynthesis pathway in *A. thaliana* [425]. In *Nicotiana tabacum*, MPK and SA signaling may function separately, however both are reportedly being regulated by GSH redox potential [215]. HGLs, a transgenic line over-expressing high GSH content, revealed an activation of WIPK and SIPK. Additionally, SIPK and WIPK activation was also noted in wild-type tobacco when fed with exogenous GSH/GSSG [215]. Ghanta et al. 2011a [243], also reported that in *Nicotiana tabacum* transgenic line exhibiting high GSH content (*NtGB*) and GSH-fed BY2 cell lines, up-regulation of *NtMPKK* gene was observed along with other stress-related gene like *NtNPR1, NtPR1, NtPR4, NtGLS* etc. The microarray analysis in GSH-fed Col-0 seedling confirmed the up-regulation of *MPKKK19* with respect to Col-0 [77]. Together, in this present study we found out that GSH-mediated regulation of MPK3 in *A. thaliana*.

1.2. Transgenic plants

Over many decades, transgenic plants are gaining importance for applied and basic research. Advanced technologies allowing stable integration of foreign DNA in plant system, termed as 'transgenic plants', have overcome several issues related to improvement of crops. The advantages of using transgenic plants are better yield, improved quality and introduction to stress-resistant varieties. The first genetically engineered crop for commercial production was the FlavrSavr tomato (United States, 1994). Various methods have been developed and employed for generating transgenic plants. 'Direct gene transfer' methods gained popularity especially with the monocotyledonous plants. Apart from these, some transformation methods are based on utilizing *Agrobacterium* sp. (*Agrobacterium tumefaciens* and *Agrobacterium rhizogenes*), a pathogen capable of infecting dicot plants and transferring genes into the plant genome. The *Agrobacterium*-mediated transformation method has many advantages over direct gene transfer methods. It is relatively less cumbersome with minimal equipment costs, results in a single copy insertion or low copy number of transgene, leads to stable integration and so on.

1.3. Agrobacterium tumefaciens: a powerful tool useful for plant transformation

Agrobacterium tumefaciens is a bacterium found in soil and it is much popular among plant biologists as well as biotechnologists. It causes 'crown gall' disease in plants. The chance of crown gall (tumourous growth) formation depends on the potentiality of A. *tumefaciens* to transfer its genes into the plant system, an astonishing feature of inter-kingdom gene transfer. Crown gall formation takes places due to the partial transfer of a plasmid present in *A. tumefaciens* genome known as the 'Ti (tumour-inducing) plasmid'. Exploiting this feature, plant biologists have developed methods to transfer the genes of their interest into the plant genome.

2. Materials and Methods

2.1. Plant samples used and growth conditions maintained for A. thaliana and Lycopersicon esculentum seedling, GSH/GSSG feeding

All *Arabidopsis* seeds were procured from NASC. Col-0 (NASC ID: N1092; ABRC stock number: CS1092) used as wild-type, *Arabidopsis* mutants named *pad2.1* (N3804) which has a mutated γ-*ECS* gene and have only 22 % of the Col-0 GSH content [198] and *mpk3* (SALK_151594) null mutant [426]. *L. esculentum* wild-type seeds were purchased from the local market. The specimen was identified by Botanical Survey of India (BSI, Shibpur, West Bengal) and deposited to the Central National Herbarium, BSI with the specimen number Le101 (vide. CNH/22/2011/Tech.II/412 dt. 21.03.2011). All seeds were surface sterilized according to standard protocol. The seeds were allowed to imbibe overnight in sterile milliQ water (smw) and washed thrice with smw under aseptic conditions. The seeds were then incubated in 1 % sodium hypochlorite and 5 µL of Tween-20 for 30 minutes with shaking. Again, the washing steps were repeated thrice. The seeds were then rinsed with 70 % ethanol for 30 seconds and the washing steps were repeated for three times. The seeds were then transferred to MS media [292] for germination and maintained under *in vitro* conditions at 22±1°C having 16 hours of 150 µE m^{-2} sec^{-1} light and 8 hours dark cycles [293].

GSH feeding is performed according to the protocol mentioned in **Chapter I** under **Materials & Methods** section. The protocol of GSSG feeding is complementary to GSH feeding in which three week old seedlings of Col-0 were transferred to MS medium containing 100 µM GSSG, which was maintained under same growth condition for 72 hours.

2.2. Combined (osmotic+cold) abiotic stress treatment

The protocol of combined (osmotic+cold) abiotic stress treatment is similar to that described in **Chapter I** under **Materials & Methods** section.

2.3. BSO, DTT, ST treatments to A. thaliana seedlings

All feeding experiments were done by placing the seedlings (three week old) in half strength MS medium containing 1 % sucrose and the corresponding chemical in the desired concentration.

Buthionine sulphoximine (BSO) inhibits the action of the first enzyme in GSH biosynthetic pathway thereby resulting in marked reduction in GSH content in *Arabidopsis* [427]. For BSO treatment, 1 mM BSO solution was used to treat all the seedlings for 72 hours [214]. Dithiothreitol (DTT) forms reducing environment in plants [428]. *A. thaliana* seedlings were treated with 5 mM DTT solution [214]. Staurosporine (ST) is also known to be general protein kinase inhibitor [429]. ST treatment was performed with 50 μM of it for 3 hours [430].

2.4. RNA extraction, quantitative RT-PCR analysis

Arabidopsis leaves was used for total RNA extraction by TRIzol@ method (Invitrogen) as described in **Chapter I** under **Materials & Methods** section. cDNA had been prepared from 1 μg RNA sample utilizing the RevertAidHMinus cDNA synthesis kit (ThermoScientific) as standardized before [214]. The protocol of which is similar to that described in **Chapter I** under **Materials & Methods** section.

All qRT-PCR analysis were performed using the FastStart DNA SYBR Green Master Mix (Roche Applied Science, USA) and a set of two qPCR primers (forward and reverse) specific for the target region were used in the Light Cycler 96 System (Roche Applied Science). The synthesized cDNA was diluted 1:100 times with sterile molecular biology grade nuclease free water. The reaction mixture is listed in **Table 1**. The instrument setup and amplification cycles of qRT-PCR analysis are given in **Table 2**. The list of primer pairs along with their sequences have been presented in **Table 3**. Primers were procured from Eurofins Genomics India Pvt. Ltd. (India). The *tubulin* expression was used for the normalization of gene expression analysis by the comparative Ct method. Single plant for each sample was used from the three separate batches and their RNA was pooled for extraction.

Table 1: Components to prepare the reaction mixture for qRT-PCR analysis

Components	Volumes (µL)
2 X SYBR Green Master Mix	10
10 µM Forward Primer	1
10 µM Reverse Primer	1
Water	7
Template DNA	1

Table 2: The instrument setup and amplification cycles of qRT-PCR analysis

Temperature (°C)	Ramp (°C/s)	Duration (s)	Acquisition mode
Pre-incubation			
95	4.4	600	None
3-Step amplification (No. of cycles 45)			
95	4.4	10	None
55	2.2	10	None
72	4.4	10	Single
Melting			
95	4.4	10	None
65	2.2	60	None
97	0.1	1	5 Readings/°C

Table 3: List of primer sequences

Gene	Forward primer (5'- 3')	Reverse primer (5'- 3')
LeMPK3(CDS cloning)	ACTCTAGAGCATGGTTGATGC TAATATGGGTGC	AGCGAGCTCGCGTTAAGCATAT TCAGGATTCAACGCC
nptII	GAGGCTATTCGGCTATGACTG	ATCGGGAGGGGCGATACCGTA
MPK3 (promoter cloning)	AGCTCTAGAGCTCTTAAAAAT CATAATTGAATAGTATCT3	TCGCCATGGTCGTTCTCTCTCAA TTGATCAAAGTCGAGATTC
AtPR1	CCGTGAACATGTGGGTTAG	CTCACTGACTTTCTCCAAACA
AtHSP70	CTGTTCAAGCGGATAAG	AGGAGAACCAAGGAAAG
AtHSP18.2	TGATGTGGCAGCGTTTAC	AACCTTGACTTCTTCCTTCTTC
AtMPKKK19	GTCGGAACAAGGAAGAGATT	CGGTTACAAATGGATGGTTTAG
AtMKK1	AGAGATGGGAGCTAGGTTTAT	TCCTTGACAGCAAAGAAGTC
AtMKK2	TGGCGCAATCTCACTAATC	ATAACGGTACTCACACCAAAG
AtMPK1	CCATCTTCGACATGAGA	GCAACTGGAACAAGAAG
AtMPK2	CCAAATACGTGCCTATC	CCCTAAGAGTCCTCAAC
AtMPK3	GTTCCACCACCACTAAGAAG	CGAAGTAGCTGGTACAAGAAG
AtMPK4	GAAAGTATGTTCCTCCTCTTC	GCATCGAGATTTGAAACCTAG
AtMPK6	CGGTGGTTCAGGTCAACCGG	AATTTTCTTAATCGCAACGCTCT C
Aty-ECS	TTTGGGTTTGAGCAGTATGT	ACCTCTCATCTCCAAGTATCT
MPK3; pair 1	GGCCAAACGTAGAGAACGAG	GTGGGAGTTGCCTGACGTAT
MPK3; pair 2	TGGGTGCTGCTCAATTTC	CACGTCCAATAGGCATGATAG
GUS	GTAGAAACCCCAACCCGTGA	AGTCTGCCAGTTCAGTTCGTT
AtWRKY75	AATGGGTCGTTGTATGCTCC	GACGGCCTTTTGGCCATATT3
AtWRKY18	AAGGAGGTCTCAGTTTTGGC3	CTGAGTCCAATAGGAAAGCC3
AtWRKY3	TTTTTTAGCGGTGGCGTTGG	CAAAGAAGCTCGGAGAATCC3
AtWRKY40	ATCAAATCAGCCCTCCCAAG	TGACAGAACAGCTTGGAGCA3
AtZAT6	CTCTTCCTACTCCGATCTACA A	GGTGGCGAACGATTTATGA
AtERF6	ATTACAGAGGAGTGAGGATG A	GTCTCTCTTCCGTTTGTTGT
AtMYB44	CGTGAAGAATCACTGGAACT	AGCTCAACGGAAGGTAATATC
AtTUBULIN	AGTCTAAGCTTGGTTTTACCA	GTCTGGAACTCAGTGATATC
AtMPK3 (ChIP)	AACCATCGTAAACCACACATG	ATGAGTTTTCGCGGTAATTGC

2.5. Protein isolation, Estimation, Immunoblotting

2 g of leaf tissues were grounded in 50 mM potassium phosphate solution (pH 7.8) mixed with 15 % Triton X-100. The protocol followed for protein isolation is same as mention in **chapter 1** under **Materials & Methods** section.

For measuring protein concentration, BSA was used as a standard [431]. The protein samples (2 µL) were mixed with 100 µL of Bradford reagent and kept at 37˚C for 10 minutes with mild shaking. Absorbance was noted at 595 nm in the Synergy H1 Hybrid reader and protein concentration was estimated using the standard curve for known concentrations of BSA (0.25 mg mL^{-1}–2 mg mL^{-1}).

30 µg of protein were prepared and 5 X loading dye (composition is mentioned in **Table 4**) was mixed to every protein samples to make a final concentration of 1 X. Resolving and stacking gels were prepared according to **Table 5** and **Table 6**.

Table 4: Composition of 5 X loading dye

Components	Concentration
Tris-HCl (pH 6.8)	250 mM
SDS	10 %
Glycerol	50 %
Bromophenol blue	0.1 %
β-mercaptoethanol	10 %

Table 5: Composition of various concentrations of resolving gel

Components	**Resolving gel**	
	8 %	**10 %**
1.5 M Tris-HCl buffer (pH 8.8)	2.5 mL	2.5 mL
40 % Acrylamide	2.0 mL	2.5 mL
Double distilled water	5.5 mL	5 mL
10 % SDS	100 µL	100 µL
10 % Ammonium persulfate	50 µL	50 µL
N,N,N,N-Tetramethylethylenediamine (TEMED)	10 µL	10 µL

Table 6: Composition of various concentrations of stacking gel

Components	**Stacking gel (8 %)**
0.5 M Tris-HCl buffer (pH 6.8)	2.5 mL
40 % Acrylamide	1 mL
Double distilled water	6.5 mL
10 % SDS	100 µL
10 % Ammonium persulfate	100 µL
N,N,N,N-Tetramethylethylenediamine (TEMED)	20 µl

Protein gel running buffer (composition is mentioned in **Table 7)** was prepared and an equal amount of samples were loaded. The gel was run at 90 V.

Table 7: Composition of protein gel running buffer

Components	Concentration
Tris Base	25 mM
Glycine	192 mM
SDS	3.5 mM

A Bio-Rad wet transfer system was used for transfer in a Mini Ve transfer apparatus using Millipore PVDF membrane (IPVH000-10). The membrane had a pore size of 0.45 μm, hydrophobic in nature, and activated using methanol. The transfer was done in a 1 X transfer buffer (composition is mentioned in **Table 8**) at 90 V.

Table 8: Composition of transfer buffer

Components	Concentration
Tris Base	25 mM
Glycine	192 mM
Methanol	20 %

Next, blocking of PVDF membrane was performed using 5 % skimmed milk in TBST for 1 hour [214]. The membrane was then washed with TBST (composition is mentioned in **Table 9**) thrice for 5 minutes each and then the membrane was incubated with respective primary (1^o) antibodies (list of which is presented in **Table 10**) at 4˚C overnight. Next day, the membrane was again washed with TBST and it was incubated with secondary (2^o) antibody (details listed in **Table 10**) at room temperature (RT) for 1 hour. Protein bands were identified with the help of Super Signal West Pico chemiluminescent substrate (Thermo Scientific, USA) followed by exposure to X-ray film (Carestream XBT, USA).

Table 9: Composition of TBST

Components	Concentration
Tris Base	50 mM
NaCl	150 mM
Tween20 (pH-7.4)	0.1 %

Table 10: Details of antibodies used

Type	Name	Manufacturer	Species raised in
Primary	MPK3	Sigma, USA	Rabbit
Primary	γ-ECS	Agrisera, Sweden	Rabbit
Primary	WRKY40	Ab-mart, China	Rabbit
Primary	Tubulin α chain	Agrisera, Sweden	Rabbit
Secondary	Anti-rabbit, HRP conjugated	Agrisera, Sweden	Goat

2.6. Estimating total GSH content, GSH:GSSG ratio

Arabidopsis leaves were used for GSH extraction [296]. GSH content was measured by HPLC that had been standardized before [214] following the protocol described in **Chapter I** under **Materials & Methods** section.

GSH:GSSG ratio was also determined following the protocol mentioned in **Chapter I** under **Materials & Methods** section.

2.7. Cloning of LeMPK3 and raising of over-expression line (viz. AtMPK3 line) in Arabidopsis

2.7.1. **Cloning of *MPK3* gene into *pGEMT-Easy* vector system**

RNA was isolated from *L. esculentum* seedlings and cDNA was prepared from 1 µg RNA following the protocol mentioned above. Gene specific forward and reverse primers were

designed to amplify the full coding sequence (cds) of *LeMPK3* (Gene ID: 823706) having a length of 1122 bp with *XbaI/SacI* recognition sites at the 5' ends of each of the primers. The forward primer bearing a sequence 5'ACTCTAGAGCATGGTTGATGCTAATATGGGTGC3' and reverse primer 5'AGCGAGCTCGCGTTAAGCATATTCAGGATTCAACGCC3' (**Table 3**). The PCR product of *LeMPK3* was cloned inside *pGEM-T Easy* vector (Promega, USA) according to manufacturer's instruction [243]. Next step was to run the PCR product on 1 % agarose gel followed by its gel extraction with the help of QIAquick gel extraction kit (Qiagen, Germany) as per manufacturer's instruction. The PCR program used is as follows:-

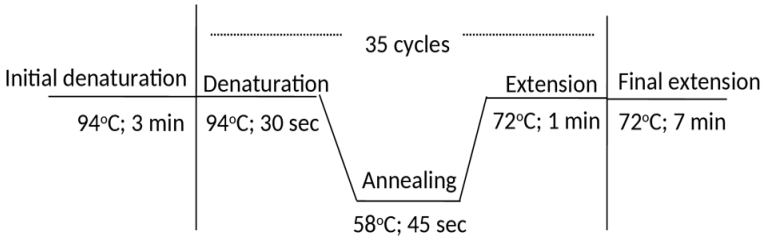

Ligation of the PCR purified product with *pGEMT-Easy* vector was carried out and transformed into chemically competent DH5α strain of *Escherichia coli*. Chemically competent cells were prepared and bacterial transformation was performed following standard protocols [295]. The transformed cells were selected on the basis of blue/white selection in presence of ampicillin. Plasmid was isolated from the overnight grown cultures of white colonies. The positive clones were confirmed by digestion with *EcoRI* and PCR amplification with the primer pair mentioned above (**Table 3**). The accuracy of the sequence cloned was checked by sequencing with M13 forward primer (Eurofins Genomics India Pvt. Ltd.).

2.7.2. Sub-cloning of *MPK3* gene into *pBI121* vector system

The positive clones of *LeMPK3* cDNA were next sub-cloned inside *pBI121* plasmid situated upstream of *CaMV35S* promoter [214]. For that, both the *LeMPK3-pGEMT-Easy* clones and the *pBI121* vector were digested with the corresponding restriction enzymes (*XbaI* and *SacI*) at 37°C for 1 and ½ hour following manufacturer's instruction. The digested DNA products (vector and insert) were then gel purified as mentioned above and quantified. Ligation of the digested insert and the vector were carried out at 4°C for 18 hours using T4 DNA ligase (Promega, USA)

according to manufacturer's guidelines subsequently followed by transformation of the ligated product into *E. coli* DH5α competent strain as described above. The selection of putatively transformed bacterial colonies was performed on LB plates in presence of kanamycin. The positive clones were selected by *XbaI/SacI* digestion and PCR amplification. The directional cloning of the gene of interest was confirmed by sequencing (Eurofins Genomics India Pvt. Ltd.). The resulting construct *pCaMV35S:LeMPK3* was maintained as glycerol stock at -80°C. All cloning and molecular biology protocols were performed according to Sambrook and Russell, 2001 [295].

2.7.3. Transformation of *A. tumefaciens* for floral dip

In the present study, *A. tumefaciens* GV3101 strain had been used. The strain was maintained in LB medium in presence of rifampicin (100 μg mL^{-1}) at 30°C overnight under shaking condition. For preparing competent cells, overnight grown cells of 5 mL culture (OD-0.6) were pelleted down (5,000 rpm; 5 minutes; 4°C), which were dissolved using 1 mL chilled 0.15 M NaCl solution. Next, to the centrifuged cells (5,000 rpm; 5 minutes; 4°C), 100 μL of chilled 20 mM $CaCl_2$ solution was added to re-suspend the cells again and stored at 4°C overnight. For each set of transformation, 2 sets of competent cells (200 μL) were pooled in a microfuge tube. 1 μg of the *pCaMV35S:LeMPK3* construct was mixed to it and incubated on ice for 30 minutes. The tube was then frozen in liquid N_2 for 1 minute and immediately shifted to a water bath (37°C) for 10 minutes. Fresh LB medium was then aseptically mixed to it and allowed to grow for additional 2–4 hours. After incubation, the bacterial culture was pelleted (5,000 rpm; 5 minutes) and dissolved in 100 μL of fresh LB medium and plated on solid LB medium having kanamycin (100 μg mL^{-1}). The plate was incubated at 30°C for 48 hours.

2.7.4. Selection of putatively transformed *A. tumefaciens* colonies

Several colonies from the transformed plate were selected and cultured overnight in 5 mL LB medium under conditions mentioned. From this overnight grown culture, plasmid DNA (*pCaMV35S:LeMPK3* construct) was isolated using standard protocol. Briefly, the cells were pelleted (10,000 rpm; 1 minute) and dissolved in 187.5 μL of GETL (40 μL lysozyme + 1 mM of Solution I; Solution I:50 mM glucose, 25 mM Tris-base, 10 mM EDTA) followed by incubation

at RT for 5 minutes. 375 µL of solution II (1 % SDS, 10 N NaOH) was added to it, mixed by inverting and placed on ice (5 minutes). To it, 312 µL of 3 M potassium acetate was added and kept on ice (10 minutes) with occasional mixing. After spinning the mixture (13,000 rpm; 10 minutes), to the supernatant, 2.5 µL of RNaseA added to it. It was then incubated at RT for 20 minutes. Up next, equal portion of phenol:chloroform:isoamyl alcohol (25:24:1) was added. After few minutes of incubation, the cells were spinned down (13,000 rpm; 5 minutes), and upper aqueous layer was separated. The previous step of adding phenol:chloroform:isoamyl alcohol was repeated once again to remove excess phenol. The mixture was spinned again and upper aqueous layer was separated. An equal amount of isopropanol was added and then it was incubated at -20°C (30 minutes). The mixture was again spinned down and 70 % ethanol was added to the pellet for washing. Next, it was air-dried and dissolved in 20 µL of sterile milliQ water.

For confirming whether the construct has been transformed into the *A. tumefaciens* strain, PCR analysis was performed. The isolated plasmid DNA was used as template for PCR analysis using gene-specific primers for *MPK3* gene mentioned in **Table 3**.

2.7.5. *Arabidopsis* transformation by floral dip method

Col-0 plants transformation with *pCaMV35S:LeMPK3* construct was carried out following the standard floral dip method [432]. The overnight grown cells of transformed *A. tumefaciens* were spinned down (4,000 × g; 10 minutes) and re-suspended in equal volume of half strength MS medium (supplemented with 5 % sucrose + 0.02 % Silwet L-77). The inflorescence of the plant was dipped in this cell suspension for 10 seconds with gentle agitation. The excess liquid was drained for 3 to 5 seconds and the plant was covered in a plastic bag and kept in horizontal position for 18 hours in dark at 21°C. After 18 hours, the plant was taken out from the plastic bag and maintained in growth chamber at 21±1°C under long day condition till seed set. Two separate homozygous transgenic lines (*AtMPK3-1, AtMPK3-15*) were produced. The seeds of both the *AtMPK3* lines were sown and collected. From T1 plantlets, seeds of T2 generation were set. The transgenic lines were selected and maintained in growth chambers with conditions similar to that used for growing Col-0 plants.

2.7.6. Antibiotic screening of the primary transformants (T_1)

The T1 seeds were screened by germinating them on MS medium in presence of kanamycin (100 μg mL^{-1}). The seeds were surface sterilized using standard protocol mentioned earlier. Next, the seeds were spread on petri-plates containing MS medium with 100 μg mL^{-1} kanamycin. After germination, seedlings were sub-cultured on the same medium every 3 days. Only the seedlings that remained green and healthy for 15 days on antibiotic plates were transferred to MS medium without antibiotic and maintained there for 15 days. Then the plants were transferred to autoclaved soil with a top layer of soil-rite and shifted to growth chambers (21±1 °C, 75 % RH) under short day conditions for vegetative growth. Further, genomic DNA PCR for the *nptII* gene of the transgenic lines was also carried out using forward primer (5'GAGGCTATTCGGCTATGACTG3') and reverse primer (5'ATCGGGAGGGGCGATACCGTA3') as mentioned in **Table 3**. To initiate bolting, plants were transferred to long day condition and maintained till seed set. Independent transgenic lines were maintained upto T_2 generation.

2.7.7. Genomic DNA isolation from leaves and validation of transgenic *AtMPK3* lines

The protocol followed for genomic DNA isolation from leaves is the standard CTAB (cetyl trimethyl aminobromide) method [295]. Firstly, 100-500 mg of tissue was grounded in liquid N_2 and the powder was transferred to 10 mL tube. Next, 1 mL freshly prepared CTAB extraction buffer (composition is mentioned in **Table 11**) was added to it and mixed very well. Next, the tube was placed in a shaking water bath (60°C; 1 hour). To the slurry, equal amount of chloroform and isoamyl alcohol (24:1) mixture was added and incubated (RT; 15 minutes) under shaking condition. The mixture was spinned down (8,000 rpm; 10 minutes). To the collected upper aqueous phase, 5 M NaCl solution (500 μL) was mixed. To it, 0.6 volume of isopropanol was added and the mixture was again stored at RT for an hour (or overnight). DNA was pelleted (10,000 rpm; 10 minutes), rinsed with 80 % ethanol, air-dried and then re-dissolved in 0.5 mL of TE buffer (composition is mentioned in **Table 12**). Next, RNase A (5 μL) was mixed, followed by its incubation for 30 minutes in water bath (37°C). After incubation, equal proportion of chloroform and isoamyl alcohol (24:1) was added and then the mixture was pelleted down centrifuged (8,000 rpm; 10 minutes). Ice-cold absolute ethanol was added to the upper aqueous

phase, after which it was spinned down (10,000 rpm; 10 minutes). DNA pellet was rinsed with 80 % ethanol, air-dried, mixed with 20 µL of sterile milliQ water and stored at -20°C. Genomic DNA was run using 1 % agarose gel (protocol of gel preparation mentioned in **Chapter I** under **Materials & Methods** section**)**.

Over-expression was validated in both the transgenic lines viz. *AtMPK3-1* and *AtMPK3-15* by MPK3 gene amplification from genomic DNA. PCR of *nptII* and *Le-MPK3* gene were done to select the putative transgenic lines. Over-expression of MPK3 was analyzed at gene and protein level. Protocols followed were similar to that described above.

Table 11: Composition of CTAB extraction buffer

Components	**Concentration**
Tris HCl (pH 8.0)	100 mM
EDTA	25 mM
NaCl	1.5 M
CTAB	2.5 %
β-mercaptoethanol	0.2 %
Polyvinylpyrrolidone	1 %

Table 12: Composition of TE buffer

Components	**Concentration**
Tris HCl (pH 8.0)	10 mM
EDTA	1 mM
NaCl	1 M

2.8. Promoter activity by GUS staining

MPK3 promoter (672 bp of intergenic region upstream of the TSS) was PCR amplified from Col-0 genomic DNA with *XbaI/NcoI* recognition sites. The forward primer bearing a sequence of 5'AGCTCTAGAGCTCTTAAAAATCATAATTGAATAGTATCT3' and the reverse primer bearing sequence of 5'TCGCCATGGTCGTTCTCTCTCAATTGATCAAAGTCGAGATTC3' (**Table 3**). The PCR product of *MPK3* promoter was cloned inside the *pGEM-T Easy* vector (Promega) as per manufacturer's guidelines [243]. The PCR products were gel purified using Gel Extraction Kit (Qiagen) following manufacturer's instructions and then transformed into *E. coli* DH5α strain following the protocol described above. After which the promoter sequences were sub-cloned into *pCAMBIA1303* plasmid which harbours *GUS (uidA)-GFP* genes, as standardized before [214]. Next, *Agrobacterium*-mediated Col-0 plant transformation by floral dip technique was performed with the resultant construct *proMPK3:GUS-GFP* [432]. The transgenic line thus developed was named as *pMPK3*.

Histochemical GUS staining of *Arabidopsis* seedlings was performed as per the standardized protocol [214]. Briefly, seedlings were kept in cold 90 % acetone for 15 minutes and then washed using 100 mM phosphate buffer (twice). Next step includes soaking the seedlings in GUS staining solution (composition is mentioned in **Table 13**) and then a mild negative pressure was applied to all the samples. Once again the seedlings were soaked in the GUS staining solution (16 hours), fixed using 70 % ethanol followed by visualization under microscope. The transcript analysis of the *gus* gene in GSH-fed seedlings of *pMPK3* were also conducted.

Table 13: Composition of GUS staining solution

Components	Concentration
5-bromo-4-chloro-3-indolylb-glucuronic acid	0.5 mg/mL
Potassium ferrocyanide	0.5 mM
Potassium ferricyanide	0.5 mM
Triton X-100	0.1 % (v/v)
Phosphate buffer (pH 7.0)	100 mM
EDTA	10 mM

2.9. Isolation of protoplast and its transformation

Briefly, protoplasts were isolated from *Arabidopsis* leaves [433]. Excluding the mid-rib, the rest of the portion of leaves were sliced into small strips (1 mm thickness) and soaked in enzyme solution (composition is mentioned in **Table 14**). The next step included incubation in dark (3 hours; 22°C) under gently shaking condition. To this solution, equal amount of W5 solution (composition is mentioned in **Table 15**) was added and filtration with a nylon mesh was done. The filtrate was spinned down (100 × g; 2 minutes) and pellet was mixed in MMG solution (composition is mentioned in **Table 16**).

The protoplast transformation with *proMPK3:GUS-GFP* construct using PEG and $CaCl_2$ was performed [214]. For that, *proMPK3:GUS-GFP* construct (20 µg in 10 µL volume) was added to 100 µL of the protoplast solution and mixed gently. To it, 110 µL of freshly prepared PEG-calcium transformation solution (composition is mentioned in **Table 17**) was mixed by gentle tapping and incubation was done in a dark space for 5 minutes for transformation to take place. Next, in order to stop transformation, 400 µL of W5 solution was mixed gently. It was then spinned down (100 × g; 2 minutes) and then dissolved in 1 mL of WI solution (composition is mentioned in **Table 18**) followed by incubation at 22°C for 5 hours. The GFP expression levels in *Arabidopsis* protoplasts were visualized under confocal laser scanning microscope. GFP fluorescence was determined with the help of ImageJ software. The fluorescence of each whole protoplast (× 60 magnifications) was measured. The fluorescence per area unit of each and every

protoplast was evaluated. Lastly, the mean of fluorescence/area of all the protoplasts present in a particular field was measured and then the fluorescence/area of the transformed protoplasts was normalized with the value of the control.

GSH and BSO-feeding of the protoplasts was performed by maintaining them in a medium containing GSH and BSO for 5 hours at RT. In case of combined (osmotic+ cold) abiotic stress, 30 % PEG solution was mixed to the maintenance medium and stored at 4°C for additional 15 minutes.

Table 14: Composition of enzyme solution for protoplast isolation

Components	**Concentration**
MES (pH 5.7)	20 mM
Cellulase	1.5 %
Pectinase	0.4 %
Mannitol	0.4 M
KCl	20 mM
$CaCl_2$	10 mM
BSA	0.1 %

Table 15: Composition of W5 solution

Components	**Concentration**
MES (pH 5.7)	2 mM
NaCl	154 mM
KCl	5 mM
$CaCl_2$	125 mM

Table 16: Composition of MMG solution

Components	Concentration
MES (pH 5.7)	4 mM
Mannitol	0.4 mM
$MgCl_2$	15 mM

Table 17: Composition of PEG-calcium transformation solution

Components	Concentration
PEG4000 (w/v)	20 %
Mannitol	0.2 mM
$CaCl_2$	100 mM

Table 18: Composition of WI solution

Components	Concentration
MES (pH 5.7)	4 mM
Mannitol	0.5 mM
KCl	20 mM

2.10. Co-transformation assay in Arabidopsis protoplasts

WRKY40 gene (909 bp) was cloned inside *pAM-PAT-YFP* vector situated upstream of *CaMV35S* promoter [434]. Co-transformation of the resultant construct (*YFP-WRKY40*) along with *proMPK3:GUS-GFP* construct using PEG and $CaCl_2$ was performed. The GFP and YFP fluorescence were observed under a confocal microscope, and fluorescence was determined.

2.11. Stress tolerance assay

Arabidopsis plants (three week old) were treated with biotic stress viz. *P. syringae pv. tabaci* [286]. *P. syringae* was maintained in LB medium till OD reaches 0.7. The cells were then pelleted down and re-suspended in 10 mM $MgCl_2$ [435]. 5 µL of this re-suspended inoculum was spread on the upper side of the leaves. The culture containers were sealed to maintain a highly humid condition. They were then maintained inside growth chambers and observed for 5 days post-infection. Plants treated with 10 mM $MgCl_2$ served as experimental control. Next, infected leaves were collected to carry on further experiments. For CFU count, leaf discs were homogenized in $MgCl_2$, serially diluted and plated over YEP medium (composition is mentioned in **Table 19**) in presence of kanamycin and rifampicin.

For abiotic salt stress assay, three week old soil-grown plants grown were treated with 200 mM NaCl on 1st, 3rd, 5th, 7th, and 9th day for 5 times. So all together, the plants were treated for 5 times. The control of the experiment was plant samples sprayed with water [214].

Table 19: Composition of YEP medium

Components	Concentration
Yeast extract	10 g L^{-1}
Peptone	10 g L^{-1}
NaCl	5 g L^{-1}
Agar	15 g L^{-1}

2.12. In-gel kinase assay

The in-gel kinase assay was conducted following the standard protocol [399**,**410]. 20 µg of protein was used for the assay and run on 10 % polyacrylamide gel. Bovine brain myelin basic protein (0.25 mg mL^{-1}; Sigma) was mixed with the gel. Following this step, the gel was rinsed (thrice) with washing buffer (composition is mentioned in **Table 20**) for 30 minutes at RT, thrice with renaturation buffer (composition is mentioned in **Table 21**) for 12 hours at 4°C. The next

step includes a washing step with reaction buffer (composition is mentioned in **Table 22)** for 30 minutes at RT. Incubation was done in reaction buffer (12.5 mL) with non-labelled ATP (250 nM) and labelled ones (1.85 MBq [y-32P] ATP; 3000 Ci $mmol^{-1}$) for 1.5 hour at RT. Last washing step is performed with washing solution (5 % TCA, 1 % pyrophosphoric acid) for five times. The gel was dried and exposed to X-ray film (Carestream XBT).

Table 20: Composition of washing buffer

Components	Concentration
Tris-HCl (pH 7.5)	25 mM
DTT	0.5 mM
Na_3VO_4	0.1 mM
NaF	5 mM
BSA	0.5 mg mL^{-1}
Triton X-100	0.1 %

Table 21: Composition of renaturation buffer

Components	Concentration
Tris-HCl (pH 7.5)	25 mM
DTT	1 mM
Na_3VO_4	0.1 mM
NaF	5 mM

Table 22: Composition of reaction buffer

Components	Concentration
Tris-HCl (pH 7.5)	25 mM
EGTA	2 mM
$MgCl_2$	12 mM
DTT	1 mM
Na_3VO_4	0.1 mM

2.13. In silico study to identify the TFs binding MPK3 promoter

In order to identify the TFs that has binding sites in the promoter region of *MPK3* gene, the Plant Promoter Analysis Navigator, PlantPan; http://PlantPan2.itps.edu.tw [436] was used. On the basis of above mentioned *in silico* study, TFs having high number of binding sites in the *MPK3* promoter were short-listed and mutants of those TFs were procured from NASC, i.e., *wrky75* (N121513), *wrky18* (N593916), *wrky3* (N607019), *wrky40* (N119583), *zat6* (N678573), *myb44* (N539074), and *erf6* (N530723).

2.14. Protein immunoprecipitation and immunoblotting

3 mg of total proteins were isolated following the protocol mentioned in **chapter 1** under **Materials & Methods** section and the isolated proteins were dissolved in isolation buffer containing protein A (magnetic beads, Millipore, USA) as per the protocol followed by Kumar and Chattopadhyay, 2018 [437]. The anti-γ-ECS primary antibody (Agrisera, Sweden) was added to the buffer for immunoprecipitation (overnight at 4°C). Next, the solution was pelleted down and washed with the protein isolation buffer. To it, 20 µL of loading dye was added and it was heated at 70°C for 10 minutes. Using the upper layer of protein samples, immunoblotting was conducted. Proteins expression was determined using the anti-WRKY40 primary antibody (Ab-mart, China).

2.15. ChIP-qPCR assay

Arabidopsis leaves were used for this analysis [214] using the EZ-ChIP kit (Millipore, USA). For pulling down the chromatin, anti-WRKY40 antibody (Ab-mart) was used. A buffer (composition is mentioned in **Table 23)** was used for soaking the leaves in a vacuum condition for 15 minutes in order to crosslink the chromatins. For terminating the crosslinking process, 0.1 M glycine was added and stored for additional 5 minutes. The leaves were then collected and homogenised well. Leaf samples were then re-suspended in PBS buffer. Binding of RNA polymerase II to *GAPDH* promoter was used as control. The primers used are listed in **Table 3**. Three independent experiments were performed with similar results. Data are mean values of three replicates ± SD.

Table 23: Composition of ChIP-qPCR buffer

Components	Concentration
Sucrose	0.4 M
Tris HCl (pH 8.0)	10 mM
EDTA	1 mM
PMSF	1 mM
Formaldehyde	1 %

2.16. Determination of H_2O_2 content

Foliar H_2O_2 contents were measured according to Velikova et al. 2000 [438], with slight modifications. Leaf samples (200 mg) were used for this assay. Leaf tissues were grounded and dissolved in 0.1 % trichloroacetic acid (2 mL) and spinned down (12,000 × g; 20 minutes). 500 µL of the supernatant was added to equal amount of a mixture containing 10 mM sodium-phosphate buffer (pH 7.5) and 1 M potassium iodide. The absorbance at 390 nm was then noted.

DAB staining was performed for H2O2 detection with slight modifications [439]. Briefly, *A. thaliana* leaves were soaked in DAB solution (1 mg mL^{-1}) for 12 hours. Samples were then bleached after staining using a solution of ethanol, acetic acid and glycerol (3:1:1) for 5 minutes in boiling water bath and put in a fresh bleaching solution for additional 30 minutes. Samples were lastly mounted and visualized through microscope.

2.17. Chlorophyll content estimation

Estimation of total chlorophyll was done from *A. thaliana* leaves [440]. Briefly, leaf samples (200 mg) were homogenised in 95 % ethanol (2 mL) and incubated for 12 hours. Then samples were spinned down (10,000 rpm; 2 minutes). The OD of the supernatant was determined at 664/648 nm using a spectrophotometer (Shimadzu, Japan). Chlorophyll content was measured using spectrophotometer and calculated using the following formula:

$$\text{Chlorophyll}_{a+b} = 5.24 \times A_{664} + 22.24 \times A_{648}$$

[$Chlorophyll_{a+b}$: Total chlorophyll content in μg mL^{-1}; A_{664}: Absorbance at 664 nm; A_{648}: Absorbance at 648 nm].

2.18. Physiological responses

The free proline content was measured following the protocol by Bates et al. 1973 [441]. For that, 500 mg of crushed leaves was dissolved in 5 mL of 3 % 5-sulphosalicylic acid. After centrifuging, the soup was collected and to it equal quantity of glacial acetic acid and 2.5 % ninhydrin were added. The sample mixture was then kept at 100°C for 30 minutes, after which it was kept on ice for few minutes, followed by addition of an equal volume of toluene and mixed really well. Thereafter, the absorbance of the upper layer was noted at 520 nm.

The extent of lipid peroxidation was estimated in *A. thaliana* leaves spectrophotometrically by determining malondialdehyde (MDA) concentration, as described by Hodges et al. 1999 [442]. Leaf samples were grounded and dissolved in 0.1 % TCA (2 mL). Samples were then spinned down (20,000 × g; l0 minutes). The soup (1 mL) was collected and to it 20 % TCA (4 mL) containing 0.5 % TBA was added. The samples were boiled at 95°C for 30 minutes followed by quick chill. Up next, samples were centrifuged (20,000 × g; 10 minutes) and the OD of the supernatant was measured spectrophotometrically at 532 nm.

2.19. Statistical analysis

Every experiment was performed in three biological replicas and the data presented are the mean of them (± standard error). Statistical analysis was performed using multiple t test (two-stage step-up method of Benjamini, Kreiger and Yekutieli comparison test). The software used was GraphPad InStat software (version 8). $P<0.33$, 0.002, 0.001 was considered to be statistically significant.

3. Results

3.1. Varied GSH content modulates MPK3 both at gene and protein level in Arabidopsis

To find out whether GSH has any role to play in inducing MPK3, the transcript profiling of few selective *MPK* isoforms that includes *MPKKK19, MKK1, MKK2, MKK5, MPK1, MPK2, MPK3, MPK4* and *MPK6* was performed in wild-type Col-0, GSH-mutant *pad2.1* and GSH-fed Col-0 samples both in absence (henceforth mentioned as control condition/samples) and presence of stress conditions (combined osmotic+cold stress, henceforth mentioned as treated condition/samples).

To examine the establishment of GSH-fed condition in Col-0 samples, HPLC analysis was performed in GSH and GSSG-fed Col-0 plants. Result showed higher GSH content and increased GSH:GSSG ratio in GSH-fed Col-0 samples (**Fig. 3A,B**). The *PR1* transcript abundance in GSH-fed Col-0 showed its significant elevated expression (**Fig. 3C**). PR1 is a marker for enhanced GSH condition which also corroborated with earlier studies [300,243,246]. The physiological responses under treated condition in Col-0, *pad2.1* and GSH-fed Col-0 samples in terms of proline and chlorophyll content along with MDA concentration were also noted. Results revealed that the proline were approximately 2-fold higher in treated plant samples [443] as shown in **Fig. 3D** and the chlorophyll content was significantly less in all treated samples (**Fig. 3E)**. MDA concentration was observed to be 4-fold higher in treated samples (**Fig. 3F)** as reported earlier [52].

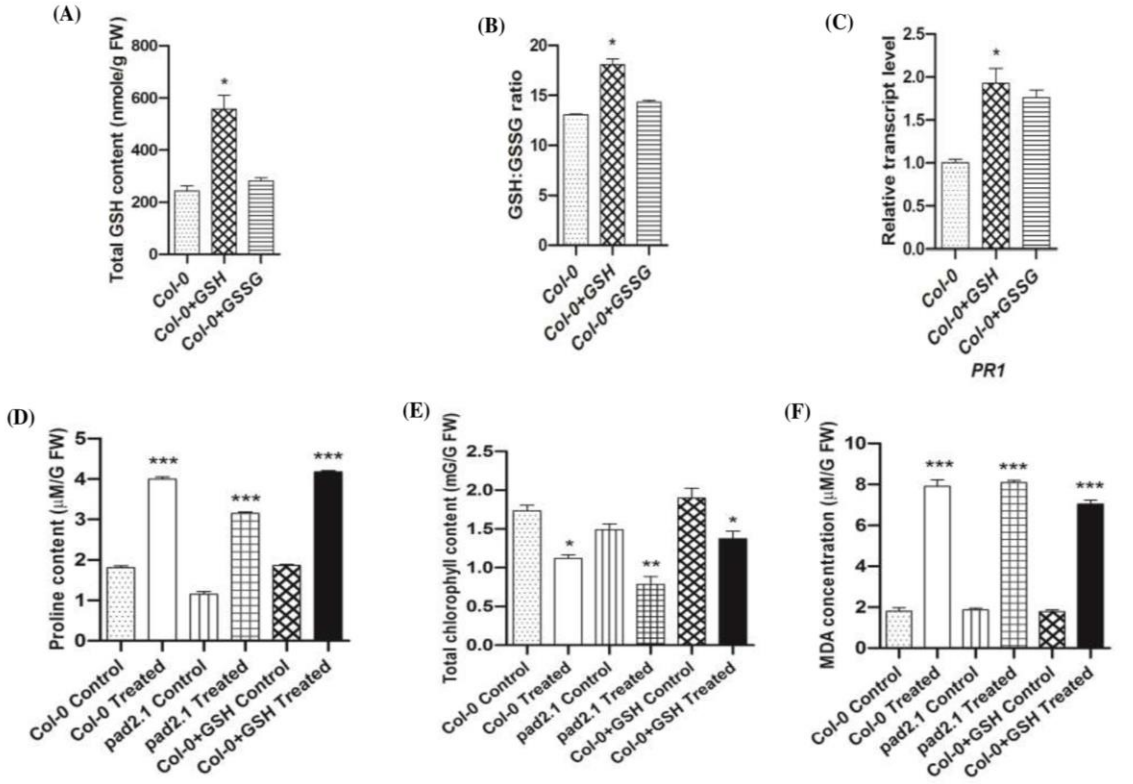

Fig. 3. Establishment of GSH-fed condition and physiological response of Col-0, *pad2.1*, and GSH-fed Col-0 plants under combine (osmotic+cold) abiotic stress. **(A)** Estimation of GSH content by HPLC analysis. **(B)** Determination of GSH:GSSG ratio. **(C)** *PR1* transcript abundance by qRT-PCR analysis in GSH and GSSG-fed Col-0 plants, where *tubulin* used as reference gene. **(D)** Estimation of proline content. **(E)** Estimation of chlorophyll content. **(F)** Estimation of MDA concentration of Col-0, *pad2.1,* and GSH-fed Col-0 plants. Data are the mean ± SE for 3 individual experiments using plants grown independently. *P<0.332, **P<0.002, ***P<0.001.

Furthermore, transcript analysis of all *MPK* isoforms under varied GSH conditions was performed. Results showed that majority of the MPK isoforms had increased expression in GSH-fed Col-0 plants as well as decreased expression in *pad2.1* mutants with respect to wild-type Col-0. It is noteworthy to mention that among all isoforms, MPK3 was significantly up-regulated in GSH-fed Col-0 plants and significantly down-regulated in *pad2.1* both under control as well as treated condition at gene and protein level (**Fig. 4**). Further, in BSO-fed Col-0, the MPK3 expression was observed was significantly less (**Fig. 5A,B**). BSO is a strong inhibitor of GSH biosynthetic pathway. The expression of *MPK3* in GSSG (oxidized form of GSH)-fed Col-0 revealed no significant change (**Fig. 5C**). It may be noted that there no difference in GSH content in GSSG-fed Col-0 plants (**Fig. 3A**). Next, it was assumed that this change in MPK3 expression

is actually not GSH-dependant but due to the altered redox homeostasis during stress. For this, DTT, a strong reducing agent, was used to treat the Col-0 plants and MPK3 expression was analysed both at gene and protein level. Results showed insignificant change in MPK3 expression in the DTT treated Col-0 samples compared to Col-0 without DTT treatment (**Fig. 5D,E**). Altogether, results suggested GSH being responsible in modulating the expression MPK3.

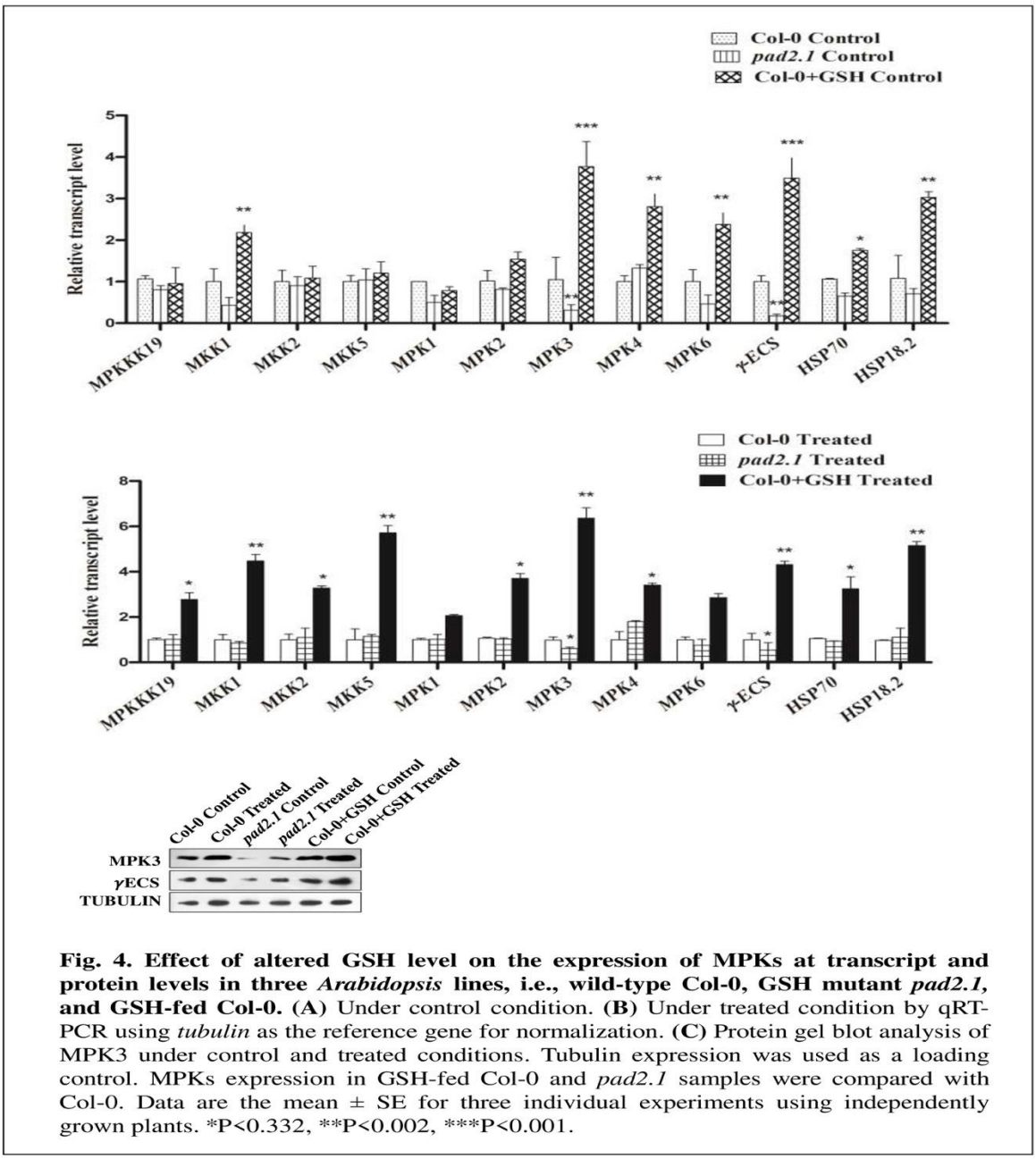

Fig. 4. Effect of altered GSH level on the expression of MPKs at transcript and protein levels in three *Arabidopsis* lines, i.e., wild-type Col-0, GSH mutant *pad2.1*, and GSH-fed Col-0. (A) Under control condition. **(B)** Under treated condition by qRT-PCR using *tubulin* as the reference gene for normalization. **(C)** Protein gel blot analysis of MPK3 under control and treated conditions. Tubulin expression was used as a loading control. MPKs expression in GSH-fed Col-0 and *pad2.1* samples were compared with Col-0. Data are the mean ± SE for three individual experiments using independently grown plants. *P<0.332, **P<0.002, ***P<0.001.

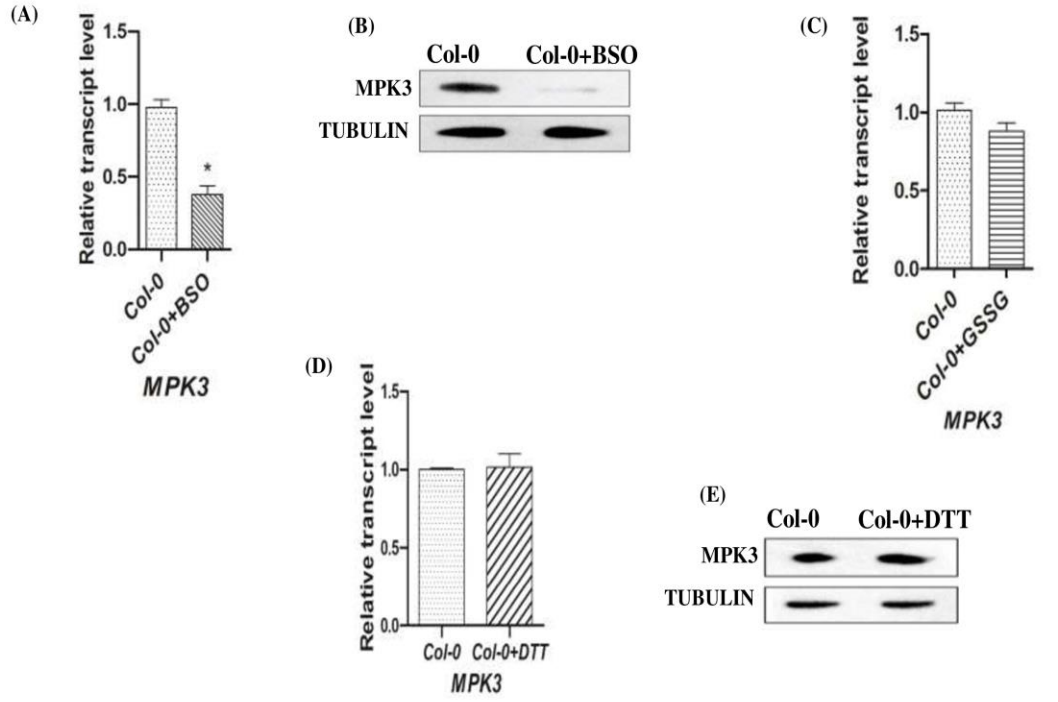

Fig. 5. MPK3 expression analysis in BSO-fed, GSSG-fed and DTT fed Col-0 plants. (**A**) *MPK3* expression in BSO-fed Col-0 at transcript level and (**B**) protein level. (**C**) *MPK3* expression in GSSG-fed Col-0 at transcript level. (**D**) *MPK3* expression at transcript level and (**E**) protein level in DTT-fed Col-0. Data are the mean ± SE for 3 individual experiments using plants grown independently. *P<0.332.

3.2. Raising transgenic A. thaliana line over-expressing MPK3

MPK3 is known to be an important member of MPK cascade. *MPK3* gene from *Lycopersicon esculentum* (Gene ID: 543880) had similarity (86.3 %) and identity (73.8 %) at DNA level as well as at protein level (94 % similarity, 81 % identity) with *A. thaliana MPK3* (Gene ID: 823706). Therefore the *LeMPK3* gene was cloned inside *pBI121* binary vector downstream of *CaMV35S* constitutive promoter forming the *pCaMV35S:LeMPK3* construct. The *pBI121* vector backbone harbouring *MPK3* gene has been shown in **Fig. 6.**

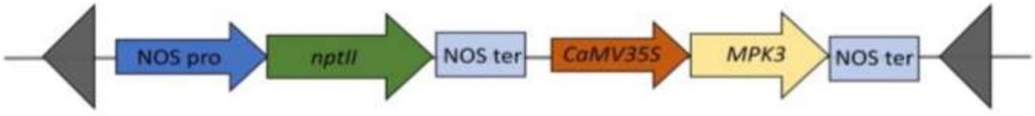

Fig. 6. The *pCaMV35S:LeMPK3* in *pBI121* vector backbone

The *pCaMV35S:LeMPK3* was then transformed to Col-0 plants by means of floral dip method for which Col-0 seeds were germinated on soil-rite and then 2 week old seedlings were transferred to autoclaved soil and maintained in growth chamber at 21±1°C and 75 % relative humidity. Initially a short day condition was maintained to facilitate vegetative growth of the plants (**Fig. 7A**). To initiate bolting, plants were then exposed to 16 hours light and 8 hours dark cycles. Floral dip was carried out at a stage when the plant bore maximum number of unopened floral buds (**Fig. 7B**). *A. tumefaciens* GV3101 strain was transformed to carry the *pCaMV35S:LeMPK3* construct and used for floral dip. After dipping, plants were maintained under long day condition till seed set (**Fig. 7C)**. Transformed seeds were collected and subjected to antibiotic (kanamycin) screening (**Fig. 7D**). During this screening, some seeds did not germinate or displayed yellowing within a few days. Only the seedlings that remained green upto 15 days were transferred to MS medium without antibiotic and were allowed to grow. These primary transformants (T1) were transferred to soil (with a top layer of soilrite) after 15 more days and maintained under short day condition in a growth chamber (**Fig. 7E**). At this stage the primary transformants were screened by genomic DNA PCR analysis for the *nptII* gene (**Fig. 7F**).

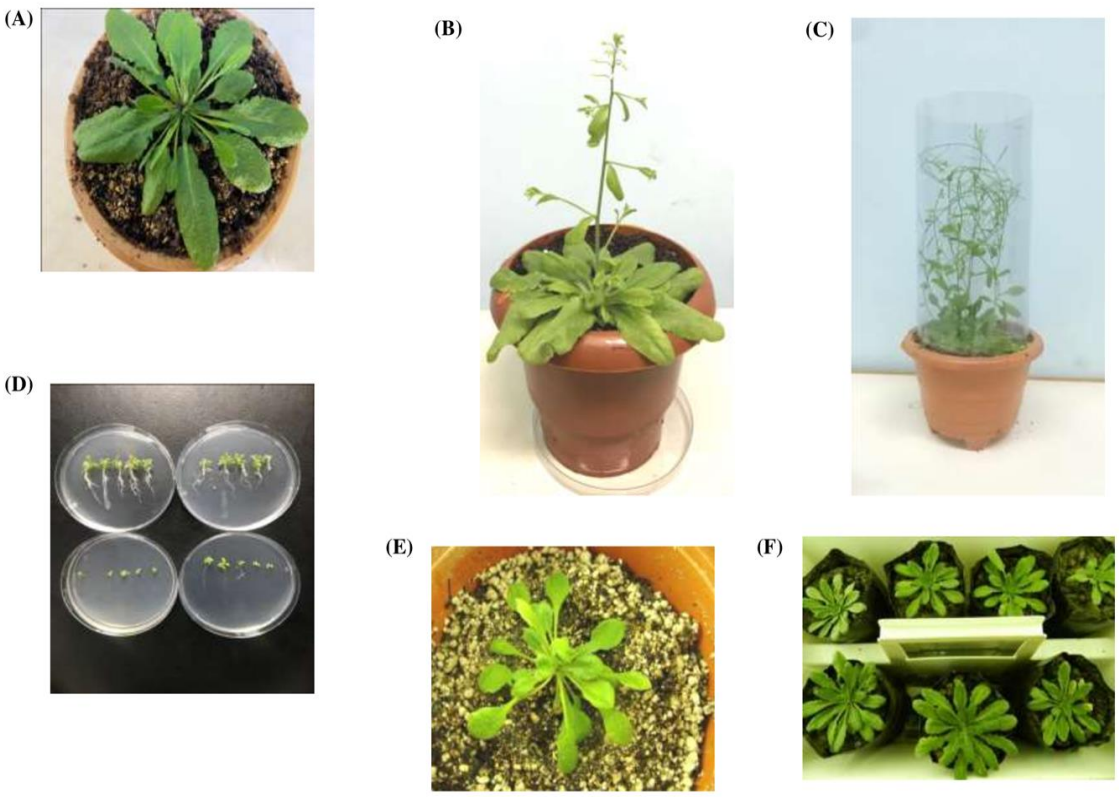

Fig. 7. Raising of *AtMPK3* line. **(A)** Col-0 at vegetative stage. **(B)** Col-0 at flowering stage. **(C)** Col-0 just after floral dip for seed set. **(D)** Antibiotic screening of primary transformants. **(E)** *AtMPK3* plant transferred to soil. **(F)** Fully mature *AtMPK3* lines at vegetative phase.

Nearly 75 % of the transformants (selected from antibiotic screening) were found to be positive. Among the various Kan^R plants, 15 PCR positive transgenic lines were initially screened, from which 2 healthy *AtMPK3* transgenic lines (*AtMPK3-1* and *AtMPK3-15*) were selected for further characterization and were maintained upto T2 generation. For each generation 50 seeds were screened for each of the 2 lines. The detail of screening has been summarized in **Table 24**.

Table 24: Screening of *AtMPK3* line for obtaining homozygous line

Lines	Generation	No. of plants		
		Screened	Positive	Negative
AtMPK3-1	T_2	50	36	14
AtMPK3-15	T_2	50	29	21

3.3. Comparison of morphology and enhanced expression of MPK3 gene in the AtMPK3 lines

The visual appearance of the *AtMPK3* lines at the seedling stage was similar to the wild-type Col-0 plants. Absence of any striking morphological differences were noted in Col-0 and the fully grown transgenic lines viz. *AtMPK3* lines (**Fig. 8A**).

To compare the expression levels of the *MPK3* gene in the *AtMPK3* lines (T2 generation) with the wild-type Col-0 plants, we performed genomic DNA PCR of *nptII* and MPK3. Result of which showed positive *nptII* bands in both the transgenic lines (**Fig. 8B**). Up-regulated *MPK3* expression was also noted in both the *AtMPK3* lines compared to Col-0 (**Fig. 8B**) which corroborated with qRT-PCR data, revealing the *AtMPK3* lines which exhibited more than 2-fold up-regulation of *MPK3* expression in *AtMPK3* transgenic lines (**Fig. 8C**). For qRT-PCR analysis of *MPK3,* two pair of primers was designed (**Table 3**). 'Pair 1' was designed flanking the homologous region present in both *Lycopersicon* and *Arabidopsis*. Whereas 'pair 2' was designed for flanking CDS region present exclusively in *Lycopersicon MPK3* gene and not in *Arabidopsis.* To check the level of MPK3 protein accumulation in the transgenic lines, western blot analysis was performed and proteins levels were compared in the *AtMPK3-1, AtMPK3-15* and Col-0. The two transgenic lines exhibited strong up-accumulation of the MPK3 protein as compared to Col-0 (**Fig. 8D**). Among both the transgenic lines, *AtMPK3-1* was used for subsequent experiments.

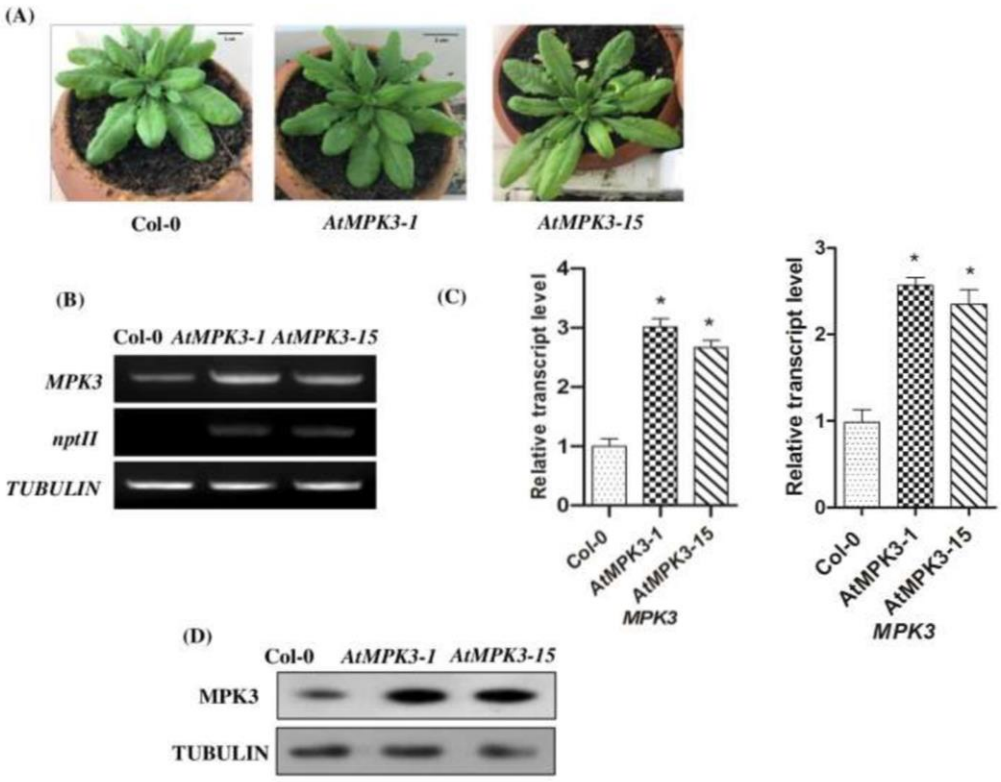

Fig. 8. Characterization of *AtMPK3* lines. **(A)** Morphological images. **(B)** Genomic DNA PCR screening of *MPK3* and *nptII* in *AtMPK3* lines. *Tubulin* expression was used as the loading control. **(C)** qRT-PCR analysis for *MPK3* expression using primer pair 1 and 2 respectively in *AtMPK3* lines. *Tubulin* was used for normalization. **(D)** Protein gel blot analysis of *AtMPK3* lines. Tubulin expression was used as a loading control. All experiments were repeated thrice. Data are the mean ± SE for three individual experiments using independently grown plants. *P<0.332.

3.4. Varied MPK3 level modulates γ-ECS expression at gene and protein level

MPK3 is one of the well characterized MPKs that play a fundamental role in MPK cascade during stress. In order to check the response of varied MPK3 level on γ-ECS expression, *AtMPK3-1* transgenic line was utilized along with *mpk3* mutant line and staurosporine (ST)-fed Col-0. The physiological responses with respect to changes in proline, chlorophyll content and MDA concentration were analyzed in combined (osmotic+ cold) abiotic stress treated *AtMPK3-1* and *mpk3* samples. Data of which showed more than 2-fold increase in proline content (**Fig. 9A**),

2 to 4-fold depletion in chlorophyll content (**Fig. 9B**), and 3-fold higher MDA concentration in the treated samples compared to samples without stress treatment (**Fig. 9C**).

In *AtMPK3-1* samples, significantly elevated transcript abundance of *γ-ECS* was noted (**Fig. 10A**). Consequently, lesser transcript abundance of *γ-ECS* in *mpk3* mutants was observed under control conditions (**Fig. 10A**). Interestingly, similar expression pattern was also observed under treated condition but the magnitude of expression was higher compared to control condition (**Fig. 10B**). In the next step of experiments, Col-0 plants were fed with a MPK inhibitor, viz. staurosporine (ST). Extremely diminished *γ-ECS* expression was noted in ST-fed Col-0 plants (**Fig. 10 A,B**). The above transcript data corroborated with protein data where expression of γ-ECS varied in presence of altered MPK3 content in *A. thaliana* under both control and treated conditions (**Fig. 10 C,D**). Thus, results further confirmed a correlation between γ-ECS and MPK3.

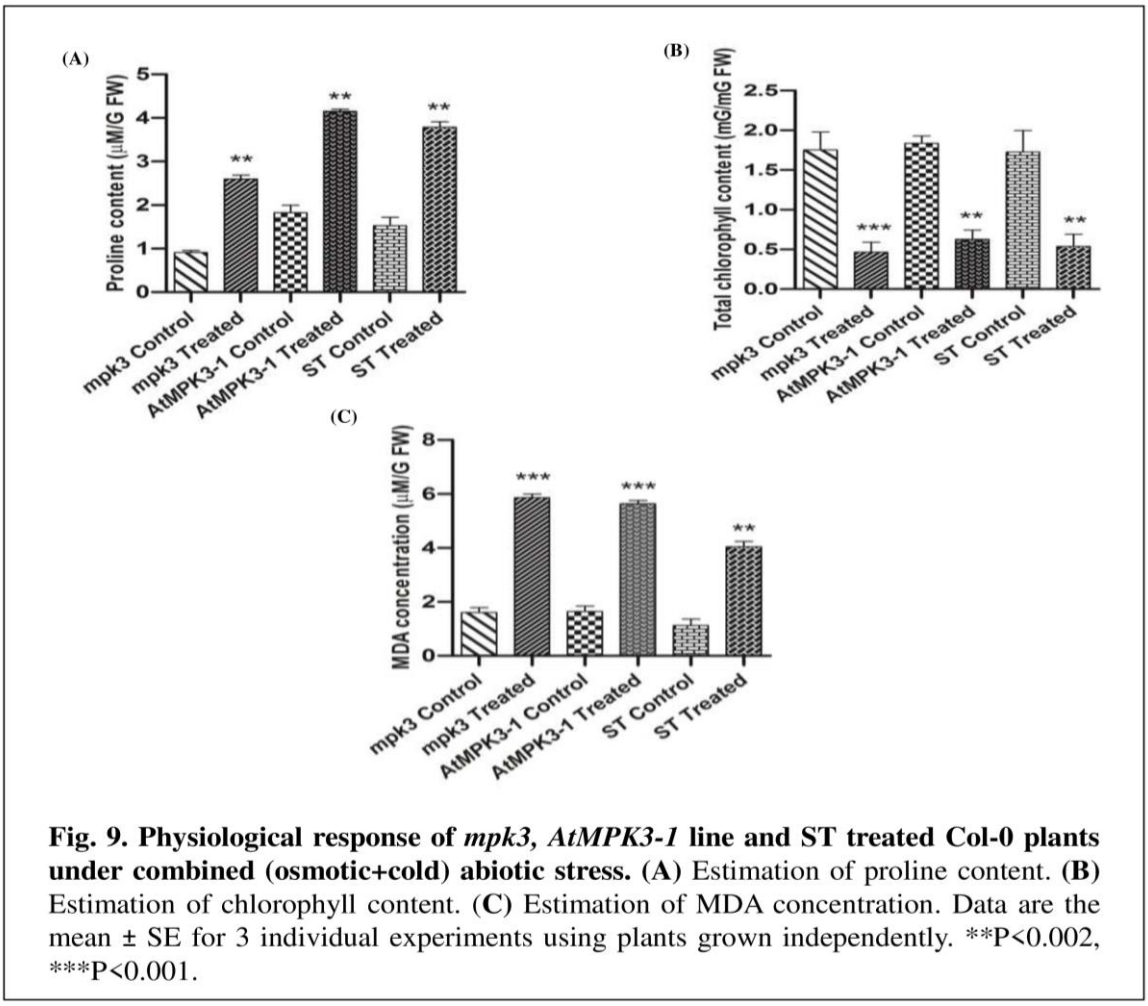

Fig. 9. Physiological response of *mpk3*, *AtMPK3-1* line and ST treated Col-0 plants under combined (osmotic+cold) abiotic stress. **(A)** Estimation of proline content. **(B)** Estimation of chlorophyll content. **(C)** Estimation of MDA concentration. Data are the mean ± SE for 3 individual experiments using plants grown independently. **P<0.002, ***P<0.001.

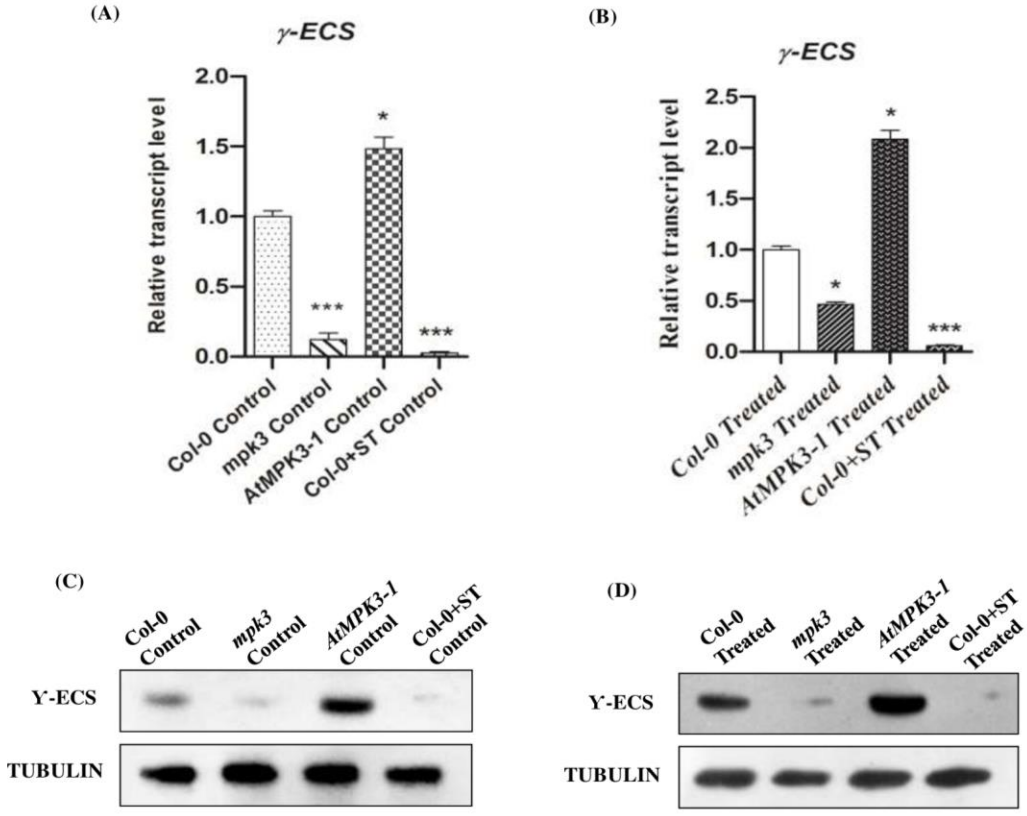

Fig. 10. Effect of altered MPK levels on γ-ECS expression at transcript and protein level in four *Arabidopsis lines*, i.e., Col-0, *mpk3* mutant, *AtMPK3-1* line, and staurosprorine (ST) treated Col-0. **(A)** *γ-ECS* expression under control condition **(B)** and treated condition (combine abiotic stress) by qRT-PCR analysis. *Tubulin* was used for normalization. **(C)** Protein gel blot analysis of γ-ECS protein under control condition **(D)** and treated condition. Tubulin expression was used as the loading control. γ-ECS expression in transgenic *AtMPK3-1* and *mpk3* mutant and ST-treated Col-0 were compared with Col-0. Data are the mean ± SE for three individual experiments using independently grown plants. *P<0.332, ***P<0.001.

3.5. GSH plays a role in activating *MPK3* promoter

To explore GSH's function on inducing *MPK3*, promoter of *MPK3* (intergenic region of 627 bp upstream from TSS) was fused with *GUS* and *GFP* in the backbone of *pCAMBIA1303* backbone forming the resultant construct named *proMPK3:GUS-GFP* (**Fig. 11**). The *proMPK3:GUS-GFP*

construct was transformed into Col-0 samples. Eventually, GUS staining revealed that the *MPK3* promoter was greatly induced in response to GSH (**Fig. 12A**). Similarly, transcript analysis of *GUS* gene also revealed a similar result like the previous one (**Fig. 12B**). Briefly these observations indicated that GSH induces the promoter activity of *MPK3*. In addition, *proMPK3:GUS-GFP* construct was transformed into *Arabidopsis* protoplasts viz. Col-0, *pad2.1*, GSH-fed Col-0 and BSO-fed Col-0. Results revealed elevated level of GFP expression in terms of its fluorescence in GSH-fed Col-0 protoplasts and lesser GFP fluorescence in *pad2.1* protoplasts both under control and treated conditions. However, the amplitude of GFP fluorescence was much higher in all treated protoplasts compared to control ones (**Fig. 12C**). On top of that, GFP fluorescence was remarkably reduced in BSO-fed Col-0 protoplasts both under control and treated conditions (**Fig. 12C**). Thus from the above findings it was inferred that GSH has a major role in inducing *MPK3* by activating its promoter.

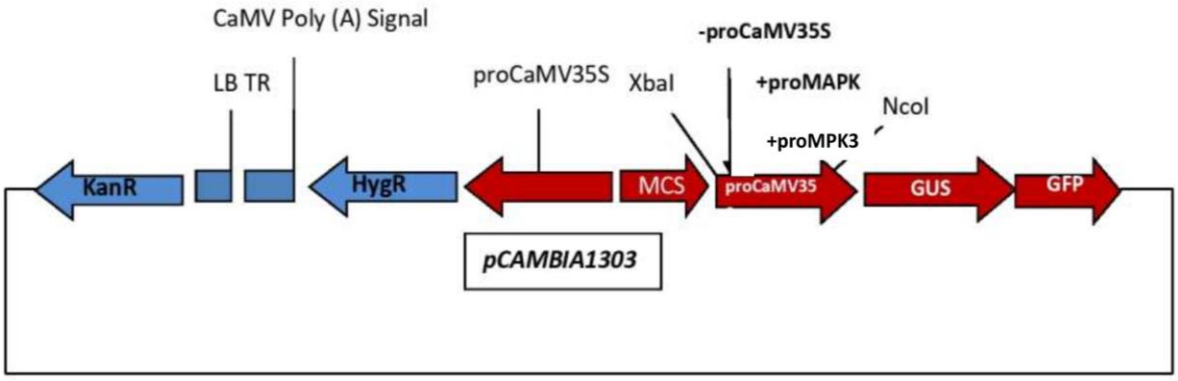

Fig. 11. The *proMPK3:GUS-GFP* construct in *pCAMBIA1303* backbone

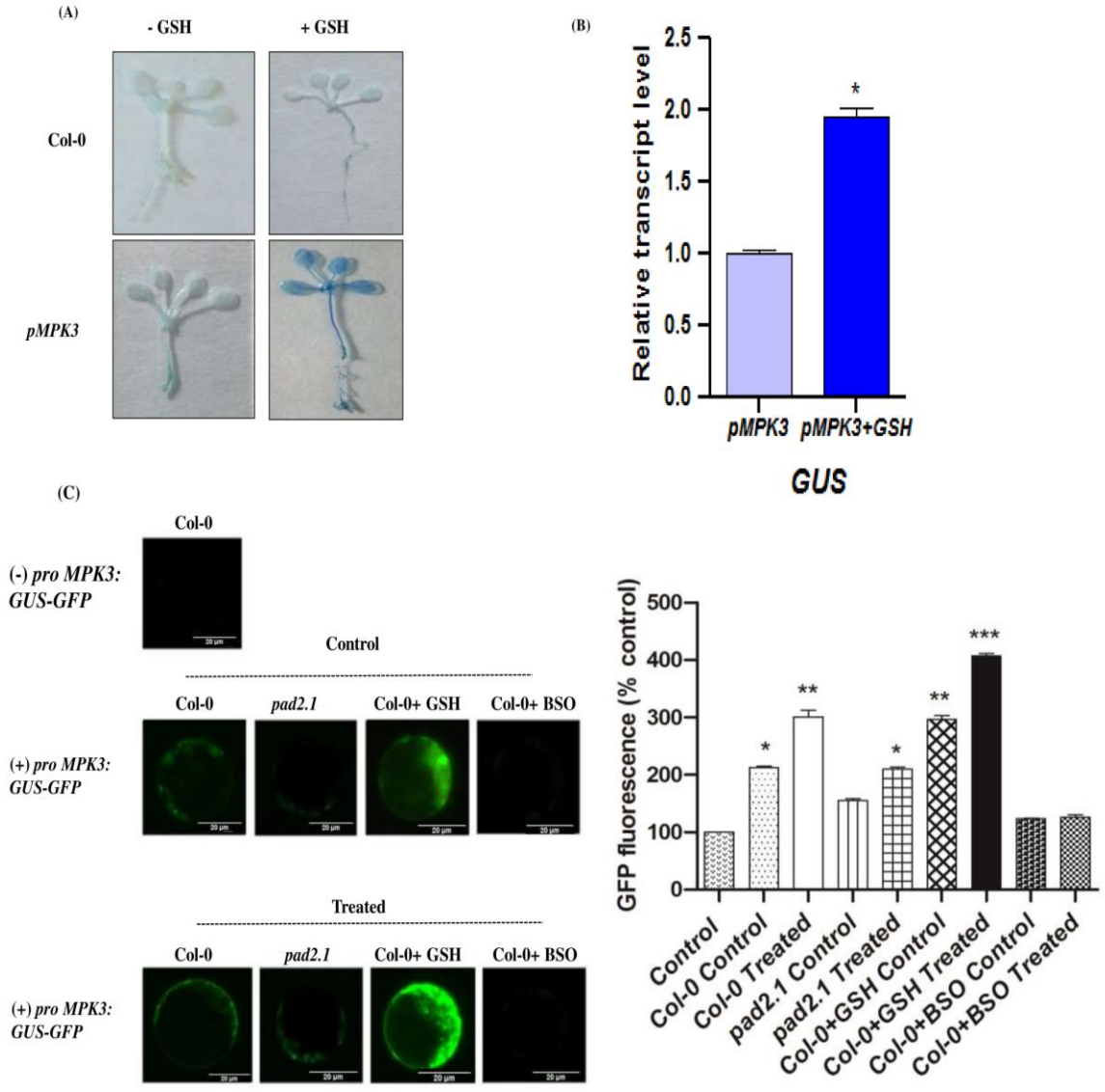

Fig. 12. Promoter analysis of *MPK3* in response to GSH using *proMPK3:GUS-GFP* construct. **(A)** GUS staining assay where Col-0 plants in the absence of GSH feeding has been used as a negative control. **(B)** The expression analysis of *GUS* in *pMPK3* transgenic line upon GSH feeding. *Tubulin* was used for normalization. **(C)** Protoplasts of Col-0, *pad2.1*, Col-0 GSH-fed, and Col-0 BSO-fed were transformed with *proMPK3:GUS-GFP* construct, and GFP expression levels were monitored under control and treated conditions (combined abiotic stress) by confocal laser scanning microscope (fluorescence under 488 nm). (-) *proMPK3:GUS-GFP* (lacking *MPK3* promoter): negative control. GFP fluorescence in *pad2.1*, GSH- and BSO-fed Col-0 samples was compared to Col-0. Experiments were performed with three biological replicates. Bar: 20 µm. *P<0.332, **P<0.002, ***P<0.001.

3.6. Essential role of GSH-MPK3 cross-talk in conferring plant stress tolerance

To investigate the importance of GSH-MPK3 cross-talk in imparting plant stress tolerance, different stress tolerant assays were performed. Previous studies have very well deciphered MPK3's role under both biotic stress viz. *Pseudomonas syringae* infection and abiotic stresses [444,445]. Hence, three stress treatments were performed to determine the importance of GSH-MPK3 interplay under stress viz. *P. syringae* infection, combined (osmotic+cold) abiotic stress and salt stress. Therefore, four week old Col-0, *AtMPK3-1* and *mpk3* plants were treated with *P. syringae* infection and samples were scored for 5 days post-infection. As a result of this infection, yellowing of the affected leaf parts was observed. Stress assay further exhibited enhanced resistance of *AtMK3-1* lines to *P. syringae* infection while *mpk3* mutants were noted to be severely infected. The quantification of *P. syringae* infection with respect to CFU count was determined which revealed lesser CFU count (~5 log CFU cm^{-2}) of *P. syringae* bacterial colonies from leaf discs of *AtMPK3-1* lines (**Fig. 13A**). Similar results in terms of change in morphology were also noted during salt stress assay (**Fig. 14A**). Under salt stress, the treated samples showed clear wilting of plants, where *AtMPK3-1* plants showed the least and *mpk3* plants showed highest wilting compared to Col-0 (**Fig. 14A**). Besides, the transcript abundance of *γ-ECS* was higher in the *P. syringae* infected Col-0, *AtMPK3-1*, and *mpk3* mutant plants (**Fig. 13B**). 2-fold higher H_2O_2 concentration was revealed in H_2O_2 content determination and DAB staining assays (**Fig. 13C,D**), whereas the amount of chlorophyll were noted to be remarkably reduced in all the infected plants (**Fig. 13E**).

Whether, the MPK3-dependent resistance can also be regulated by GSH. To address this question, Col-0, *mpk3* mutant and *AtMPK3-1* line were treated with exogenous GSH and then infected with *P. syringae*. Results showed that the *AtMPK3-1* line exhibited better response to *P. syringae* infection when fed with GSH, whereas *mpk3* mutant plants were sensitive to *P. syringae* infection (**Fig. 13A**). Alongside, H_2O_2 content was low and chlorophyll amount was high in *P. syringae* infected GSH-fed *AtMPK3-1* line (**Fig. 13C-E**). Similarly, Col-0, *mpk3* mutant and *AtMPK3-1* line were fed with GSH and then treated with combined (osmotic+cold) stress which revealed similar results like *P. syringae* infected GSH-fed samples (**Fig. 14B-F**). In nutshell, it can be concluded that GSH-MPK3 crosstalk helps in imparting resistance to biotic viz. *P. syringae* infection and abiotic stress factors.

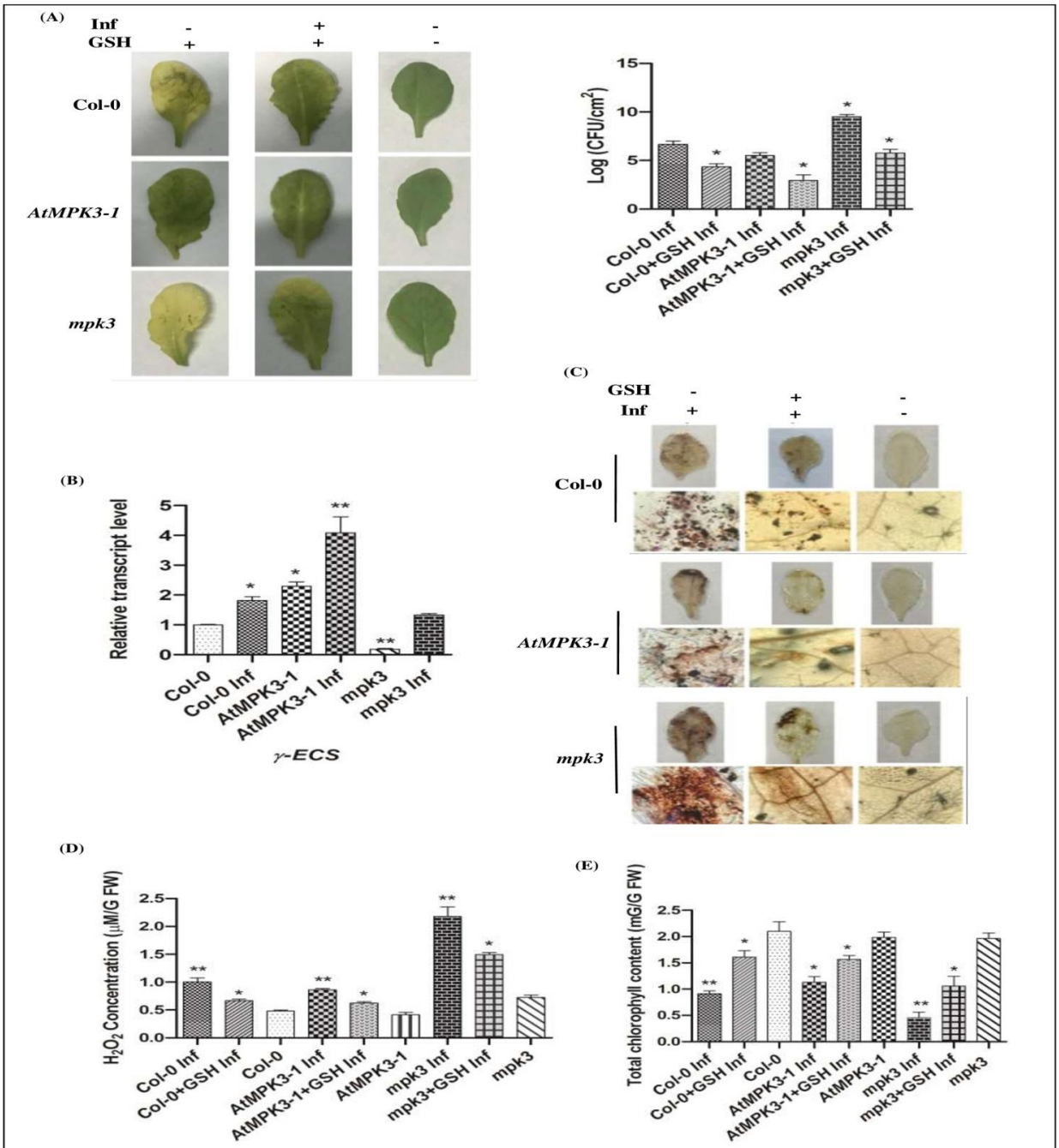

Fig. 13. Stress tolerance assay of Col-0, *AtMPK3-1* and *mpk3* mutants after *P. syringae* infection (inf) with and without GSH feeding. **(A)** Morphological images, quantification of *P. syringae* infection. Infected samples were compared with non-infected samples in presence or absence of GSH. **(B)** qRT-PCR analysis of *γ-ECS* in Col-0, *AtMPK3-1* and *mpk3* plants in response to *P. syringae* infection. *Tubulin* used as reference gene for normalization. Infected samples were compared with non-infected samples. **(C)** Determination of H_2O_2 by DAB staining with microscopic view (10x) and **(D)** Determination of H_2O_2 without and with GSH feeding. **(E)** Chlorophyll content estimation without and with GSH feeding. Col-0, *AtMPK3-1* and *mpk3* plants (without stress treatment) has been used as control. Data are the mean ± SD for 3 individual experiments using plants grown independently. *P<0.332, **P<0.002.

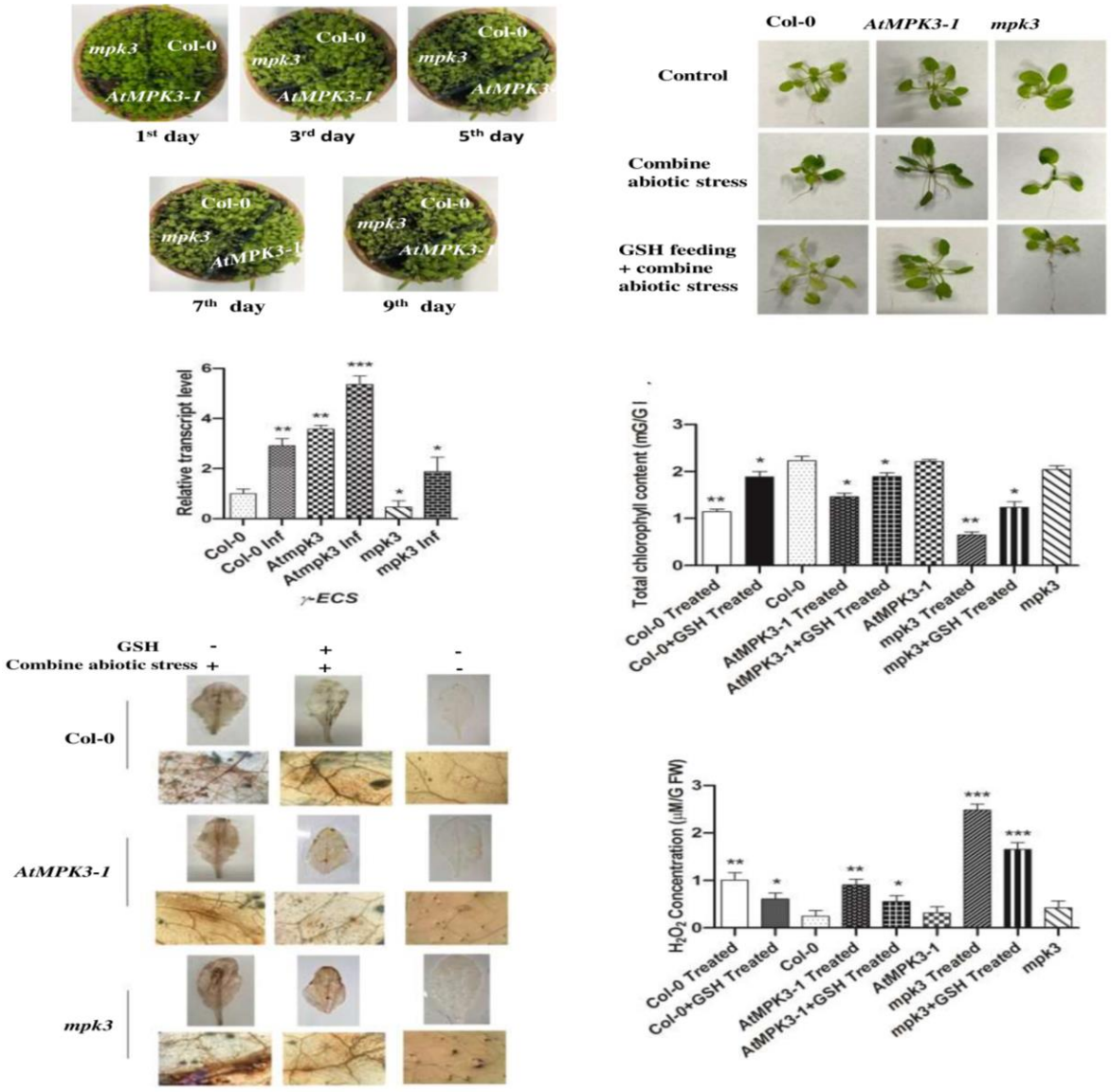

Fig. 14. Stress tolerance assay of Col-0, *AtMPK3-1* and *mpk3* plants under salt as well as combined (osmotic+cold) abiotic stress treatment. (A) Morphological images after salt stress treatment. **(B)** Morphological images after combined (osmotic+cold) abiotic stress treatment in presence and absence of GSH feeding. **(C)** qRT-PCR analysis of *γ-ECS* in Col-0, *AtMPK3-1* and *mpk3* plants in response to combined (osmotic+cold) abiotic stress treatment where Col-0 (without stress treatment) was used as control. **(D)** Chlorophyll content estimation under combined cold and osmotic stress treatment in presence and absence of GSH feeding. Col-0, *AtMPK3-1* and *mpk3* plants (without stress treatment) have been used as control. **(E)** Detection of H_2O_2 by DAB staining with microscopic view (10 X) under combined (osmotic+cold) abiotic stress treatment in presence and absence of GSH feeding. **(F)** Determination of H_2O_2 under combined (osmotic+cold) abiotic stress treatment in presence and absence of GSH feeding. Col-0, *AtMPK3-1* and *mpk3* plants (without stress treatment) have been used as control. Data are the mean ± SD for 3 individual experiments using plants grown independently. *P<0.332, **P<0.002, ***P<0.001.

3.7. Varied GSH content regulates the kinase activity of MPK3

The next question we had addressed was whether the kinase activity of MPK3 is also GSH-dependant or not. Therefore, in-gel kinase assay of MPK3 using MBP as substrate was examined in *AtMPK3-1* line. Elevated level of kinase activity in *AtMPK3-1* line was noted with respect to Col-0 plants at 0 minute itself under combined (osmotic+ cold) abiotic stress treated condition (**Fig. 15A**). With increase in time, the kinase activity also got higher at 10 and 20 minutes intervals in treated samples of Col-0 and *AtMPK3-1* line compared samples at 0 minute. Moreover, to further find out whether GSH has any role to play in modulating the kinase activity of MPK3, similar in-gel kinase activity was performed using GSH and BSO-fed samples of Col-0 and *AtMPK3-1* line. It was noted that under GSH-fed condition, the kinase activity got higher and under BSO-fed condition the kinase activity got lessened (**Fig. 15B,C**). Altogether, this result proved that the kinase activity of MPK3 being altered by GSH.

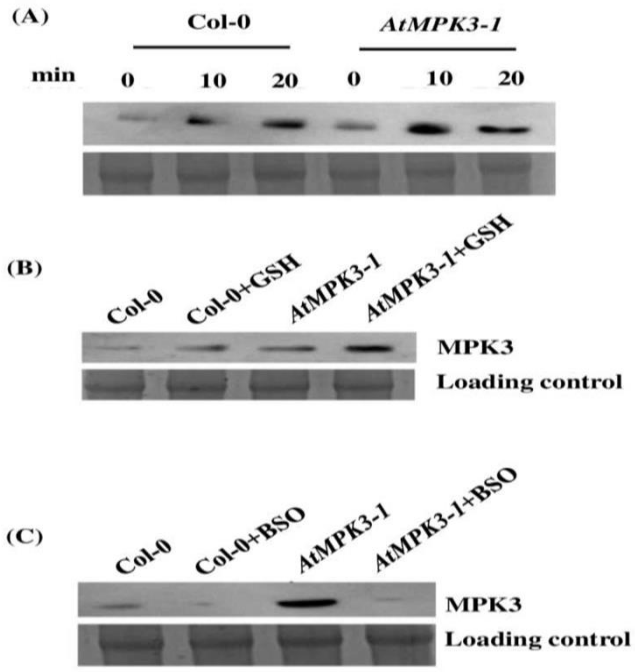

Fig. 15. In-gel kinase assay of MPK3 using MBP in Col-0 and *AtMPK3-1* plants. (A) Under combined (osmotic+cold) abiotic stress conditions. **(B)** Under GSH-fed condition. **(C)** Under BSO-fed condition. Coomassie staining of samples is the loading control. MPK3 phosphorylation in *AtMPK3-1* (without GSH-fed) and GSH-fed Col-0, *AtMPK3-1* were compared with Col-0 (without GSH feeding).

3.8. Procuring the TFs binding to MPK3 promoter

Unravelling the mechanism involved in GSH-MPK3 cross-talk was the next plan. PlantPan software [436] was utilised for shortlisting some TFs that might be responsible behind this cross-talk. The TFs having many binding sites in *MPK3* promoter region were selected viz. WRKY75, WRKY18, WRKY3, WRKY40, ZAT6, MYB44 and ERF6 and their conserved binding regions were GTCAA/TTGA, TTGAC, TGAC, TTGAC, CACT, CGGTT and CGGC respectively (**Fig. 16**). Depending on this *in silico* analysis, the above chosen TF mutants were procured from NASC to perform subsequent experiments.

CTTAAAAATCATAATTGAATAGTATCTTTTGTTTTTAAACTAATTTAGTCTATATAATAATAATATTATTA
ACCATCGTAAACCACACATGATATTCAATACTTATAATAAATTAATCGCATAAAATACAATACTTAAAA
CGAGTGTTATATAATTTTACGTAACGTAAAACAATACAAAATTTTAATTCCTGAACGAATAAAACGAG
TATATTAATTAATTTATTGATCGTATTAAAACGAATATGATCCAATTAAGATTACAATTACTAAAATCCC
CACACTATTATTGTCATTATTTAACTATGGCAGATAGATAGATACAGAACCGTAAAGGACGTTAGGAA
GAGGAAGAACGTTGACGAAGTCAACAACGAACAGAAACCGTCGATTTGAGGCGGCTCTAATCTCA
ACCACACGATCTTCTCTGCCTTTCCCTCTTCTCTCTTCTTCTTCTTCATCTTCTTCCTCGCAATTA
CCGCGAAAACTCATCTCTGCTCAATCCTCAATCTCAGTCTCTCTGTTGACTCCGACTGTTATATAAAA
CCATACAAATACCTTCAGATTCACTACTTCAAACCTCAAAGCAACCACTGAATCTCGACTTTGATCA
ATTGAGAGAGAA

Fig. 16. Promoter sequences of *MPK3*. Red, violet, deep green, pink, yellow and light green letters denote the binding sequences for transcription factors WRKY75, WRKY18, WRKY3, WRKY40, ZAT6, MYB44 and ERF6 respectively. TFs binding sequences were analyzed by PlantPan software.

3.9. WRKY40 is essential for GSH-mediated transcriptional activation of MPK3

It is obvious that GSH cannot directly regulate MPK3 activity. Therefore it became obligatory to identify the factor involved in this cross-talk. Accordingly, transcript analysis of all TFs mentioned above was performed in *pad2.1* mutant and GSH-fed Col-0 samples both under control and treated conditions. It may be noted that under control and treated conditions, among all the TFs, *WRKY40* revealed remarkably higher expression in GSH-fed Col-0 samples and

lower expression in *pad2.1* mutants (**Fig. 17A,B**). This data corroborated with immunoblot data (**Fig. 17C,D**). Further, WRKY40 expression was analysed in BSO-fed Col-0 samples. Results revealed its significantly reduced expression at both transcript and protein level (**Fig. 18A,B**). Thus, from the results it was hinted that WRKY40 might be the one that is required for the GSH-dependant regulation of MPK3 in *A. thaliana*.

Next, two separate groups of treatment were set viz. feeding with 100 μM GSH and treating with combined (osmotic+ cold) abiotic stress to the above selected TFs mutant plants as well as Col-0 as control. The transcript abundance of *MPK3* was analyzed in all TF mutant lines. Although *MPK3* expression level did not change much in any of the TF mutants except *wrky40* mutant under control condition (without GSH or stress treatment). Nonetheless, differential expression of *MPK3* transcript was noted upon feeding of GSH and *P. syringae* infection/abiotic stress treatment in *wrky75, wrky18, wrky3, zat6, myb44* and *erf6* mutants. Thus the result pointed towards the fact that GSH-MPK3 cross-talk does not involve these TFs. Fascinatingly, upon GSH-feeding and infection/abiotic stress treatment there was absence of any notable change in *MPK3* expression pattern in *wrky40* mutants (**Fig. 17E,F**). Similar data was observed at protein level (**Fig. 17G,H**). Hence, the result demonstrated that WRKY40 is very much needed in GSH-dependant MPK3 regulation. Additionally, we transfected *wrky40* mutant protoplasts with *proMPK3:GUS-GFP* construct and found no change in GFP fluorescence under GSH-fed condition (**Fig. 17I**).

Above results impelled us to perform co-transfection assay of *wrky40* mutant protoplast. Co-transfecting *YFP-WRKY40* **(**CDS of *WRKY40* was fused with YFP of *pAM-PAT-YFP***)** along with *proMPK3:GUS-GFP* construct in *wrky40* protoplast, showed the restoration of GFP florescence in the co-transfected protoplasts. Additionally, co-transfected protoplasts under GSH-fed condition revealed elevated GFP expression (**Fig. 17J**). Therefore, it can be concluded that WRKY40 is necessary for *MPK3* promoter activity in presence of GSH.

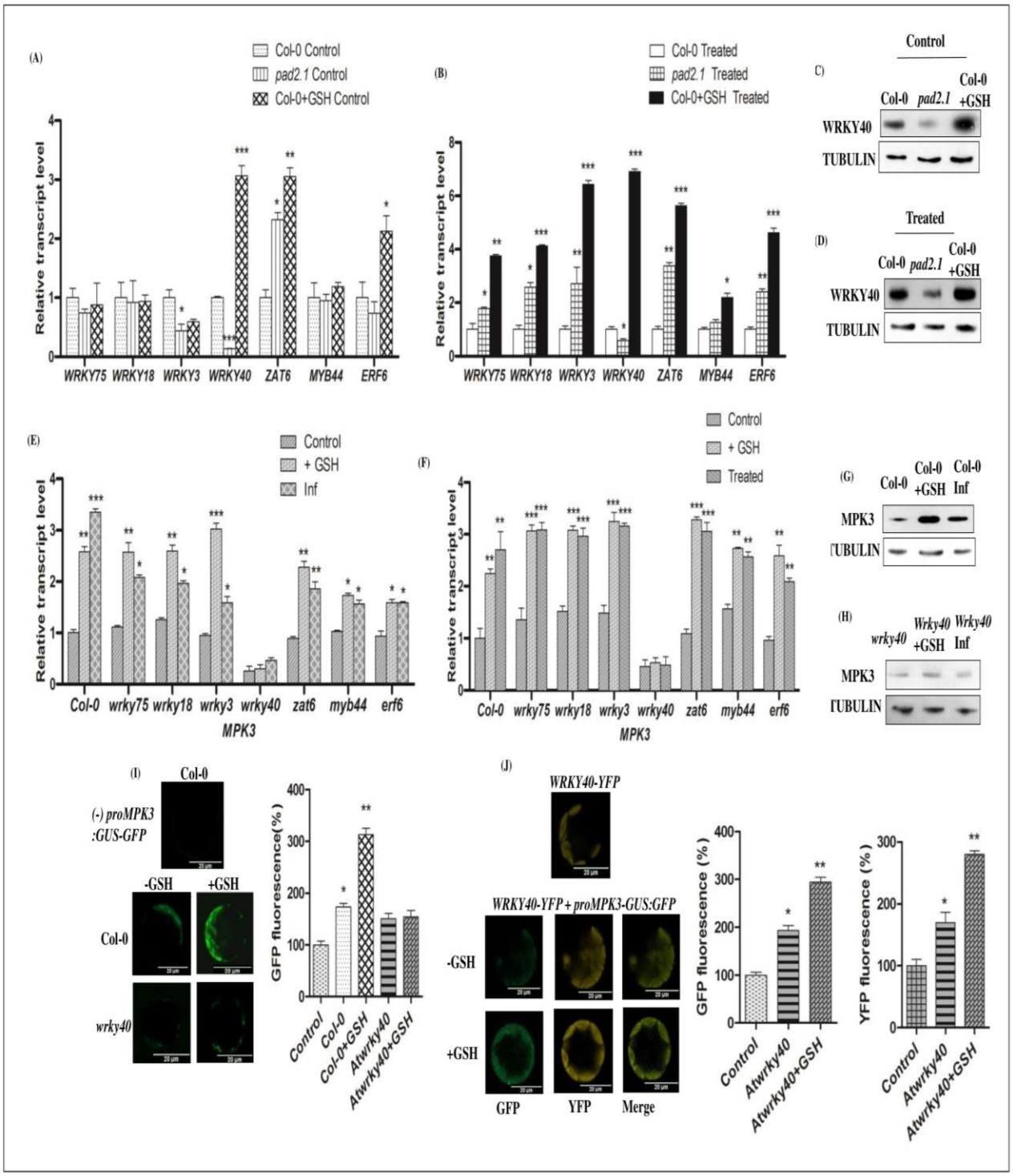
(A)
Col-0 Control
pad2.1 Control
Col-0+GSH Control
Relative transcript level
WRKY75 WRKY18 WRKY3 WRKY40 ZAT6 MYB44 ERF6
(B)
Col-0 Treated
pad2.1 Treated
Col-0+GSH Treated
Relative transcript level
WRKY75 WRKY18 WRKY3 WRKY40 ZAT6 MYB44 ERF6
C)
Control
Col-0 pad2.1 Col-0 +GSH
WRKY40
TUBULIN
(D)
Treated
Col-0 pad2.1 Col-0 +GSH
WRKY40
TUBULIN
(E)
Control
+ GSH
Inf
Relative transcript level
Col-0 wrky75 wrky18 wrky3 wrky40 zat6 myb44 erf6
MPK3
(F)
Control
+ GSH
Treated
Relative transcript level
Col-0 wrky75 wrky18 wrky3 wrky40 zat6 myb44 erf6
MPK3
(G)
Col-0 Col-0 +GSH Col-0 Inf
MPK3
TUBULIN
(H)
wrky40 Wrky40 +GSH Wrky40 Inf
MPK3
TUBULIN
(I)
Col-0
(-) proMPK3 :GUS-GFP
-GSH +GSH
Col-0
wrky40
GFP fluorescence(%)
Control Col-0 Col-0+GSH Atwrky40 Atwrky40+GSH
(J)
WRKY40-YFP
WRKY40-YFP + proMPK3-GUS:GFP
-GSH
+GSH
GFP YFP Merge
GFP fluorescence (%)
Control Atwrky40 Atwrky40+GSH
YFP fluorescence (%)
Control Atwrky40 Atwrky40+GSH

Fig. 17. WRKY40-mediated transcriptional induction of MPK3 by GSH. **(A)** Effect of altered GSH level on the expression profile of all TFs under control condition and **(B)** treated condition at the genetic level by qRT-PCR analysis. *Tubulin* was used as a reference gene for normalization. **(C)** Effect of altered GSH level on the expression profile of WRKY40 under control condition and **(D)** treated condition at the protein level by protein gel blot analysis. Tubulin expression was used as a loading control. Expression of TFs in GSH-fed Col-0 and *pad2.1* compared with Col-0. **(E)** Expression analysis of *MPK3* in TF mutants upon GSH feeding and *P. syringae* infection (inf). **(F)** *MPK3* expression analysis in TF mutants after GSH feeding, combined cold and osmotic stress treatment and **(G,H)** by protein gel blot analysis. MPK3 expression in GSH-fed and infected Col/ TFs mutants were compared with non-GSH-fed and infected Col/ TFs mutants. **(I)** Measurement of GFP fluorescence when *wrky40* mutant protoplasts were transformed with *proMPK3:GUS-GFP* upon GSH feeding. (-) *proMPK3:GUS-GFP* (lacking *MPK3* promoter): negative control. **(J)** Protoplasts of *wrky40* mutants were transformed with *WRKY40:YFP* construct and YFP expression monitored. Next, protoplasts of *wrky40* mutant lines were co-transformed with *WRKY40:YFP* and *proMPK3:GUS-GFP* constructs. YFP and GFP expression levels with or without GSH treatment were monitored. *WRKY40:YFP* was the positive control. Experiments were performed in triplicate. Bar = 20 µm. Data are the mean ± SE for three individual experiments using independently grown plants. *P<0.332, **P<0.002, ***P<0.001.

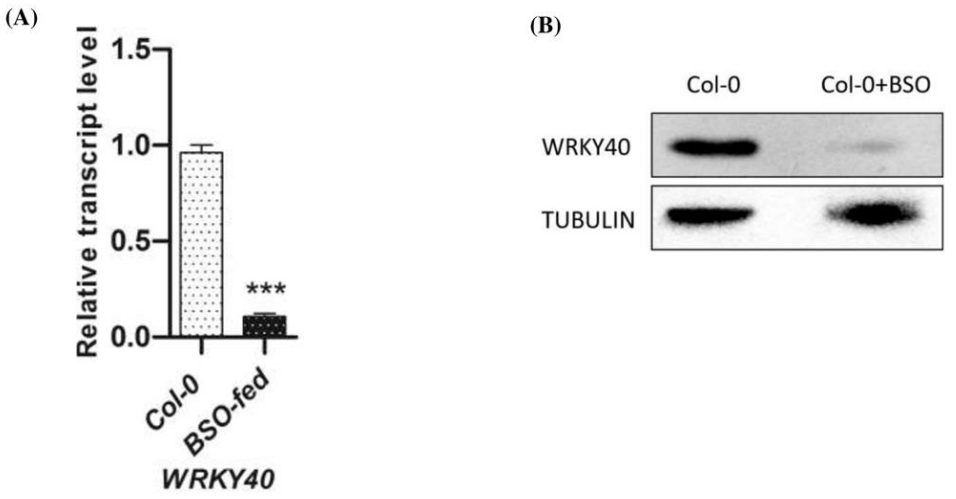

Fig. 18. WRKY40 expression analysis in BSO-fed Col-0 at (A) transcript level and **(B)** protein level in BSO-fed Col-0. Data are the mean ± SE for 3 individual experiments using plants grown independently. ***P<0.001.

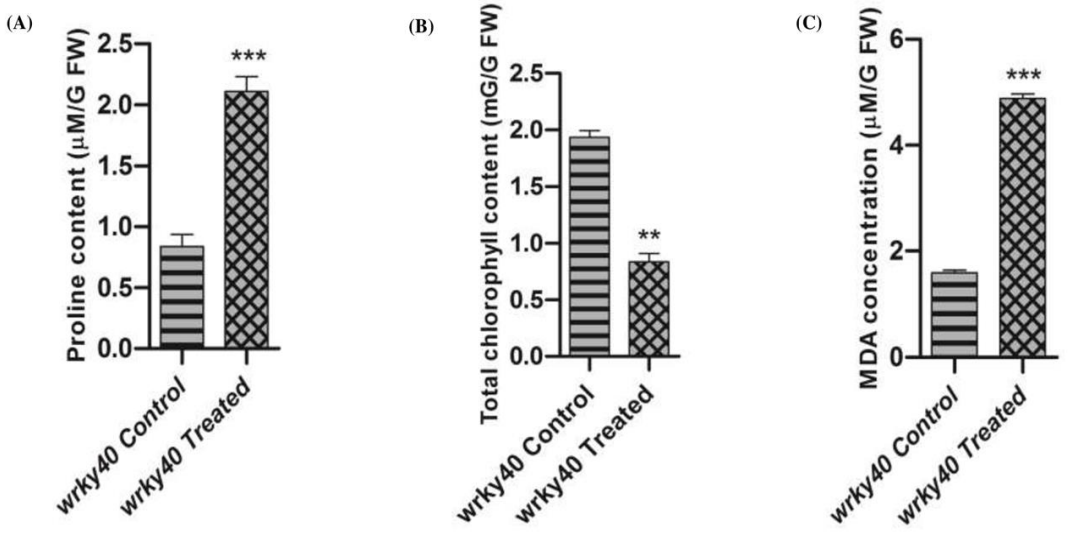

Fig. 19. Physiological response of *wrky40* mutant under combined cold and osmotic stress. **(A)** Estimation of proline content. **(B)** Estimation of chlorophyll. **(C)** Estimation of MDA concentration. Data are the mean ± SE for 3 individual experiments using plants grown independently. **P<0.002, ***P<0.001.

3.10. γ-ECS-WRKY40 interaction takes place under GSH-fed condition in A. thaliana

STRING 10 software analysis was used to exemplify protein interaction of γ-ECS, WRKY40 and MPK3 (**Fig. 20A**). Immunoprecipitating total proteins (Col-0, *pad2.1*, and GSH-fed Col-0) using anti-γ-ECS primary antibody and performing immunoblot assay of WRKY40, revealed higher expression of WRKY40 in GSH-fed Col-0 plants and lower expression in case of *pad2.1* plants (**Fig. 20B**), further confirmed the association between γ-ECS and WRKY40.

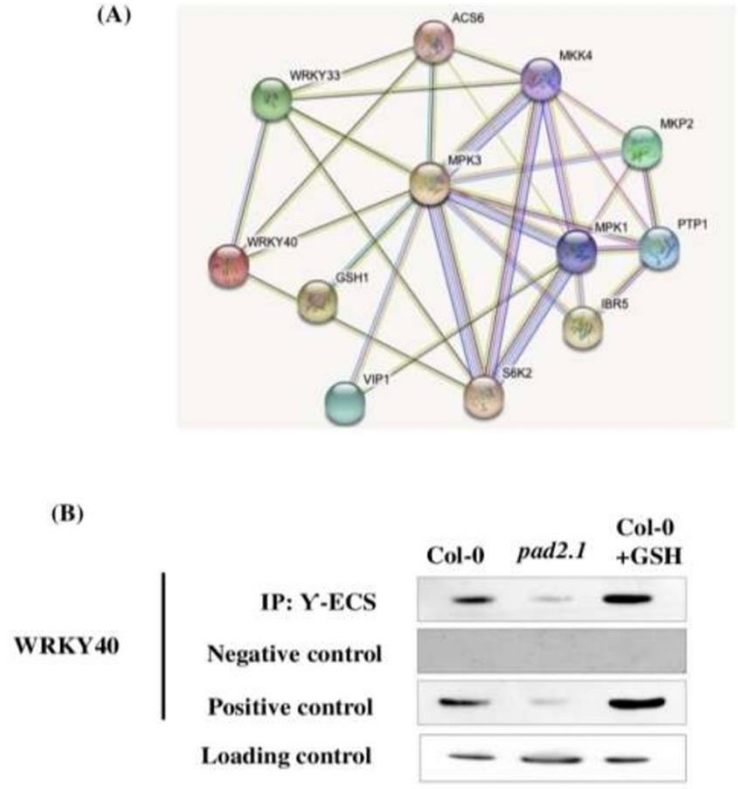

Fig. 20. Association γ-ECS and WRKY40. (A) In-silico analysis using STRING 10 software showing protein interactions among γ-ECS, WRKY40, and MPK3 proteins. **(B)** Protein immunoprecipitation followed by protein gel blot analysis showed an interaction between γ-ECS and WRKY40 under altered GSH conditions. Three types of controls were used: positive control (protein gel blot analysis of γ-ECS), negative control (non-specific binding control), and loading control. Experiments were repeated with three biological samples.

3.11. Increased Binding of WRKY40 to MPK3 promoter in response to GSH

To confirm GSH-WRKY40-MPK3 interaction, chromatin immunoprecipitation (ChIP)-quantitative PCR (qPCR) analysis of *WRKY40* on *MPK3* promoter was conducted under GSH-fed condition. Fascinatingly, results revealed that the percentage of input for *MPK3* promoter was 2.1 % in GSH-fed Col-0 plants and 0.45 % in *pad2.1* plants (**Fig. 21**) which further substantiated the importance of GSH in elevated binding of WRKY40 towards *MPK3* promoter, thus leading to higher rate *MPK3* transcription.

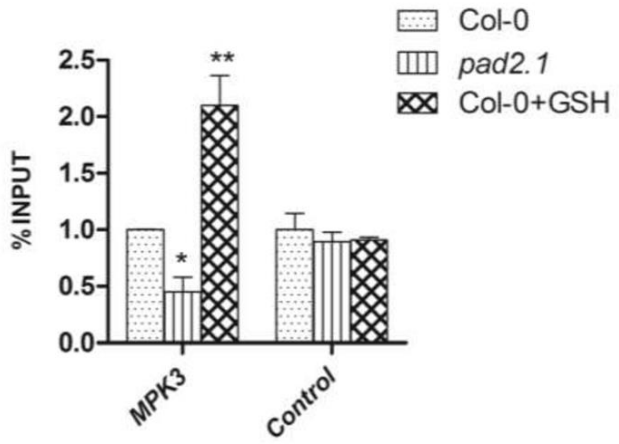

Fig. 21. Analysis of association of WRKY40 with promoters of MPK3 under altered GSH conditions. Association of RNA polymerase II with *GAPDH* promoter was used as control. Experiments were repeated with three biological samples. *P<0.332, **P<0.002.

4. Discussion

Stress factors (abiotic and biotic) viz. high temperature, chilling, salinity, heavy metals toxicity, light stress, pathogen invasion etc. greatly influence agricultural productivity by disturbing the metabolism and cellular homeostatic balance in plants. Under such stressful circumstances, plants exhibit pan-transcriptomic/proteomic changes by activating various stress-responsive programs leading to different phenotypic changes which includes altering the guard cell response via regulating the expression of genes related to opening and closing of stomata, variation in the response of root morphogenesis, accumulation of antioxidants, osmoprotectants and many more to deceive all the stress-driven impairment in the cells [85,446,447]. It is a widely known fact that GSH has an indispensable role in the context of plant stress tolerance [63,448,244,91]. Previous studies from our laboratory pointed out GSH's importance in controlling different types of protein, which includes proteins related to MPK cascade, under differential stress [244,77]. Few years back, interplay of GSH and SIPK/WIPK in combating *P. syringae* infection has been studied [215]. Nonetheless, the mechanism underlying the GSH and MPK interaction under stress is still unexplored. The present work elucidated that stress-driven GSH augmentation regulated MPK3 activation in a WRKY40-dependant manner.

The proteomics data of ***Chapter* 1** hinted towards GSH and MPK connection as MPK3 was noted to be up-accumulated in GSH-fed under stress treated condition. Therefore, the transcript analysis of a few *MPK* orthologs was conducted. The *MPK* orthologs were selected based on the previously mentioned proteomics study and earlier reports from our laboratory. Among the chosen MPK orthologs, MPK3 was observed to be notably up-accumulated in response to GSH feeding both in presence and absence of combined (osmotic+cold) abiotic stress (**Fig. 4**).

To further examine the GSH-mediated MPK3 regulation, the pattern of MPK3 expression was checked in Col-0 treated with BSO which showed remarkably less expression with respect to Col-0 without BSO treatment (**Fig. 5A,B**). This suggested that the GSH is responsible in increasing MPK3 expression in *A. thaliana*. We postulated that changes in cellular redox balance could be the reason for increased MPK3 expression. To rule out that point we checked MPK3 expression in Col-0 plant treated with DTT (strong reducing agent). No variation in MPK3 expression was noted under DTT-fed condition (**Fig. 5D,E**). Therefore, the result thus confirmed that this change in MPK3 expression is not for reducing environment induced by DTT but for any other factor/factors.

Next, MPK3 was over-expressed in *A. thaliana* and transgenic lines viz. *AtMPK3* was developed. The reason behind cloning *LeMPK3* in *Arabidopsis*, with 94 % similarity (81 % identity) at protein level was to investigate the cell-autonomous effect of MPK3 across all plant species. Two homozygous *AtMPK3* transgenic lines viz. *AtMPK3-1* and *AtMPK3-15* were developed, from which *AtMPK3-1* line revealed better MPK3 over-expression and thus was further utilized in later experiments. The stress tolerance capacity of *AtMPK3-1* line was evaluated which revealed better tolerance capacity to biotic stress viz. *P. syringae* infection and abiotic stress (salt stress and combined abiotic stress treatment), exhibiting the importance of MPK3 in plant stress tolerance (**Fig. 13,14**). Additionally, treatment with exogenous GSH ameliorated the stress tolerance potential of *Arabidopsis* under biotic stress (**Fig. 13A,C-E**). The phosphorylating capacity of MPK3 was better induced in response to GSH feeding (**Fig. 15**). Together, all the above results demonstrated the stress-driven interaction of GSH and MPK3. Thereafter, the expression check of γ-ECS at elevated MPK3 level showed increased expression in *AtMPK3-1* lines (**Fig. 10**).

The significant participation of the MPK signaling cascade in developing plant stress tolerance is a well-known fact [449]. Evidently, GSH is known to coordinate various stress responses by controlling various genes and proteins at different levels forming a very complex networking system. Consequently, our work primarily emphasized on unravelling the GSH-MPK3 cross-talk. This cross-talk/interaction can happen in many ways. For example, GSH can influence *MPK3* expression by increasing its promoter activity, or increased production of GSH under stress can result in activating MPK3. On that account, exploring the probable mechanism/pathway underlying the GSH and MPK3 cross-talk under stress conditions would be fascinating.

The promoter transformation assay with *MPK3* promoter fused with GFP (*proMPK3:GUS-GFP*) showed higher promoter activity (GFP fluorescence) in response to GSH feeding within Col-0 protoplasts in absence of stress conditions. Additionally, this GFP fluorescence increased further under treated conditions (**Fig. 12C**). In *pad2.1* mutants, the fluorescence got notably diminished both in presence and absence of combined (osmotic+ cold) abiotic stress conditions which is probably due to fact that *pad2.1* mutants contains only 22 % of the total GSH amount of wild-type Col-0.

Till now it was evident there is an inter-relationship between GSH and MPK3 under environmental stress. No matter how it was not known what factor/s is/are behind this cross-talk. It is obvious that GSH alone is unable to bind to the promoter region of *MPK3* and determine its expression. For that reason, it was required to find out that factor/factors activating *MPK3* in presence of GSH. WRKYs are a group of TFs that are known to regulate different plant processes, including the responses to biotic and abiotic stresses [450]. Besides, WRKY40 has the ability to bind to its own promoter and auto-regulate its activity [451]. Similarly, *in silico* analysis revealed that the promoter region of *MPK3* had binding sites for WRKY40 [452,453], whose expression was also noted higher under GSH-fed condition in Col-0. Whereas WRKY40 showed lower expression in *pad2.1* under control and treated conditions (**Fig. 17A-D**). Upon GSH feeding/*P. syringae* infection/different abiotic stress treatments, the *wrky40* mutant line did not exhibit any variation in *MPK3* activation (**Fig. 17E-J**). This result was substantiated with co-transformation assay in *wrky40* mutant protoplasts co-transformed with *YFP-WRKY40* and *proMPK3:GUS-GFP* that appeared to re-establish GFP fluorescence (**Fig. 17J**). The above

results clearly showed that GSH augmentation in plants induced the *MPK3* expression in a WRKY40-dependent manner.

STRING 10 protein-protein interaction analysis elucidated the relationship between γ-ECS and WRKY40 (**Fig. 20A**). The protein immunoprecipitation assay detected by protein immunoblot assay unveiled an elevated level of WRKY40 expression under GSH-fed condition in plant cells (**Fig. 20B**). ChIP-qPCR analysis further demonstrated that high cellular GSH level increased the binding of WRKY40 to *MPK3* promoter, leading to increased expression of this gene (**Fig. 21**). Altogether, we suggested GSH induces *MPK3* transcription in a WRKY40-mediated manner under stress conditions, increasing the transcript level of *MPK3*.

The proposed model for this GSH-MPK3 interplay has been summarized in **Fig. 22** where it has been shown that GSH positively regulates the expression levels of MPK3. It was further established that GSH induces MPK3 by up-regulating the expression of WRKY40, which plays a pivotal role in activating the promoters of MPK3.Under stress, elevated GSH content inside the cell is inducing the expression of WRKY40. Increased level of WRKY40 is leading to higher expression of MPK3 by binding to its promoter. However, apart from WRKY40 mediated modulation of MPK3 by GSH, there might be other factor/s working with WRKY40 in this GSH-MPK3 interplay, which is yet to be explored. This will be another interesting area that will increase the understanding of stress mitigation.

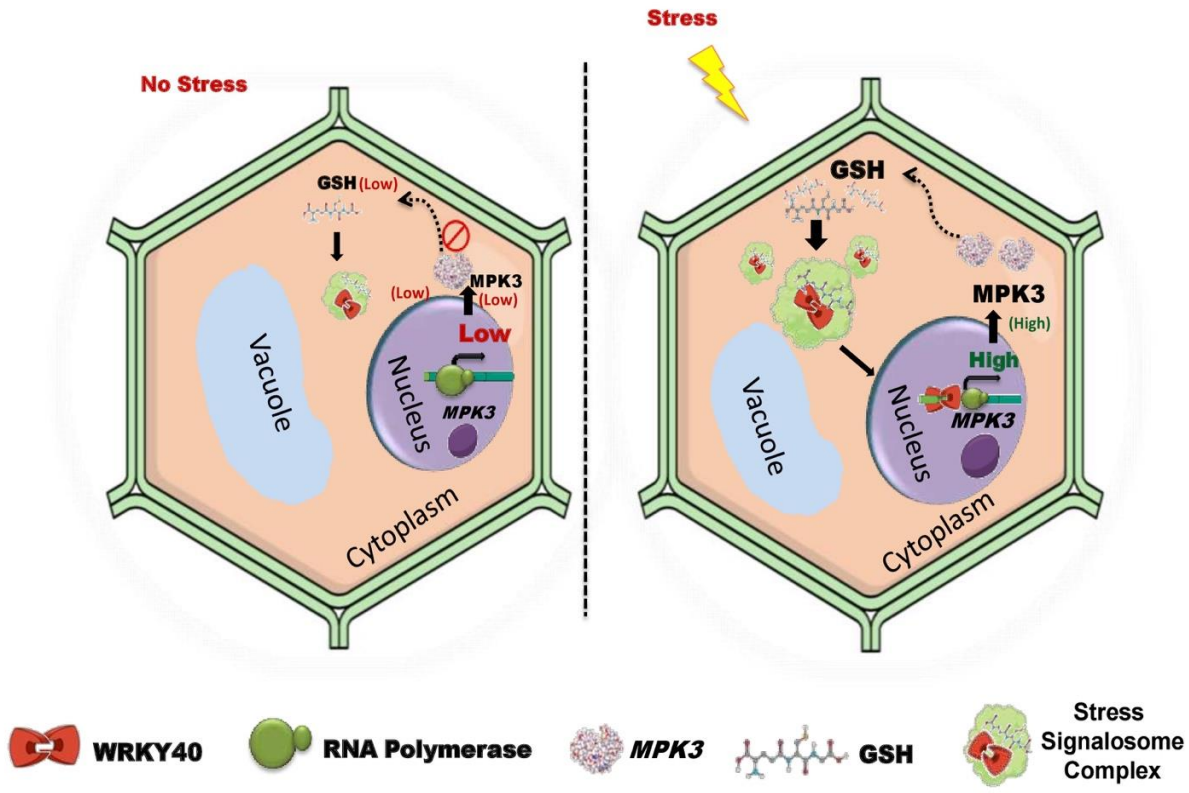

Fig. 22. Proposed model for the modulation of MPK3 by GSH. Under stress conditions, enhanced GSH content increased the expression of the WRKY40 transcription factor, which increased the binding of WRKY40 to the *MPK3* promoter, thereby inducing *MPK3* expression.

SUMMARY

[SUMMARY]

Plant defense response is regulated by a network of signal transduction pathways in which GSH is one of the vital players. Previous studies also reported the involvement of GSH in a multi-step crosstalk with MPK cascade to combat environmental stresses as well as alteration of *MPK* genes under varied GSH conditions [243,215,77]. Nonetheless, the mechanism of GSH-MPK interplay is still largely unexplored. With this background, the present research aims to unravel the role of GSH in plant defense.

Initially, the proteome response of GSH-fed Col-0 (wild-type), under combined (osmotic+cold) abiotic stress was studied. Interestingly, many stress-responsive proteins involved in PTI-related first line of defense and proteins taking part in many signaling pathways were up-accumulated signifying a dynamic role of GSH in plant defense. MPK3 was up-accumulated under stress in GSH-fed Col-0 samples.

To obtain a deeper insight, the expressions of few MPK isoforms were checked in GSH-fed Col-0 plants and *pad2.1*, a GSH-deficient *Arabidopsis* mutant. Interestingly, MPK3 was significantly up-regulated in GSH-fed Col-0 and down-regulated in *pad2.1*. Promoter activation assay further established that GSH feeding activates MPK3 expression in *A. thaliana* by inducing its promoter. Next, *MPK3* was overexpressed in *A. thaliana* and independent transgenic (*AtMPK3*) lines were raised and characterized by genomic DNA PCR, qRT-PCR, and Western blot analysis. Surprisingly, transcript and protein level of γ-ECS (the rate-limiting enzyme of GSH biosynthesis) was higher in *AtMPK3-1* transgenic line. An in-gel kinase assay exhibited hyperphosphorylation of MBP in the GSH-fed *AtMPK3* transgenic line. Additionally, GSH-fed *AtMPK3-1* plants exhibited resistance against various stress factors representing a key role of GSH-MPK3 interplay in plant stress tolerance.

Furthermore, expression analysis of few selected TFs (based on *in-silico* analysis) during control and combined abiotic stress treated conditions revealed the up-regulated expression of WRKY40 under enhanced GSH condition. Interestingly, GSH feeding was rendered ineffective in altering MPK3 expression in the *Atwrky40* mutant, emphasizing the involvement of WRKY40 in GSH-MPK3 interplay. This was further confirmed by a *wrky40* co-transformation assay. STRING 10 software analysis illustrated the interaction between γ-ECS and WRKY40. The immunoprecipitation assay followed by ChIP-qPCR showed a significant increase in the binding of WRKY40 to *MPK3* promoter upon GSH feeding. Together, the study demonstrated that GSH modulates MPK3 expression via WRKY40 in response to stress.

REFERENCES

1. Mittler R, Vanderauwera S, Gollery M, Van Breusegem F (2004) Reactive oxygen gene network of plants. Trends Plant Sci. 9: 490–498.

2. Asada K (2006) Production and scavenging of reactive oxygen species in chloroplasts and their functions. Plant Physiol. 141: 391–396.

3. Miller G, Coutu J, Shulaev V, Mittler R (2008) Reactive oxygen signalling in plants. Intracellular Signalling in Plants (ed. Yang Z.) Annu. Plant Rev. 33: 189–201.

4. García-Mata C, Lamattina L (2001) Nitric oxide induces stomatal closure and enhances the adaptive plant responses against drought stress. Plant Physiol. 126: 1196–1204.

5. Zeidler D, Zähringer U, Gerber I, Dubery I, Hartung T, Bors W, Hutzler P, Durner J (2004) Innate immunity in *Arabidopsis thaliana*: lipopolysaccharides activate nitric oxide synthase (NOS) and induce defense genes. Proc. Nat. Acad. Sci. 101: 15811–15816.

6. Creelman RA, Mullet JE (1995) Jasmonic acid distribution and action in plants: regulation during development and response to biotic and abiotic stress. Proc. Natl. Acad. Sci. 92: 4114–4119.

7. Paschold A, Halitschke R, Baldwin IT (2007) Co(i)-ordinating defenses: NaCOI1 mediates herbivore-induced resistance in *Nicotiana attenuata* and reveals the role of herbivore movement in avoiding defenses. Plant J. 51: 79–91.

8. Pieterse CM, Leon-Reyes A, Van der Ent S, Van Wees SC (2009) Networking by small-molecule hormones in plant immunity. Nat. Chem. Biol. 5: 308.

9. Vlot AC, Dempsey DA, Klessig DF (2009) Salicylic acid, a multifaceted hormone to combat disease. Annu. Rev. Phytopathol. 47: 177–206.

10. Cutler SR, Rodriguez PL, Finkelstein RR, Abrams SR (2010) Abscisic acid: emergence of a core signaling network. Annu. Rev. Plant Biol. 61: 651–679.

11. Hartman S, Liu Z, Van Veen H, Vicente J, Reinen E, Martopawiro S, Zhang H, van Dongen N, Bosman F, Bassel GW, Visser EJW, Bailey-Serres J, Theodoulou FL, Hebelstrup KH, Gibbs DJ, Holdsworth MJ, Sasidharan R, Voesenek LACJ (2019) Ethylene-mediated nitric oxide depletion pre-adapts plants to hypoxia stress. Nat. Comm. 10: 1–9.

12. Prakash V, Singh VP, Tripathi DK, Sharma S, Corpas FJ (2021) Nitric oxide (NO) and salicylic acid (SA): A framework for their relationship in plant development under abiotic stress. Plant Biol. 23: 39–49.

13. Flors V, Ton J, Jakab G, Mauch-Mani B (2005) Abscisic acid and callose: team players in defence against pathogens? J. Phytopathol. 153: 377–383.

14. Cui W, Lee JY (2016) *Arabidopsis* callose synthases CalS1/8 regulate plasmodesmal permeability during stress. Nat. Plants 2: 1–9.

15. Hunter K, Kimura S, Rokka A, Tran HC, Toyota M, Kukkonen JP, Wrzaczek M (2019) CRK2 enhances salt tolerance by regulating callose deposition in connection with PLDα1. Plant Physiol. 180: 2004–2021.

16. Wang Y, Li X, Fan B, Zhu C, Chen Z (2021) Regulation and Function of Defense-Related Callose Deposition in Plants. Int. J. Mol. Sci. 22: 2393.

17. Liu J, Liu Y, Wang S, Cui Y, Yan D (2022) Heat Stress Reduces Root Meristem Size via Induction of Plasmodesmal Callose Accumulation Inhibiting Phloem Unloading in *Arabidopsis*. Int. J. Mol. Sci. 23: 2063.

18. Zhang S, Klessig DF (2001) MAPK cascades in plant defense signaling. Trends Plant Sci. 6: 520–527.

19. Meng X, Zhang S (2013) MAPK cascades in plant disease resistance signaling. Annu. Rev Phytopathol. 51: 245–266.

20. Li J, Liu X, Wang Q, Huangfu J, Schuman MC, Lou Y (2019) A group D MAPK protects plants from autotoxicity by suppressing herbivore-induced defense signaling. Plant Physiol. 179: 1386–1401.

21. Dong X (1998) SA, JA, ethylene, and disease resistance in plants. Curr. Opin. Plant Biol. 1: 316–323.

22. Thomma BPHJ, Eggermont K, Penninckx IAMA, Mauch-Mani B, Vogelsang R, Cammue BPA, Broekaert WF (1998) Separate jasmonate dependent and salicylate dependent defense-response pathways in *Arabidopsis* are essential for resistance to distinct microbial pathogens. Proc. Natl. Acad. Sci. USA 95: 15107–15111.

23. Singh KB, Foley RC, Oñate-Sánchez L (2002) Transcription factors in plant defense and stress responses. Curr. Opin. Plant Biol. 5: 430-436.

24. Loake G, Grant M (2007) Salicylic acid in plant defence-the players and protagonists. Curr. Opin. Plant Biol. 10: 466–472.

25. Qin F, Sakuma Y, Tran LS, Maruyama K, Kidokoro S, Fujita Y, Fujita M, Umezawa T, Sawano Y, Miyazono KI, Tanokura M, Shinozaki K, Yamaguchi-Shinozaki K (2008) *Arabidopsis* DREB2A-interacting proteins function as RING E3 ligases and negatively regulate plant drought stress-responsive gene expression. Plant Cell 20: 1693–1707.

26. Lata C, Prasad M (2011) Role of DREBs in regulation of abiotic stress responses in plants. J. Exp. Bot. 62: 4731–4748.

27. Yoshida T, Fujita Y, Maruyama K, Mogami J, Todaka D, Shinozaki K, Yamaguchi-Shinozaki K. (2015) Four *Arabidopsis* AREB/ABF transcription factors function predominantly in gene expression downstream of SnRK2 kinases in abscisic acid signalling in response to osmotic stress. Plant Cell Environ. 38: 35–49.

28. Javed T, Shabbir R, Ali A, Afzal I, Zaheer U, Gao SJ (2020) Transcription factors in plant stress responses: Challenges and potential for sugarcane improvement. Plants 9: 491.

29. Oh MH, Wang X, Wu X, Zhao Y, Clouse SD, Huber SC (2010) Autophosphorylation of Tyr-610 in the receptor kinase BAK1 plays a role in brassinosteroid signaling and basal defense gene expression. Proc. Natl. Acad. Sci. 107: 17827–17832.

30. Belkhadir Y, Jaillais Y, Epple P, Balsemão-Pires E, Dangl JL, Chory J (2012) Brassinosteroids modulate the efficiency of plant immune responses to microbe-associated molecular patterns. Proc. Natl. Acad. Sci. 109: 297–302.

31. Zhang DW, Deng XG, Fu FQ, Lin HH (2015) Induction of plant virus defense response by brassinosteroids and brassinosteroid signaling in *Arabidopsis thaliana*. Planta 241: 875–885.

32. Nolan TM, Vukašinović N, Liu D, Russinova E, Yin Y (2020) Brassinosteroids: Multidimensional regulators of plant growth, development, and stress responses. Plant Cell 32: 295–318.

33. Kour J, Kohli SK, Khanna K, Bakshi P, Sharma P, Singh AD, Ibrahim M, Devi K, Sharma N, Ohri P, Skalicky M (2021) Brassinosteroid Signaling, Crosstalk and, Physiological Functions in Plants Under Heavy Metal Stress. Front. Plant Sci. 12.

34. Shi H, Li Q, Luo M, Yan H, Xie B, Li X, Zhong G, Chen D, Tang D (2022) BRASSINOSTEROID-SIGNALING KINASE1 modulates MAP KINASE15 phosphorylation to confer powdery mildew resistance in Arabidopsis. Plant Cell 34: 1768–1783.

35. Romeis T, Piedras P, Jones JD (2000) Resistance gene-dependent activation of a calcium-dependent protein kinase in the plant defense response. Plant Cell 12: 803–815.

36. Dubiella U, Seybold H, Durian G, Komander E, Lassig R, Witte CP, Schulze WX, Romeis T (2013) Calcium-dependent protein kinase/NADPH oxidase activation circuit is required for rapid defense signal propagation. Proc. Natl. Acad. Sci. 110: 8744–9749.

37. Liao C, Zheng Y, Guo Y (2017) MYB30 transcription factor regulates oxidative and heat stress responses through ANNEXIN-mediated cytosolic calcium signaling in *Arabidopsis*. New Phytol. 216: 163–177.

38. Manishankar P, Wang N, Köster P, Alatar AA, Kudla J (2018) Calcium signaling during salt stress and in the regulation of ion homeostasis. J. Exp. Bot. 69: 4215–4226.

39. Mittler R, Vanderauwera S, Suzuki N, Miller GA, Tognetti VB, Vandepoele K, Gollery M, Shulaev V, Van Breusegem F (2011) ROS signaling: the new wave? Trends Plant Sci. 16: 300–309.

40. Suzuki N, Miller G, Morales J, Shulaev V, Torres MA, Mittler R (2011) Respiratory burst oxidases: the engines of ROS signaling. Curr. Opin. Plant Biol. 14: 691–699.

41. Bergmann L, Rennenberg H (1993) Glutathione metabolism in plants. In: LJ De Kok, I Stulen, H Rennenberg, C Brunold, WE Rauser (eds) *Sulfur Nutrition and Sulfur Assimilation in Higher Plants*. SPB Academic Publishers, The Hague, The Netherlands, pp. 109–123.

42. Meister A, Anderson ME (1983) Glutathione. Annu. Rev. Biochem. 52: 711–760.

43. Kunert KJ, Foyer CH (1993) Thiol/disulphide exchange in plants. In: De Kok LJ, Stulen I, Rennenberg H, Brunhold C, Rausen W (eds) *Sulfur Nutrition and Assimilation in*

Higher Plants. Regulatory, Agricultural and Environmental Aspects. SPB Academic Publishers, The Hague, The Netherlands, pp. 139–151.

44. Rennenberg H (1997) Molecular approaches to glutathione biosynthesis. In: Cram WJ, DeKok LJ, Stulen I, Brunold C, Rennenberg H (eds) *Sulphur Metabolism in Higher Plants.* Backhuys Publishers, Leiden, The Netherlands, pp. 59–70.

45. Kalinina EV, Chernov NN, Novichkova MD (2014) Role of glutathione, glutathione transferase, and glutaredoxin in regulation of redox-dependent processes. Biochemistry 79: 1562–1583.

46. Li H, Xu H, Graham DE, White RH (2003) Glutathione synthetase homologs encode alpha-L-glutamate ligases for methanogenic coenzyme F420 and tetrahydrosarcinapterin biosyntheses. Proc. Natl. Acad. Sci. USA 100: 9785–9790.

47. Foyer CH, Halliwell B (1976) The presence of glutathione and glutathione reductase in chloroplasts: a proposed role in ascorbic acid metabolism. Planta 133: 21–25.

48. Foyer CH, and Noctor G (2011) Ascorbate and glutathione: the heart of the redox hub. Plant Physiol. 155: 2–18.

49. Noctor G, Mhamdi A, Chaouch S, Han Y, Neukermans J, Marquez- Garcia B, Queval G, Foyer CH (2012) Glutathione in plants: an integrated overview. Plant Cell Environ. 35: 454–484.

50. Rennenberg H (1995) Processes involved in glutathione metabolism. In: RM Wallsgrove (ed) *Amino Acids and their Derivatives in Higher Plants*. Cambridge University Press, Cambridge, UK, pp. 155–171.

51. Foyer CH, Souriau N, Perret S, Lelandais M, Kunert KJ, Pruvost C, Jouanin L (1995) Overexpression of glutathione reductase but not glutathione synthetase leads to increases in antioxidant capacity and resistance to photoinhibition in poplar trees. Plant Physiol. 109: 1047–1057.

52. Foyer CH, Noctor G (2005) Redox homeostasis and antioxidant signaling: a metabolic interface between stress perception and physiological responses. Plant Cell 17: 1866–1875.

53. Meister A (1988) Glutathione metabolism and its selective modification. J. Biol. Chem. 263: 17205–17208.

54. Hell R, Bergmann L (1990) γ-Glutamylcysteine synthetase in higher plants: catalytic properties and subcellular localization. Planta 180: 603–612.

55. Schneider S, Bergmann L (1995) Regulation of glutathione synthesis in suspension cultures of parsley and tobacco. Bot. Acta. 108: 34–40.

56. Rüegsegger A, Brunold C (1992) Effect of cadmium on γ-glutamylcysteine synthesis in maize seedlings. Plant Physiol. 99: 428–433.

57. Strohm M, Jouanin L, Kunert K-J, Pruvost C, Polle A, Foyer CH, Rennenberg H (1995) Regulation of glutathione synthesis in leaves of transformed poplar (*Populus tremula* X *P. alba*) overexpressing glutathione synthetase. Plant J. 7: 141–145.

58. Wachter A, Wolf S, Steininger H, Bogs J, Rausch T (2005) Differential targeting of GSH1 and GSH2 is achieved by multiple transcription initiation: implications for the compartmentation of glutathione biosynthesis in the Brassicaceae. Plant J. 41: 15–30.

59. Pasternak M, Lim B, Wirtz M, Hell R, Cobbett CS, Meyer AJ (2008) Restricting glutathione biosynthesis to the cytosol is sufficient for normal plant development. Plant J. 53: 999–1012.

60. Maughan SC, Pasternak M, Cairns N, Kiddle G, Brach T, Jarvis R, Haas F, Nieuwland J, Lim B, Müller C, Salcedo-Sora E, Kruse C, Orsel M, Hell R, Miller AJ, Bray P, Fover CH, Murray JA, Meyer AJ, Cobbett CS (2010) Plant homologs of the *Plasmodium falciparum* chloroquine-resistance transporter, PfCRT, are required for glutathione homeostasis and stress responses. Proc. Natl. Acad. Sci. USA 107: 2331–2336.

61. Lu SC (2009) Regulation of glutathione synthesis. Mol. Aspects Med. 30: 42–59.

62. Noctor G, Gomez L, Vanacker H, Foyer CH (2002) Interactions between biosynthesis, compartmentation and transport in the control of glutathione homeostasis and signalling. J. Exp. Bot. 53: 1283–1304.

63. Noctor G, Foyer CH (1998) ASCORBATE AND GLUTATHIONE: Keeping active oxygen under control. Annu. Rev. Plant Physiol. Plant Mol. Biol. 49: 249–279.

64. Meyer AJ, May MJ, Fricker M (2001) Quantitative *in vivo* measurement of glutathione in *Arabidopsis* cells. Plant J. 27: 67–78.

65. Bielawski W, Joy KW (1986) Reduced and oxidised glutathione and glutathione-reductase activity in tissues of *Pisum sativum*. Planta 169: 267–272.

66. Ball L, Accotto GP, Bechtold U, Creissen G, Funck D, Jimenez A, Kular B, Leyland N, Mejia-Carranza J, Reynolds H, Karpinski S, Mullineaux PM (2004) Evidence for a direct link between glutathione biosynthesis and stress defense gene expression in *Arabidopsis*. Plant Cell 16: 2448–2462.

67. Hartmann T, Hönicke P, Wirtz M, Hell R, Rennenberg H, Kopriva S (2004) Regulation of sulphate assimilation by glutathione in poplars (*Populus tremula*× *P. alba*) of wild type and overexpressing γ-glutamylcysteine synthetase in the cytosol. J. Exp. Bot. 55: 837–845.

68. Gutierrez-Alcala G, Gotor C, Meyer AJ, Fricker M, Vega JM, Romero LC (2000) Glutathione biosynthesis in *Arabidopsis* trichome cells. Proc. Natl. Acad. Sci. USA 97: 11108–11113.

69. Meyer AJ, Fricker MD (2000) Direct measurement of glutathione in epidermal cells of intact *Arabidopsis* roots by two-photon laser scanning microscopy. J. Microscopy 198: 174–181.

70. Mou Z, Fan W, Dong X (2003) Inducers of plant systemic acquired resistance regulate NPR1 function through redox changes. Cell 113: 935–944.

71. Su T, Xu J, Li Y, Lei L, Zhao L, Yang H, Feng J, Liu G, Ren D (2011) Glutathione-indole-3-acetonitrile is required for camalexin biosynthesis in *Arabidopsis thaliana*. Plant Cell 23: 364–380.

72. Rouhier N, Lemaire SD, Jacquot JP (2008) The role of glutathione in photosynthetic organisms: emerging functions for glutaredoxins and glutathionylation. Annu. Rev. Plant Biol. 59: 143–166.

73. Zaffagnini M, Bedhomme M, Marchand CH, Morisse S, Trost P, Lemaire SD (2012) Redox regulation in photosynthetic organisms: focus on glutathionylation. Antioxid. Redox Signal. 16: 567–586.

74. Pasternak T, Asard H, Potters G, Jansen MAK (2014) The thiol compounds glutathione and homoglutathione differentially affect cell development in alfalfa (*Medicago sativa* L.). Plant Physiol. Biochem. 74: 16–23.

75. Bossio E, Diaz Paleo A, del vas M, baroli I, Acevedo A, Rios RD (2013) Silencing of the glutathione biosynthetic pathway inhibits somatic embryogenesis in wheat. Plant Cell Tiss. Org. Cult. 112: 239–248.

76. Xin X, Tian Q, Yin G, Chen X, Zhang J, Ng S, Lu X (2014) Reduced mitochondrial and ascorbate-glutathione activity after artificial ageing in soybean seed. J. Plant Physiol. 171: 140–147.

77. Sinha R, Kumar D, Datta R, Hazra S, Bhattacharyya D, Mazumdar AB, Mukhopadhyay R, Sultana A, Chattopadhyay S (2015) Integrated transcriptomic and proteomic analysis of *Arabidopsis thaliana* exposed to glutathione unravels its role in plant defense. Plant Cell Tiss. Org. Cult. 120: 975–988.

78. Vernoux T, Wilson RC, Seeley KA, Reichheld JP, Muroy S, Brown S, Maughan SC, Cobbett CS, Van Montagu M, Inzé D, May MJ, Sung ZR (2000) The *root meristemless1*/*cadmium sensitive 2 g*ene defines a glutathione-dependent pathway involved in initiation and maintenance of cell division during postembryonic root development. Plant Cell 122: 97–109.

79. Cairns NG, Pasternak M, Wachter A, Cobbett CS, Meyer AJ (2006) Maturation of *Arabidopsis* seeds is dependent on glutathione biosynthesis within the embryo. Plant Physiol. 141: 446–455.

80. Speiser A, Silbermann M, Dong Y, Haberland S, Uslu VV, Wang S, Bangash SA, Reichelt M, Meyer AJ, Wirtz M, Hell R (2018) Sulfur partitioning between glutathione and protein synthesis determines plant growth. Plant Physiol. 177: 927–937.

81. Basu U, Upadhyaya HD, Srivastava R, Daware A, Malik N, Sharma A, Bajaj D, Narnoliya L, Thakro V, Kujur A, Tripathi S, Bharadwaj C, Hedge VS, Pandey AK, Singh AK, Tyagi AK, Parida SK (2019) ABC transporter-mediated transport of glutathione conjugates enhances seed yield and quality in chickpea. Plant Physiol. 180: 253–275.

82. García-Quirós E, Alché JD, Karpinska B, Foyer CH (2020) Glutathione redox state plays a key role in flower development and pollen vigour. J. Exp. Bot. 71: 730–741.

83. Pareek A, Dhankher OP, Foyer CH (2020) Mitigating the impact of climate change on plant productivity and ecosystem sustainability. J. Exp. Bot. 71: 451–416.

84. Takahashi S, Murata N (2008) How do environmental stresses accelerate photoinhibition? Trends Plant Sci. 13: 178–182.

85. Gill SS, Tuteja N (2010) Reactive oxygen species and antioxidant machinery in abiotic stress tolerance in crop plants. Plant Physiol. Biochem. 48: 909–930.

86. Liu YJ, Yuan Y, Liu YY, Liu Y, Fu JJ, Zheng J, Wang GY (2012) Gene families of maize glutathione-ascorbate redox cycle respond differently to abiotic stresses. J. Plant Physiol. 169: 183–192.

87. Szarka A, Tomasskovics B, Bánhegyi G (2012) The Ascorbate-glutathione-α-tocopherol triad in abiotic stress response. Int. J. Mol. Sci. 13: 4458–4483.

88. Schnaubelt D, Schulz P, Hannah MA, Yocgo RE, Foyer CH (2013) A phenomics approach to the analysis of the influence of glutathione on leaf area and abiotic stress tolerance in *Arabidopsis thaliana*. Front. Plant Sci. 4: 416.

89. Heyneke E, Luschin-Ebengreuth N, Krajcer I, Wolkinger V, Müller M, Zechmann B (2013) Dynamic compartment specific changes in glutathione and ascorbate levels in *Arabidopsis* plant exposed to different light intensities. BMC Plant. Biol. 13: 104.

90. Borgohain P, Saha B, Agrahari R, Chowardhara B, Sahoo S, van der Vyver C, Panda SK (2019) SlNAC2 overexpression in *Arabidopsis* results in enhanced abiotic stress tolerance with alteration in glutathione metabolism. Protoplasma 27: 1–3.

91. Hasanuzzaman M, Bhuyan MH, Anee TI, Parvin K, Nahar K, Mahmud JA, Fujita M (2019) Regulation of ascorbate-glutathione pathway in mitigating oxidative damage in plants under abiotic stress. Antioxidants 8: 384.

92. Ruiz JM, Blumwald E (2002) Salinity-induced glutathione synthesis in *Brassica napus*. Planta 214: 965–969.

93. Mittova V, Tal M, Volokita M, Guy M (2003) Up-regulation of the leaf mitochondrial and peroxisomal antioxidative systems in response to salt-induced oxidative stress in the wild salt-tolerant tomato species *Lycopersicon pennellii*. Plant Cell Environ. 26: 845–856.

94. Singla-Pareek SL, Reddy MK, Sopory SK (2003) Genetic engineering of the glyoxalase pathway in tobacco leads to enhanced salinity tolerance. Proc. Natl. Acad. Sci. USA 100: 14672–14677.

95. Singla-Pareek SL, Yadav SK, Pareek A, Reddy MK, Sopory SK (2007) Enhancing salt tolerance in a crop plant by overexpression of glyoxalase II. Transgenic Res. 17: 171–180.

96. Chen JH, Jiang HW, Hsieh EJ, Chen HY, Chien CT, Hsieh HL, Lin TP (2012) Drought and salt stress tolerance of an *Arabidopsis* glutathione S-transferase U17 knockout mutant are attributed to the combined effect of glutathione and abscisic acid. Plant Physiol. 158: 340–351.

97. Anjum NA, Aref IM, Duarte AC, Pereira E, Ahmad I, Iqbal M (2014) Glutathione and proline can coordinately make plants withstand the joint attack of metal (loid) and salinity stresses. Front. Plant Sci. 5: 662.

98. Fatma M, Asgher M, Masood A, Khan NA (2014) Excess sulfur supplementation improves photosynthesis and growth in mustard under salt stress through increased production of glutathione. Environ. Exp. Bot. 107: 55–63.

99. Teh CY, Mahmood M, Shaharuddin NA, Ho CL (2015) In vitro rice shoot apices as simple model to study the effect of NaCl and the potential of exogenous proline and glutathione in mitigating salinity stress. Plant Growth Regul. 75: 771–781.

100. Chan C, Lam HM (2014) A putative lambda class glutathione S-transferase enhances plant survival under salinity stress. Plant Cell Physiol. 55: 570–579.

101. Csiszár J, Horváth E, Váry Z, Gallé Á, Bela K, Brunner S, Tari I (2014) Glutathione transferase supergene family in tomato: salt stress-regulated expression of representative genes from distinct GST classes in plants primed with salicylic acid. Plant Physiol. Biochem. 78: 15–26.

102. Xu J, Xing XJ, Tian YS, Peng RH, Xue Y, Zhao W, Yao QH (2015) Transgenic *Arabidopsis* plants expressing tomato glutathione S-transferase showed enhanced resistance to salt and drought stress. PLoS One 10: e0136960.

103. Wu TM, Lin WR, Kao CH, Hong CY (2015) Gene knockout of glutathione reductase 3 results in increased sensitivity to salt stress in rice. Plant. Mol. Biol. 87: 555–564.

104. Zhou Y, Diao M, Chen X, Cui J, Pang S, Li Y, Hou C, Liu HY (2019) Application of exogenous glutathione confers salinity stress tolerance in tomato seedlings by modulating ions homeostasis and polyamine metabolism. Sci. Hortic. 250: 45–58.

105. Ahanger MA, Aziz U, Alsahli AA, Alyemeni MN, Ahmad P (2020) Influence of exogenous salicylic acid and nitric oxide on growth, photosynthesis, and ascorbate-glutathione cycle in salt stressed *Vigna angularis*. Biomolecules 10: 42.

106. Song JQ, Liu XH, Li XL, Zhang B, Li AJ, Ye XF, Wang J, Wang P (2021) Thymol improves salinity tolerance of tobacco by increasing the Na+ efflux and enhancing the content of NO and GSH.

107. Xu L, Song JQ, Wang YL, Liu XH, Li XL, Zhang B, Li AJ, Ye XF, Wang J, Wang P (2022) Thymol improves salinity tolerance of tobacco by increasing the sodium ion efflux and enhancing the content of nitric oxide and glutathione. BMC Plant Biol. 22: 1–1.

108. Anderson JV, Chevone BI, Hess JL (1992) Seasonal variation in the antioxidant system of eastern white pine needles evidence for thermal dependence. Plant Physiol. 98: 501–508.

109. Leipner J, Fracheboud Y, Stamp P (1999) Effect of growing season on the photosynthetic apparatus and leaf antioxidative defenses in two maize genotypes of different chilling tolerance. Environ. Exp. Bot. 42: 129–139.

110. Kocsy G, Szalai G, Vágújfalvi A, Stéhli L, Orosz G, Galiba G (2000) Genetic study of glutathione accumulation during cold hardening in wheat. Planta 210: 295–301.

111. Guo Z, Ou W, Lu S, Zhong Q (2006) Differential responses of antioxidative system to chilling and drought in four rice cultivars differing in sensitivity. Plant Physiol. Biochem. 44: 828–836.

112. Gomez LD, Noctor G, Knight MR, Foyer CH (2004) Regulation of calcium signalling and gene expression by glutathione. J. Exp. Bot. 55: 1851–1859.

113. Laureau C, Bligny R, Streb P (2011) The significance of glutathione for photoprotection at contrasting temperatures in the alpine plant species *Soldanella alpina* and *Ranunculus glacialis*. Physiol. Plant. 143: 246–260.

114. Bai X, Chen J, Kong X, Todd CD, Yang Y, Hu X, Li D (2012) Carbon monoxide enhances the chilling tolerance of recalcitrant *Baccaurea ramiflora* seeds via nitric oxide-mediated glutathione homeostasis. Free Radic. Biol. Med. 53: 710–720.

115. Kim YJ, Jang MG, Noh HY, Lee HJ, Sukweenadhi J, Kim JH, Kim SY, Kwon WS, Yang DC (2014) Molecular characterisation of two glutathione peroxidase genes of *Panax ginseng* and their expression analysis under environmental stresses. Gene 535: 33–41.

116. Zhang YP, Xu S, Yang SJ, Chen YY (2017) Melatonin alleviates cold-induced oxidative damage by regulation of ascorbate-glutathione and proline metabolism in melon seedlings (*Cucumis melo* L.). J. Horti. Sci. Biotech. 92: 313–324.

117. Liu F, Zhang X, Cai B, Pan D, Fu X, Bi H, Ai X (2020) Physiological response and transcription profiling analysis reveal the role of glutathione in H_2S-induced chilling stress tolerance of cucumber seedlings. Plant Sci. 291: 110363.

118. Yao M, Ge W, Zhou Q, Zhou X, Luo M, Zhao Y, Wei B, Ji S (2021) Exogenous glutathione alleviates chilling injury in postharvest bell pepper by modulating the ascorbate-glutathione (AsA-GSH) cycle. Food Chem. 352: 129458.

119. Boro P, Sultana A, Mandal K, Chattopadhyay S (2022) Interplay between glutathione and mitogen-activated protein kinase 3 via transcription factor WRKY40 under combined osmotic and cold stress in *Arabidopsis*. J. Plant Physiol. 153664.

120. Nieto-Sotelo J, Ho T-HD (1986) Effect of heat shock on the metabolism of glutathione in maize roots. Plant Physiol. 82: 1031–1035.

121. Dash S, Mohanty N (2002) Response of seedlings to heat-stress in cultivars of wheat: Growth temperature-dependent differential modulation of photosystem 1 and 2 activity, and foliar antioxidant defense capacity. J. Plant Physiol. 159: 49–59.

122. Ma YH, Ma FW, Zhang JK, Li MJ, Wang YH, Liang D (2008) Effects of high temperature on activities and gene expression of enzymes involved in ascorbate–glutathione cycle in apple leaves. Plant Sci. 175: 761–766.

123. Zhao FY, Liu W, Zhang SY (2009) Different responses of plant growth and antioxidant system to the combination of cadmium and heat stress in transgenic and non-transgenic rice. J. Integr. Plant Biol. 51: 942–950.

124. Nahar K, Hasanuzzaman M, Alam MM, Fujita M (2015a) Exogenous glutathione confers high temperature stress tolerance in mung bean (*Vigna radiata L.*) by modulating antioxidant defense and methylglyoxal detoxification system. Environ. Exp. Bot. 112: 44–54.

125. Zou M, Yuan L, Zhu S, Liu S, Ge J, Wang C (2016) Response of osmotic adjustment and ascorbate-glutathione cycle to heat stress in a heat-sensitive and a heat-tolerant genotype of wucai (*Brassica campestris L.*). Sci. Hortic. 211: 87.

126. Liang D, Gao F, Ni Z, Lin L, Deng Q, Tang Y, Wang X, Luo X, Xia H (2018) Melatonin improves heat tolerance in kiwifruit seedlings through promoting antioxidant enzymatic activity and glutathione S-transferase transcription. Molecules 23: 584.

127. Tiwari YK, Yadav SK (2019) Effect of High-Temperature Stress on Ascorbate–Glutathione Cycle in Maize. Agri. Res. 4: 1–9.

128. Iqbal N, Umar S, Khan NA, Corpas FJ (2021) Nitric oxide and hydrogen sulfide coordinately reduce glucose sensitivity and decrease oxidative stress via ascorbate-glutathione cycle in heat-stressed wheat (*Triticum aestivum L.*) plants. Antioxidants 10: 108.

129. Dhindsa RS (1987) Glutathione status and protein synthesis during drought and subsequent rehydration in *Tortula ruralis*. Plant Physiol. 83: 816–819.

130. Wang CY (1995) Temperature Preconditioning Affects Glutathione Content and Glutathione Reductase Activity in Chilled Zucchini Squash. J. Plant Physiol. 145: 148–152.

131. Morabito D, Guerrier G (2000) The free oxygen radical scavenging enzymes and redox status in roots and leaves of *Populus x Euramericana*in response to osmotic stress, desiccation and rehydration. J. Plant Physiol. 157: 74–80.

132. Shan C, Liang Z (2010) Jasmonic acid regulates ascorbate and glutathione metabolism in *Agropyron cristatum* leaves under water stress. Plant Sci. 178: 130–139.

133. Shan CJ, Zhang SL, Li DF, Zhao YZ, Tian XL, Zhao XL, Wu YX, Wei XY, Liu RQ (2011) Effects of exogenous hydrogen sulfide on the ascorbate and glutathione metabolism in wheat seedlings leaves under water stress. Acta Physiol. Plant. 33: 2533.

134. Xing X, Zhou Q, Xing H, Jiang H, Wang S (2016) Early abscisic acid accumulation regulates ascorbate and glutathione metabolism in soybean leaves under progressive water stress. J. Plant Growth Reg. 35: 865–876.

135. Munemasa S, Muroyama D, Nagahasi H, Nakamura Y, Mori IC, Murata Y (2013) Regulation of reactive oxygen species-mediated abscisic acid signalling in guard cells and drought tolerance by glutathione. Front. Plant Sci. 20: 472.

136. Nahar K, Hasanuzzaman M, Alam MM, Fujita M (2015b) Glutathione-induced drought stress tolerance in mung bean: coordinated roles of the antioxidant defence and methylglyoxal detoxification systems. AoB Plants 7: plv069.

137. Liting W, Lina W, Yang Y, Pengfei W, Tiancai G, Guozhang K (2015) Abscisic acid enhances tolerance of wheat seedlings to drought and regulates transcript levels of genes encoding ascorbate-glutathione biosynthesis. Front. Plant Sci. 6: 458.

138. Zhang L, Yu D, Wei T (2018) Overexpression of the glutathione peroxidase 5 (RcGPX5) gene from *Rhodiola crenulata* increases drought tolerance in *Saliva miltiorrhiza*. Front. Plant Sci. 9: 1950.

139. Nguyen KH, Mostofa MG, Watanabe Y, Tran CD, Rahman MM, Tran LS (2019) Overexpression of GmNAC085 enhances drought tolerance in *Arabidopsis* by regulating glutathione biosynthesis, redox balance and glutathione-dependent detoxification of reactive oxygen species and methylglyoxal. Environ. Exp. Bot. 161: 242–254.

140. Raja V, Wani UM, Wani ZA, Jan N, Kottakota C, Reddy MK, Kaul T, John R (2021) Pyramiding ascorbate–glutathione pathway in *Lycopersicum esculentum* confers tolerance to drought and salinity stress. Plant Cell Rep. 12: 1–9.

141. Nerva L, Guaschino M, Pagliarani C, De Rosso M, Lovisolo C, Chitarra W (2022) Spray-induced gene silencing targeting a glutathione S-transferase gene improves resilience to drought in grapevine. Plant Cell Environ. 45: 347–361.

142. Aono M, Kubo A, Saji H, Tanaka K, Kondo N (1993) Enhanced tolerance to photooxidative stress of transgenic *Nicotiana tabacum* with high chloroplastic glutathione reductase activity. Plant. Cell Physiol. 34: 129–135.

143. Melchiorre M, Robert G, Trippi V, Racca R, Lascano HR (2009) Superoxide dismutase and glutathione reductase overexpression in wheat protoplast: photooxidative stress tolerance and changes in cellular redox state. Plant Growth Regul. 57: 57-68.

144. Chang CC, Ślesak I, Jordá L, Sotnikov A, Melzer M, Miszalski Z, Mullineaux PM, Parker JE, Karpińska B, Karpiński S (2009) *Arabidopsis* chloroplastic glutathione

peroxidases play a role in cross talk between photooxidative stress and immune responses. Plant Physiol. 150: 670–683.

145. Noshi M, Yamada H, Hatanaka R, Tanabe N, Tamoi M, Shigeoka S (2017) *Arabidopsis* dehydroascorbate reductase 1 and 2 modulate redox states of ascorbate-glutathione cycle in the cytosol in response to photooxidative stress. Biosci. Biotech. Biochem. 81: 523–533.

146. König K, Vaseghi MJ, Dreyer A, Dietz KJ (2018) The significance of glutathione and ascorbate in modulating the retrograde high light response in *Arabidopsis thaliana* leaves. Physio. Plant. 162: 262–273.

147. Terai Y, Ueno H, Ogawa T, Sawa Y, Miyagi A, Kawai-Yamada M, Ishikawa T, Maruta T (2020) Dehydroascorbate reductases and glutathione set a threshold for high light-induced ascorbate accumulation. Plant Physiol. 183: 112–122.

148. Grill E, Löffler S, Winnacker E-L, Zenk MH (1989) Phytochelatins, the heavy-metal-binding peptides of plants, are synthesized from glutathione by a specific γ-glutamylcysteine dipeptidyl transpeptidase (phytochelatin synthase). Proc. Natl. Acad. Sci. USA 86: 6838–6842.

149. Clemens S, Kim EJ, Neumann D, Schroeder JI (1999) Tolerance to toxic metals by a gene family of phytochelatin synthases from plants and yeast. EMBO J. 18: 3325–3333.

150. Ha SB, Smith AP, Howden R, Dietrich WM, Bugg S, O'Connell MJ, Goldsbrough PB, Cobbett CS (1999) Phytochelatin synthase genes from *Arabidopsis* and the yeast *Schizosaccharomyces pombe*. Plant Cell 11: 1153–1164.

151. Vatamaniuk OK, Mari S, Lu Y-P, Rea PA (1999) *AtPCS1*, a phytochelatin synthase from *Arabidopsis*: isolation and in vitro reconstitution. Proc. Natl. Acad. Sci. USA 96: 7110–7115.

152. Schützendüble A, Polle A (2002) Plant responses to abiotic stresses: heavy metal-induced oxidative stress and protection by mycorrhization. J. Exp. Bot. 53: 1351–1365.

153. Queval G, Thominet D, Vanacker H, Miginiac-Maslow M, Gakière B, Noctor G (2009) H_2O_2-activated up-regulation of glutathione in *Arabidopsis* involves induction of genes encoding enzymes involved in cysteine synthesis in the chloroplast. Mol. Plant 2: 344–356.

154. Kumar A, Chakraborty A, Ghanta S, Chattopadhyay S (2009) *Agrobacterium*-mediated genetic transformation of mint with *E. coli* glutathione synthetase gene. Plant Cell Tiss. Org. Cult. 96: 117–126.

155. Wang F, Chen F, Cai Y, Zhang G, Wu F (2011a) Modulation of exogenous glutathione in ultrastructure and photosynthetic performance against Cd stress in the two barley genotypes differing in Cd tolerance. Biol. Trace Elem. Res. 144: 1275–1288.

156. Mestre TC, Garcia-Sanchez F, Rubio F, Martinez V, Rivero RM (2012) Glutathione homeostasis as an important and novel factor controlling blossom-end rot development in calcium-deficient tomato fruits. J. Plant Physiol. 169: 1719–1727.

157. Bello MH, Morin D, Epstein L (2013) γ-Glutamyltransferases (GGT) in *Colletotrichum graminicola*: mRNA and enzyme activity, and evidence that *CgGGT1* allows glutathione utilization during nitrogen deficiency. Fungal Genet. Biol. 51: 72–83.

158. Requejo R, Tena M (2012) Influence of glutathione chemical effectors in the response of maize to arsenic exposure. J. Plant Physiol. 169: 649–656.

159. Jobe TO, Sung D-Y, Akmakjian G, Pham A, Komives EA, Mendoza-Cozatl DG, Schroeder JI (2012) Feedback inhibition by thiols outranks glutathione depletion: a luciferase-based screen reveals glutathione-deficient γ-ECS and glutathione synthetase mutants impaired in cadmium-induced sulphate assimilation. Plant J. 70: 783–795.

160. Zeng F, Qiu B, Wu X, Niu S, Wu F, Zhang G (2012) Glutathione-mediated alleviation of chromium toxicity in rice plants. Biol. Trace Elem. Res. 148: 255–263.

161. Seth CS, Reman T, Keunen E, Jozefczak M, Gielen H, Opdenakker K, Weywns N, Vangronsveld J, Cuypers A (2012) Phytoextraction of toxic metals: a central role for glutathione. Plant Cell Environ. 35: 334–346.

162. Koffler BE, Polanschütz L, Zechmann B (2014) Higher sensitivity of *pad2-1* and *vtc2-1* mutants to cadmium is related to lower subcellular glutathione rather than ascorbate contents. Protoplasma 251: 755–769.

163. López-Climent MF, Arbona V, Pérez-Clemente RM, Zandalinas SI, Gómez-Cadenas A (2014) Effect of cadmium and calcium treatments on phytochelatin and glutathione levels in citrus plants. Plant Biol. 16: 79–87.

164. Ramírez L, Bartoli CG, Lamattina L (2013) Glutathione and ascorbic acid protect *Arabidopsis* plants against detrimental effects of iron deficiency. J. Exp. Bot. 64: 3169–3178.

165. Paulose B, Chhikara S, Coomey J, Jung HI, Vatamaniuk O, Dhankher OP (2013) A γ-glutamyl cyclotransferase protects *Arabidopsis* plants from heavy metal toxicity by recycling glutamate to maintain glutathione homeostasis. Plant Cell 25: 4580–4595.

166. Nakamura S, Suzui N, Nagasaka T, Komatsu F, Ishioka NS, Ito-Tanabata S, Kawachi N, Rai H, Hattori H, Chino M, Fujimaki S (2013) Application of glutathione to roots selectively inhibits cadmium transport from roots to shoots in oilseed rape. J. Exp. Bot. 64: 1073–1081.

167. Aranjuelo I, Doustaly F, Cela J, Porcel R, Muller M, Aroca R, Munne-Bosch S, Bourguignon J (2014) Glutathione and transpiration as key factors conditioning oxidative stress in *Arabidopsis thaliana* exposed to uranium. Planta 239: 817–830.

168. Sobrino-Plata J, Meyssen D, Cuypers A, Escobar C, Hernández LE (2014) Glutathione is a key antioxidant metabolite to cope with mercury and cadmium stress. Plant Soil 377: 369–381.

169. Sun C, Liu L, Yu Y, Liu W, Lu L, Jin C, Lin X (2015) Nitric oxide alleviates aluminum-induced oxidative damage through regulating the ascorbate-glutathione cycle in roots of wheat. J. Integr. Plant Biol. 57: 550–561.

170. Khan MI, Nazir F, Asgher M, Per TS, Khan NA (2015) Selenium and sulfur influence ethylene formation and alleviate cadmium-induced oxidative stress by improving proline and glutathione production in wheat. J. Plant Physiol. 173: 9–18.

171. Chen J, Yang L, Yan X, Liu Y, Wang R, Fan T, Ren Y, Tang X, Xiao F, Liu Y, Cao S (2016) Zinc-finger transcription factor ZAT6 positively regulates cadmium tolerance through the glutathione-dependent pathway in *Arabidopsis*. Plant Physiol. 171: 707–719.

172. Yang J, Gao MX, Hu H, Ding XM, Lin HW, Wang L, Xu JM, Mao CZ, Zhao FJ, Wu ZC (2016) OsCLT1, a CRT-like transporter 1, is required for glutathione homeostasis and arsenic tolerance in rice. New Phytol. 211: 658–670.

173. Hasanuzzaman M, Nahar K, Anee TI, Fujita M (2017) Exogenous silicon attenuates cadmium-induced oxidative stress in *Brassica napus L*. by modulating AsA-GSH pathway and glyoxalase system. Front. Plant Sci. 8: 1061.

174. Kim YO, Bae HJ, Cho E, Kang H (2017) Exogenous glutathione enhances mercury tolerance by inhibiting mercury entry into plant cells. Front. Plant Sci. 8: 683.

175. Zhang BL, Guo CC, Ding F, Lu YT, Fu ZW (2019) 14-3-3s function in plant cadmium response by changes of glutathione and glutathione synthesis in *Arabidopsis*. Environ. Exp. Bot. 163: 69–77.

176. Khullar S, Reddy MS (2020) Arsenic toxicity and its mitigation in ectomycorrhizal fungus *Hebeloma cylindrosporum* through glutathione biosynthesis. Chemosphere 240: 124914.

177. Trujillo-Hernandez JA, Bariat L, Enders TA, Strader LC, Reichheld JP, Belin C (2020) A glutathione-dependent control of the indole butyric acid pathway supports Arabidopsis root system adaptation to phosphate deprivation. J. Exp. Bot. 71: 4843–4857.

178. Bashri G, Singh S, Prasad SM, Ansari MJ, Usmani S, Alfarraj S, Alharbi SA, Brestic M (2021) Kinetin mitigates Cd-induced damagesto growth, photosynthesis and PS II photochemistry of Trigonella seedlings by up-regulating ascorbate-glutathione cycle. PLoS One 16: e0249230.

179. Li GZ, Chen SJ, Li NY, Wang YY, Kang GZ (2021) Exogenous Glutathione Alleviates Cadmium Toxicity in Wheat by Influencing the Absorption and Translocation of Cadmium. Bull. Environ. Contam. Toxicol. 10: 1–7.

180. Wen K, Li X, Huang R, Nian H (2022) Application of exogenous glutathione decreases chromium translocation and alleviates its toxicity in soybean (*Glycine max L*.). Ecotoxicol. Environ. Saf. 234: 113405.

181. Wingate VP, Lawton MA, Lamb CJ (1988) Glutathione causes a massive and selective induction of plant defense genes. Plant Physiol. 87: 206–210.

182. Dron M, Clouse SD, Dixon RA, Lawton MA, Lamb CJ (1988) Glutathione and fungal elicitor regulation of a plant defense gene promoter in electroporated protoplasts. Proc. Natl. Acad. Sci. USA 85: 6738–6742.

183. Bradley DJ, Kjellbom P, Lamb CJ (1992) Elector- and wound-induced oxidative cross-linking of a proline-rich plant cell wall protein: a novel, rapid defense response. Cell 70: 21–30.

184. Bolter C, Brammall RA, Cohen R, Lazarovits G (1993) Glutathione alterations in melon and tomato roots following treatment with chemicals which induce disease resistance to *Fusarium* wilt. Physiol. Mol. Plant Pathol. 42: 321–336.

185. Mauch F, Dudler R (1993) Differential induction of distinct glutathione-S-transferases of wheat by xenobiotics and by pathogen attack. Plant Physiol. 102: 1193–1201.

186. Levine A, Tenhaken R, Dixon R, Lamb C (1994) H_2O_2 from the oxidative burst orchestrates the plant hypersensitive disease resistance response. Cell 79: 583–593.

187. Jabs T, Dietrich RA, Dangl JL (1996) Initiation of runaway cell death in an *Arabidopsis* mutant by extracellular superoxide. Science 273: 1853–1856.

188. May MJ, Hammond-Kosack KE, Jones J (1996) Involvement of reactive oxygen species, glutathione metabolism, and lipid peroxidation in the Cf-gene-dependent defense response of tomato cotyledons induced by race-specific elicitors of *Cladosporium fulvum*. Plant Physiol. 110: 1367–1379.

189. Fodor J, Gullner G, Adam AL, Barna B, Komives T, Kiraly Z (1997) Local and systemic responses of antioxidants to *tobacco mosaic virus* infection and to salicylic acid in tobacco (role in systemic acquired resistance). Plant Physiol. 114: 1443–1451.

190. Xiang C, Oliver DJ (1998) Glutathione metabolic genes coordinately respond to heavy metals and jasmonic acid in *Arabidopsis*. Plant Cell 10: 1539–1550.

191. Rask L, Andreasson E, Ekbom B, Eriksson S, Pontoppidan B, Meijer J (2000) Myrosinase: gene family evolution and herbivore defense in Brassicaceae. Plant Mol. Biol. 42: 93–113.

192. Wittstock U, Gershenzon J (2002) Constitutive plant toxins and their role in defense against herbivores and pathogens. Curr. Opin. Plant Biol. 5: 300–307.

193. Barlet E, Kiddle G, Williams I, Wallsgrove R (1999) Wound-induced increases in the glucosinalte content of oilseed rape and their effect on subsequent herbivory by a crucifer specialist. In: Simpson SJ, Jennifer Mordue A, Hardie J (eds) *Proceedings of the 10th*

International Symposium on Insect-Plant Relationships. Springer, Dordrecht, pp. 163–167.

194. Mikkelsen MD, Petersen BL, Glawischnig E, Jensen AB, Andreasson E, Halkier BA (2003) Modulation of cyp79 genes and glucosinolate profiles in *Arabidopsis* by defense signaling pathways. Plant Physiol. 131: 298–308.

195. Glazebrook J (2005) Contrasting mechanisms of defense against biotrophic and necrotrophic pathogens. Annu. Rev. Phytopathol. 43: 205–227.

196. Freeman JL, Garcia D, Kim D, Hopf A, Salt DE (2005) Constitutively elevated salicylic acid signals glutathione-mediated nickel tolerance in *Thlaspi* nickel hyperaccumulators. Plant Physiol. 137: 1082–1091.

197. Van Wees SCM, Chang H-S, Zhu T, Glazebrook J (2003) Characterization of the early response of *Arabidopsis* to *Alternaria brassicicola* infection using expression profiling. Plant Physiol. 132: 606–617.

198. Parisy V, Poinssot B, Owsianowski L, Buchala A, Glazebrook J, Mauch F (2007) Identification of PAD2 as a gamma-glutamylcysteine synthetase highlights the importance of glutathione in disease resistance of *Arabidopsis*. Plant J. 49: 159–172.

199. Schlaeppi K, Bodenhausen N, Buchala A, Mauch F, Reymond P (2008) The glutathione-deficient mutant *pad2-1* accumulates lower amounts of glucosinolates and is more susceptible to the insect herbivore *Spodoptera littoralis*. Plant J. 55: 774–786.

200. Mhamdi A, Hager J, Chaouch S, Queval G, Han Y, Taconnat L, Saindrenan P, Gouia H, Issakidis-Bourguet E, Renou JP, Noctor G (2010) *Arabidopsis* GLUTATHIONE REDUCTASE 1 plays a crucial role in leaf responses to intracellular hydrogen peroxide and in ensuring appropriate gene expression through both salicylic acid and jasmonic acid signaling pathways. Plant Physiol. 153: 31144–31160.

201. Schlaeppi K, Abou-Mansour E, Buchala A, Mauch F (2010) Disease resistance of *Arabidopsis* to *Phytophthora brassicae*is established by the sequential action of indole glucosinolates and camalexin. Plant J. 62: 840–851.

202. Schlaeppi K, Mauch F (2010) Indolic secondary metabolites protect *Arabidopsis* from the oomycete pathogen *Phytophthora brassicae*. Plant Signal. Behav. 5: 1099–1111.

203. Geu-Flores F, Nielsen MT, Nafisi M, Møldrup ME, Olsen CE, Motawia MS, Halkier BA (2009) Glucosinolate engineering identifies a gamma-glutamyl peptidase. Nat. Chem. Biol. 5: 575–577.

204. Wang SD, Zhu F, Yuan S, Yang H, Xu F, Shang J, Xu MY, Jia SD, Zhang ZW, Wang JH, Xi DH, Lin HH (2011b) The roles of ascorbic acid and glutathione in symptom alleviation to SA-deficient plants infected with RNA viruses. Planta 234: 171–181.

205. Dempsey RW, Merchant A, Tausz M (2012) Differences in ascorbate and glutathione levels as indicators of resistance and susceptibility in *Eucalyptus* trees infected with *Phytophthora cinnamomi*. Tree Physiol. 32: 1148–1160.

206. Király L, Künstler A, Höller K, Fattinger M, Juhász C, Müller M, Gullner G, Zechmann B (2012) Sulfate supply influences compartment specific glutathione metabolism and confers enhanced resistance to *Tobacco mosaic virus* during a hypersensitive response. Plant Physiol. Biochem. 59: 44–54.

207. Mhamdi A, Han Y, Noctor G (2013) Glutathione-dependent phytohormone responses: teasing apart signaling and antioxidant functions. Plant Signal. Behav. 8: e24181.

208. Paudel J, Copley T, Amirizian A, Prado A, Bede JC (2013) *Arabidopsis* redox status in response to caterpillar herbivory. Front. Plant Sci. 4: 113.

209. Hiruma K, Fukunaga S, Bednarek P, Pislewska-Bednarek M, Watanabe S, Narusaka Y, Shirasu K, Takano Y (2013) Glutathione and tryptophan metabolism are required for *Arabidopsis* immunity during the hypersensitive response to hemibiotrophs. Proc. Natl. Acad. Sci. USA 110: 9589–9594.

210. Li F, Wang J, Ma C, Zhao Y, Wang Y, Hasi A, Qil Z (2013a) Glutamate receptor like channel 3.3 is involved in mediating glutathione-triggered cytosolic Ca^{+2} transients, transcriptional changes and innate immunity responses in *Arabidopsis*. Plant Physiol. 162: 1497–1509.

211. Frendo P, Baldacci-Cresp F, Benyamina SM, Puppo A (2013) Gluttahione and plant response to the biotic environment. Free Rad. Biol. Med. 65: 724–730.

212. Samalova M, Meyer AJ, Gurr SJ, Fricker MD (2014) Robust anti-oxidant defences in the rice blast fungus *Magnaporthe oryzae* confer tolerance to the host oxidative burst. New Phytol. 201: 556–573.

213. Marquez-Garcia B, Njo M, Beeckman T, Goormachtig S, Foyer CH (2014) A new role for glutathione in the regulation of root architecture linked to strigolactones. Plant Cell Environ. 37: 488–498.

214. Datta R, Kumar D, Sultana A, Hazra S, Bhattacharyya D, Chattopadhyay S (2015) Glutathione regulates 1-aminocyclopropane-1- carboxylate synthase transcription via WRKY33 and 1-aminocyclopropane- 1-carboxylate oxidase by modulating messenger RNA stability to induce ethylene synthesis during stress. Plant Physiol. 169: 2963–2981.

215. Matern S, Peskan-Berghoefer T, Gromes R, Kiesel RV, Rausch T (2015) Imposed glutathione-mediated redox switch modulates the tobacco wound-induced protein kinase and salicylic acid-induced protein kinase activation state and impacts on defence against *Pseudomonas syringae*. J. Exp. Bot. 66: 1935–1950.

216. Banday ZZ, Nandi AK (2018) *Arabidopsis thaliana* GLUTATHIONE-S-TRANSFERASE THETA 2 interacts with RSI1/FLD to activate systemic acquired resistance. Mol. Plant Pathol. 19: 464–475.

217. Doccula FG, Luoni L, Behera S, Bonza MC, Costa A (2018) In vivo analysis of calcium levels and glutathione redox status in *Arabidopsis* epidermal leaf cells infected with the hypersensitive response-inducing bacteria *Pseudomonas syringae* pv. tomato *AvrB* (*PstAvrB*). In: Gara LD, Locato V (eds) *Plant Programmed Cell Death*. Humana Press, New York, pp. 125–141.

218. Chen X, Li S, Zhao X, Zhu X, Wang Y, Xuan Y, Liu X, Fan H, Chen L, Duan Y (2020) Modulation of (homo) glutathione metabolism and H_2O_2 accumulation during soybean cyst nematode infections in susceptible and resistant soybean cultivars. Int. J. Mol. Sci. 21: 388.

219. Künstler A, Kátay G, Gullner G, Király L (2020) Artificial elevation of glutathione contents in salicylic acid-deficient tobacco (*Nicotiana tabacum* cv. *Xanthi NahG*) reduces susceptibility to the powdery mildew pathogen *Euoidium longipes*. Plant Biol. 22: 70–80.

220. Ramzan M, Aslam MN, Akram S, Shah AA, Danish S, Islam W, Mustafa AE, Al-Ghamdi AA, Alajmi AH (2021) Exogenous glutathione revealed protection to bacterial spot disease: Modulation of photosystem II and H_2O_2 scavenging antioxidant enzyme system in *Capsicum annum L.* J. King Saud Univ. Sci. 33: 101223.

221. Zhang N, Liu D, Zhai Y, Li X, Simon JC (2022a) Functional divergence of three glutathione transferases in two biotypes of the English grain aphid, *Sitobion avenae*. Entomol. Exp. Appl. 170: 79–87.

222. Mandal S, Mallick N, Mitra A (2009) Salicylic acid-induced resistance to *Fusarium oxysporum* f. sp. *lycopersici* in tomato. Plant Physiol. Biochem. 47: 642–649.

223. Pieterse CMJ, Does DV, Zamioudis C, Leon-Reyes A, Van Wees SCM (2012) Hormonal modulation of plant immunity. Annu. Rev. Cell Dev. Biol. 28: 489–521.

224. Giri MK, Swain S, Gautam JK, Singh S, Singh N, Bhattacharjee L, Nandi AK (2014) The *Arabidopsis thaliana* At4g13040 gene, a unique member of the AP2/EREBP family, is a positive regulator for salicylic acid accumulation and basal defense against bacterial pathogens. J. Plant Physiol. 171: 860–867.

225. Sahu M, Kar RK (2018) Possible interaction of ROS, antioxidants and ABA to survive osmotic stress upon acclimation in *Vigna radiata* L. Wilczek seedlings. Plant Physiol. Biochem. 132: 415–423.

226. Grant M, Lamb C (2006) Systemic immunity. Curr. Opin. Plant Biol. 9: 414–420.

227. Van Loon LC, Geraats BPJ, Linthorst HJM (2006) Ethylene as a modulator of disease resistance in plants. Trends Plant Sci. 11: 184–191.

228. Von Dahl CC, Baldwin IT (2007) Deciphering the role of ethylene in plant herbivore interactions. J. Plant Growth Regul. 26: 201–209.

229. Howe GA, Jander G (2008) Plant immunity to insect herbivores. Annu. Rev. Plant Biol. 59: 41–66.

230. Van Wees SC, Van der Ent S, Pieterse CM (2008) Plant immune responses triggered by beneficial microbes. Curr. Opin. Plant Biol. 11: 443–448.

231. Vlot AC, Klessig DF, Park SW (2008) Systemic acquired resistance: the elusive signal(s). Curr. Opin. Plant Biol. 11: 436–442.

232. Van der Ent S, Van Wees SCM, Pieterse CMJ (2009) Jasmonate signalling in plant interactions with resistance-inducing beneficial microbes. Phytochemistry 70: 1581–1588.

233. Kunkel BN, Brooks DM (2002) Cross talk between signaling pathways in pathogen defense. Curr. Opin. Plant Biol. 5: 325–331.

234. Bostock RM (2005) Signal crosstalk and induced resistance: straddling the line between cost and benefit. Annu. Rev. Phytopathol. 43: 545–580.

235. Pieterse CMJ, Dicke M (2007) Plant interactions with microbes and insect from molecular mechanisms to ecology. Trends Plant Sci. 12: 564–569.

236. Noctor G, Mhamdi A, Queval G, Foyer CH (2013) Regulating the redox gatekeeper: vacuolar sequestration puts glutathione disulfide in its place. Plant Physiol. 163: 665–671.

237. Spoel SH, Koornneef A, Claessens SMC, Korzelius JP, Van Pelt JA, Mueller MJ, Buchala AJ, Me´traux JP, Brown R, Kazan K, van Loon LC, Dong X, Pieterse CM (2003) NPR1 modulates cross talk between salicylate- and jasmonate dependent defense pathways through a novel function in the cytosol. Plant Cell 15: 760–770.

238. Jahan MS, Ogawa K, Nakamura Y, Shimoishi Y, Mori IC, Murata Y (2008) Deficient glutathione in guard cells facilitates abscisic acid-induced stomatal closure but does not affect light-induced stomatal opening. Biosci. Biotechnol. Biochem. 10: 2795–2798.

239. Akter N, Sobahan MA, Hossain MA, Uraji M, Nakamura Y, Mori IC, Murata Y (2010) The involvement of intracellular glutathione in methyl jasmonate signaling in *Arabidopsis* guard cells. Biosci. Biotechnol. Biochem. 74: 2504–2506.

240. Okuma E, Jahan MS, Munemasa S, Hossain MA, Muroyama D, Islam MM, Ogawa K, Watanabe-Sugimoto M, Nakamura Y, Shimoishi Y, Mori IC, Murata Y (2011) Negative regulation of abscisic acid-induced stomatal closure by glutathione in *Arabidopsis*. J. Plant Physiol. 168: 2048–2055.

241. Akter N, Sobahan MA, Uraji M, Ye W, Hossain MA, Mori IC, Nakamura Y, Murata Y (2012) Effects of depletion of glutathione on abscisic acidand methyl jasmonate induced stomatal closure in *Arabidopsis thaliana*. Biosci. Biotechnol. Biochem. 76: 2032–2037.

242. Yoshida S, Tamaoki M, Ioki M, Ogawa D, Sato Y, Aono M, Kubo A, Saji S, Saji H, Satoh S, Nakajima N (2009) Ethylene and salicylic acid control glutathione biosynthesis in ozone-exposed *Arabidopsis thaliana*. Physiol Plant. 136: 284298.

243. Ghanta S, Bhattacharyya D, Sinha R, Banerjee A, Chattopadhyay S (2011a) *Nicotiana tabacum* overexpressing *γ*-ECS exhibits biotic stress tolerance likely through NPR1-dependent salicylic acid-mediated pathway. Planta 233: 895–910.

244. Ghanta S, Chattopadhyay S (2011b) Glutathione as a signaling molecule-another challenge to pathogens: another challenge to pathogens. Plant Signal. Behav. 6: 783–788.

245. Spoel SH, Loake GJ (2011) Redox-based protein modification: the missing link in plant immune signalling. Curr. Opin. Plant Biol. 14: 358–364.

246. Han Y, Chaouch S, Mhamdi A, Queval G, Zechmann B, Noctor G (2013a) Functional analysis of *Arabidopsis* mutants points to novel roles for glutathione in coupling H_2O_2 to activation of salicylic acid accumulation and signaling. Antioxid. Redox Signal. 18: 2106–2121.

247. Han Y, Mhamdi A, Chaouch S, Noctor G (2013b) Regulation of basal and oxidative stress-triggered jasmonic acid-related gene expression by glutathione. Plant Cell Env. 36: 1135–1146.

248. Li G, Peng X, Wei L, Kang G (2013b) Salicylic acid increases the content of glutathione and ascorbate and temporally regulates the related gene expression in salt-stressed wheat seedlings. Gene 529: 321–325.

249. Dai H, Jia G, Shan C (2015) Jasmonic acid-induced hydrogen peroxide activates MEK1/2 in upregulating the redox states of ascorbate and glutathione in wheat leaves. Acta Physiol. Plant. 37: 200.

250. Kovacs I, Durner J, Lindermayr C (2015) Crosstalk between nitric oxide and glutathione is required for NONEXPRESSOR OF PATHOGENESIS- RELATED GENES 1 (NPR1)-dependent defense signaling in *Arabidopsis thaliana.* New Phytol. 208: 860–872.

251. Shan C, Zhou Y, Liu M (2015) Nitric oxide participates in the regulation of the ascorbate-glutathione cycle by exogenous jasmonic acid in the leaves of wheat seedlings under drought stress. Protoplasma 252: 1397–1405.

252. Kumar D, Hazra S, Datta R, Chattopadhyay S (2016) Transcriptome analysis of *Arabidopsis* mutants suggests a crosstalk between ABA, ethylene and GSH against combined cold and osmotic stress. Sci. Rep. 6: 36867.

253. Shan C, Wang T, Zhou Y, Wang W (2018) Hydrogen sulfide is involved in the regulation of ascorbate and glutathione metabolism by jasmonic acid in *Arabidopsis thaliana*. Biol. Plant. 62: 188–193.

254. Künstler A, Király L, Kátay G, Enyedi AJ, Gullner G (2019) Glutathione Can Compensate for Salicylic Acid Deficiency in Tobacco to Maintain Resistance to *Tobacco Mosaic Virus*. Front. Plant Sci. 10: 1115.

255. Kaya C (2021) Nitrate reductase is required for salicylic acid-induced water stress tolerance of pepper by upraising the AsA-GSH pathway and glyoxalase system. Physiol. Plant. 172: 351–370.

256. Sultana A, Boro P, Mandal K, Chattopadhyay S (2020) AAL-toxin induced stress in *Arabidopsis* thaliana is alleviated through GSH-mediated salicylic acid and ethylene pathways. Plant Cell Tiss. Org. Cult. 5: 1–6.

257. Zechmann B (2020) Subcellular roles of glutathione in mediating plant defense during biotic stress. Plants 9: 1067.

258. Altaf MM, Diao XP, Wang H, Khan LU, Shakoor A, Altaf MA, Farooq TH (2022) Salicylic Acid Induces Vanadium Stress Tolerance in Rice by Regulating the AsA-GSH Cycle and Glyoxalase System. J. Soil Sci. Plant Nutr. 1–7.

259. Noctor G, Arisi A-CM, Jouanin L, Foyer CH (1998) Manipulation of glutathione and amino acid biosynthesis in the chloroplast. Plant Physiol. 118: 471–482.

260. Zhu YL, Pilon-Smits EAH, Tarun AS, Weber SU, Jouanin L, Terry N (1999) Cadmium tolerance and accumulation in Indian mustard is enhanced by overexpressing γ-glutamyl cysteine synthetase. Plant Physiol. 121: 1169–1177.

261. Noctor G, Strohm S, Jouanin L, Kunert K-J, Foyer CH, Rennenberg H (1996) Synthesis of glutathione in leaves of transgenic poplar overexpressing γ-glutamylcysteine synthetase. Plant Physiol. 112: 1071–1078.

262. Creissen G, Firmin J, Fryer M, Kular B, Leyland N, Reynolds H, Pastori G, Wellburn F, Baker N, Wellburn A Mullineaux P (1999) Elevated glutathione biosynthetic capacity in the chloroplasts of transgenic tobacco plants paradoxically causes increased oxidative stress. Plant Cell 11: 1277–1292.

263. Xiang C, Werner BL, Christensen EM, Oliver DJ (2001) The biological functions of glutathione revisited in *Arabidopsis* transgenic plants with altered glutathione levels. Plant Physiol. 126: 564–574.

264. Herschbach C, Rizzini L, Mult S, Hartmann T, Busch F, Peuke AD, Kopriva S, Ensminger I (2010) Over-expression of bacterial γ-glutamylcysteine synthetase (GSH1) in plastids affects photosynthesis, growth and sulphur metabolism in poplar (*Populus tremula* x *Populus alba*) dependent on the resulting γ-glutamylcysteine and glutathione levels. Plant Cell Environ. 33: 1138–1151.

265. Liedschulte V, Wachter A, Zhigang A, Rausch T (2010) Exploiting plants for glutathione (GSH) production: Uncoupling GSH synthesis from cellular controls results in unprecedented GSH accumulation. Plant Biotech. J. 8: 807–820.

266. Ivanova LA, Ronzhina DA, Ivanov LA, Stroukova LV, Peuke AD, Rennenberg H (2011) Overexpression of *gsh1* in the cytosol affects the photosynthetic apparatus and improves the performance of transgenic poplars on contaminated soil. Plant Biol. 13: 649–659.

267. Hatano-Iwasaki A, Ogawa K (2012) Overexpression of GSH1 gene mimics transcriptional response to low temperature during seed vernalization treatment of *Arabidopsis*. Plant Cell Physiol. 53: 1195–1203.

268. Lim B, Pasternak M, Meyer AJ, Cobbett CS (2014) Restricting glutamylcysteine synthetase activity to the cytosol or glutathione biosynthesis to the plastid is sufficient for normal plant development and stress tolerance. Plant Biol. 16: 58–67.

269. Xu J, Tian YS, Xing XJ, Peng RH, Zhu B, Gao JJ, Yao QH (2016) Over-expression of *AtGSTU19* provides tolerance to salt, drought and methyl viologen stresses in *Arabidopsis*. Physio. Plant. 156: 164–175.

270. Park SI, Kim YS, Kim JJ, Mok JE, Kim YH, Park HM, Kim IS, Yoon HS (2017) Improved stress tolerance and productivity in transgenic rice plants constitutively expressing the *Oryza sativa* glutathione synthetase *OsGS* under paddy field conditions. J. Plant Physiol. 215: 39–47.

271. Martin F, Abati V, Burel A, Clément-Vidal A, Sanier C, Fabre D, Woraathasin N, Rio M, Besret P, Farinas B, Montoro P, Leclercq J (2018) Overexpression of *EcGSH1* induces

glutathione production and alters somatic embryogenesis and plant development in *Hevea brasiliensis*. Ind. Crops Prod. 112: 803–814.

272. Park SI, Kim JJ, Kim HS, Kim YS, Yoon HS (2020) Enhanced glutathione content improves lateral root development and grain yield in rice plants. Plant Mol. Biol. 18: 1–9.

273. Zhang P, Yuan Z, Wei L, Qiu X, Wang G, Liu Z, Fu J, Cao L, Wang T (2022b) Overexpression of *ZmPP2C55* positively enhances tolerance to drought stress in transgenic maize plants. Plant Sci. 314: 111127.

274. Jorrín-Novo JV, Pascual J, Sánchez-Lucas R, Romero-Rodríguez MC, Rodríguez-Ortega MJ, Lenz C, Valledor L (2015) Fourteen years of plant proteomics reflected in Proteomics: Moving from model species and 2DE-based approaches to orphan species and gel-free platforms. Proteomics 15: 1089–1112.

275. Bhushan D, Pandey A, Choudhary MK, Datta A, Chakraborty S, Chakraborty N (2007) Comparative proteomics analysis of differentially expressed proteins in chickpea extracellular matrix during dehydration stress. Mol. Cell. Proteomics 6: 1868–1884.

276. Pandey A, Chakraborty S, Datta A, Chakraborty N (2008) Proteomics approach to identify dehydration responsive nuclear proteins from chickpea (*Cicer arietinum* L.). Mol. Cell. Proteomics 7: 88–107.

277. Hossain Z, Nouri MZ, Komatsu S (2012) Plant cell organelle proteomics in response to abiotic stress. J. Proteome Res. 11: 37–48.

278. Levitt J (1980) Responses of Plants to Environmental Stress. In: Chilling, Freezing and High Temperature Stresses. Ed 2, Vol 1. Academic Press, New York, USA.

279. Larcher W (2003) Physiological Plant Ecology. Ed 4, Springer Verlag, Berlin, Heidelberg, Germany.

280. Kosová K, Vítámvás P, Prášilová P, Prášil IT (2013). Accumulation of WCS120 and DHN5 proteins in differently frost-tolerant wheat and barley cultivars grown under a broad temperature scale. Biol. Plant. 57: 105–112.

281. Sergeant K, Renaut J (2010) Plant biotic stress and proteomics. Curr. Proteomics 7: 275–297.

282. Gonzalez-Fernandez R, Jorrin-Novo JV (2012) Contribution of proteomics to the study of plant pathogenic fungi. J. Proteome Res. 11: 3–16.

283. Ahsan N, Lee DG, Alam I, Kim PJ, Lee JJ, Ahn YO, Kwak SS, Lee IJ, Bahk JD, Kang KY, Renaut J (2008) Comparative proteomic study of arsenic-induced differentially expressed proteins in rice roots reveals glutathione plays a central role during As stress. Proteomics 8: 3561–3576.

284. Ma J, Dong W, Zhang D, Gao X, Jiang L, Shao Y, Tong D, Li C (2016) Proteomic profiling analysis reveals that glutathione system plays important roles responding to osmotic stress in wheat (*Triticum aestivum* L.) roots. PeerJ. 4: e2334.

285. Ghanta S, Datta R, Bhattacharyya D, Sinha R, Kumar D, Hazra S, Mazumdar AB, Chattopadhyay S (2014) Multistep involvement of glutathione with salicylic acid and ethylene to combat environmental stress. J. Plant Physiol. 171: 940–950.

286. Datta R, Chattopadhyay S (2015) Changes in the proteome of *pad2-1*, a glutathione depleted *Arabidopsis* mutant, during *Pseudomonas syringae* infection. J. Proteomics 126: 82–93.

287. Meinke DW, Cherry JM, Dean C, Rounsley SD, Koornneef M (1998) *Arabidopsis thaliana*: a model plant for genome analysis. Science 282: 662–682.

288. AGI (2000) Analysis of the genome sequence of the flowering plant *Arabidopsis thaliana*. Nature 408: 796–815.

289. Zimmermann P, Hirsch-Hoffmann M, Hennig L, Gruissem W (2004) GENEVESTIGATOR. *Arabidopsis* microarray database and analysis toolbox. Plant Physiol. 136: 2621–2632.

290. Cobbett CS, May MJ, Howden R, Rolls B (1998) The glutathione-deficient, cadmium-sensitive mutant, *cad2-1*, of *Arabidopsis thaliana* is deficient in γ-glutamylcysteine synthetase. Plant J. 16: 73–78.

291. Shanmugam V, Tsednee M, Yeh KC (2012) Zinc tolerance induced by iron 1 reveals the importance of glutathione in the cross-homeostasis between zinc and iron in *Arabidopsis thaliana*. Plant J. 69: 1006–1017.

292. Murashige T, Skoog F (1962) A revised medium for rapid growth and bioassays with tobacco tissue cultures. Physiol. Plant. 15: 473–497.

293. Datta R, Sinha R, Chattopadhyay S (2013) Changes in leaf proteome profile of *Arabidopsis thaliana* in response to salicylic acid. J. Biosci. 38: 317–328.

294. Kumar D, Datta R, Hazra S, Sultana A, Mukhopadhyay R, Chattopadhyay S (2015) Transcriptomic profiling of *Arabidopsis thaliana* mutant *pad2.1* in response to combined cold and osmotic stress. PLoS One 10: e0122690.

295. Sambrook J, Russell DW (2001) Molecular Cloning: A Laboratory Manual. Cold Spring Harbor Laboratory Press, USA.

296. Tsakraklides G, Martin M, Chalam R, Tarczynski MC, Schmidt A, Leustek T (2002) Sulfate reduction is increased in transgenic *Arabidopsis thaliana* expressing 5'-adenylylsulfate reductase from *Pseudomonas aeruginosa*. Plant J. 32: 879–889.

297. Ishikawa K, Yoshimura K, Harada K, Fukusaki E, Ogawa T, Tamoi M, Shigeoka S (2010) AtNUDX6, an ADP-ribose/NADH pyrophosphohydrolase in *Arabidopsis*, positively regulates NPR1- dependent salicylic acid signaling. Plant Physiol. 152: 2000–2012.

298. Isaacson T, Damasceno CMB, Saravanan RS, He Y, Catalá C, Saladié M, Rose JKC (2006) Sample extraction techniques for enhanced proteomic analysis of plant tissues. Nat. Protoc. 1: 769–774.

299. Sinha R, Chattopadhyay S (2011) Changes in the leaf proteome profile of *Mentha arvensis* in response to *Alternaria alternata* infection. J. Prot. 74: 327–336.

300. Tada Y, Spoel SH, Pajerowska-Mukhtar K, Mou ZL, Song JQ, Wang C, Zuo JR, Dong XN (2008) Plant immunity requires conformational charges of NPR1 via S-nitrosylation and thioredoxins. Science 321: 952–956.

301. Van Wijk K (2001) Challenges and prospects of plant proteomics. Plant Physiol. 126: 501–508.

302. Cui S, Huang F, Wang J, Ma X, Cheng Y, Liu J (2005) A proteomic analysis of cold stress responses in rice seedlings. Proteomics 5: 3162–3172.

303. Alvarez S, Galant A, Jez JM, Hicks LM (2011) Redox-regulatory mechanisms induced by oxidative stress in *Brassica juncea*roots monitored by 2-DE proteomics. Proteomics 11: 1346–1350.

304. Sinha R, Bhattacharyya D, Majumdar AB, Datta R, Hazra S, Chattopadhyay S (2013) Leaf proteome profiling of transgenic mint infected with *Alternaria alternata*. J. Proteomics 93: 117–132.

305. Kaul T, Reddy PS, Mahanty S, Thirulogachandar V, Reddy RA, Kumar B, Sopory SK, Reddy MK (2011) Biochemical and molecular characterization of stress-induced β-carbonic anhydrase from a C4 plant, Pennisetum glaucum. J. Plant Physiol. 168: 601–610.

306. Stefano G, Renna L, Rossi M, Azzarello E, Pollastri S, Brandizzi F, Baluska F, Mancuso S (2010) AGD5 is a GTPase-activating protein at the trans-Golgi network. Plant J. 64: 790–799.

307. Nam KH, Li J (2002) BRI1/BAK1, a receptor kinase pair mediating brassinosteroid signaling. Cell110: 203–212.

308. Chinchilla D, Zipfel C, Robatzek S, Kemmerling B, Nürnberger T, Jones JD, Felix G, Boller T (2007) A flagellin-induced complex of the receptor FLS2 and BAK1 initiates plant defence. Nature 448: 497–500.

309. Heese A, Hann DR, Gimenez-Ibanez S, Jones AM, He K, Li J, Schroeder JI, Peck SC, Rathjen JP (2007) The receptor-like kinase SERK3/BAK1 is a central regulator of innate immunity in plants. Proc. Natl. Acad. Sci. 104: 12217–12222.

310. Roux M, Schwessinger B, Albrecht C, Chinchilla D, Jones A, Holton N, Malinovsky FG, Tör M, de Vries S, Zipfel C (2011) The *Arabidopsis* leucine-rich repeat receptor–like kinases BAK1/SERK3 and BKK1/SERK4 are required for innate immunity to hemibiotrophic and biotrophic pathogens. Plant Cell 23: 2440–2455.

311. Aan den Toorn M, Albrecht C, de Vries S (2015) On the origin of SERKs: bioinformatics analysis of the somatic embryogenesis receptor kinases. Mol. Plant. 8: 762–782.

312. Wang Q, Wang S, Gan S, Wang X, Liu J, Wang X (2016) Role of specific phosphorylation sites of *Arabidopsis* Brassinosteroid-insensitive 1 receptor kinase in plant growth and development. J. Plant Growth Reg. 35: 755–769.

313. Máthé C, Freytag C, Garda T (2021) The Protein Phosphatase PP2A Plays Multiple Roles in Plant Development by Regulation of Vesicle Traffic-Facts and Questions. Int. J. Mol. Sci. 22: 975.

314. Santner A, Estelle M (2010) The ubiquitin-proteasome system regulates plant hormone signaling. Plant J. 61: 1029–1040.

315. Kriegenburg F, Poulsen EG, Koch A, Kruger E, Hartmann-Petersen R (2011) Redox control of the ubiquitin-proteasome system: from molecular mechanisms to functional significance. Antioxid. Redox. Signal. 15: 2265–2299.

316. Zhou B, Zeng L (2017) Conventional and unconventional ubiquitination in plant immunity. Mol. Plant Pathol. 18: 1313–1330.

317. Serrano I, Campos L, Rivas S (2018) Roles of E3 ubiquitin-ligases in nuclear protein homeostasis during plant stress responses. Front. Plant Sci. 9: 139.

318. Cheng D, Zhou D, Wang Y, Wang B, He Q, Song B, Chen H (2021) *Ralstonia solanacearum* type III effector RipV2 encoding a novel E3 ubiquitin ligase (NEL) is required for full virulence by suppressing plant PAMP-triggered immunity. Biochem. Biophys. Res. Commun. 550: 120–126.

319. Li Y, Kabbage M, Liu W, Dickman MB (2016) Aspartyl protease-mediated cleavage of BAG6 is necessary for autophagy and fungal resistance in plants. Plant Cell 28: 233–247.

320. Li Y, Loake GJ (2016) Redox-Regulated Plant Transcription Factors. In: Plant Transcription Factors. Academic Press, Massachusetts, USA, pp. 373–384.

321. Zhou L, Zhou J, Xiong Y, Liu C, Wang J, Wang G, Cai Y (2018) Overexpression of a maize plasma membrane intrinsic protein ZmPIP1; 1 confers drought and salt tolerance in *Arabidopsis*. PloS One 13: e0198639.

322. Mata-Pérez C, Spoel SH (2019) Thioredoxin-mediated redox signalling in plant immunity. Plant Sci. 279: 27–33.

323. Okegawa Y, Tsuda N, Sakamoto W, Motohashi K (2021) Maintaining the chloroplast redox balance through the PGR5-dependent pathway and the Trx system is required for light-dependent activation of photosynthetic reactions. Plant Cell Physiol. 63: 92–103.

324. Zhai J, Qi Q, Wang M, Yan J, Li K, Xu H (2022) Overexpression of tomato thioredoxin h (SlTrxh) enhances excess nitrate stress tolerance in transgenic tobacco interacting with SlPrx protein. Plant Sci. 315: 111137.

325. Luna Diez E, Van Hulten M, Zhang Y, Berkowitz O, López A, Pétriacq P, Sellwood MA, Chen B, Burrell MM, Van De Meene AM, Pieterse CM (2014) Plant perception of β-aminobutyric acid is mediated by an aspartyl-tRNA synthetase. Nat. Chem. Biol. 10: 450–456.

326. Lopato S, Mayeda A, Krainer AR, Barta A (1996) Pre-mRNA splicing in plants: characterization of Ser/Arg splicing factors. Proc. Natl. Acad. Sci. 93: 3074–3079.

327. Lorković ZJ, Kirk DA, Lambermon MH, Filipowicz W (2000) Pre-mRNA splicing in higher plants. Trends Plant Sci. 5: 160–167.

328. Monaghan J, Xu F, Gao M, Zhao Q, Palma K, Long C, Chen S, Zhang Y, Li X (2009) Two Prp19-like U-box proteins in the MOS4-associated complex play redundant roles in plant innate immunity. PLoS Pathog. 5: e1000526.

329. Montecucco A, Biamonti G (2013) Pre-mRNA processing factors meet the DNA damage response. Front. Genet. 4: 102.

330. Janosi L, Hara H, Zhang S, Kaji A (1996) Ribosome recycling by ribosome recycling factor (RRF)—an important but overlooked step of protein biosynthesis. Adv. Biophys. 32: 121–201.

331. Wang L, Ouyang M, Li Q, Zou M, Guo J, Ma J, Lu C, Zhang L (2010a) The *Arabidopsis* chloroplast ribosome recycling factor is essential for embryogenesis and chloroplast biogenesis. Plant Mol. Biol. 74: 47–59.

332. Ma Z, Tao L, Bechthold A, Shentu X, Bian Y, Yu X (2014) Overexpression of ribosome recycling factor is responsible for improvement of nucleotide antibiotic-toyocamycin in *Streptomyces diastatochromogenes* 1628. Appl. Microbiol. Biotechnol. 98: 5051–5058.

333. Ali SE, Chehri K, Karimi N, Karimi I (2017) Computational approaches to the in vitro antibacterial activity of *Allium hirtifolium* Boiss against gentamicin-resistant *Escherichia coli*: focus on ribosome recycling factor. In Silico Pharmacol. 5: 1–9.

334. Tashian RE (1989) The carbonic anhydrases: widening perspectives on their evolution, expression and function. Bioessays 10: 186–192.

335. Badger MR, Price GD (1994) The role of carbonic anhydrase in photosynthesis. Annu. Rev. Plant Biol. 45: 369–392.

336. Moroney JV, Bartlett SG, Samuelsson G (2001) Carbonic anhydrases in plants and algae. Plant Cell Environ. 24: 141–153.

337. Tesfaye M, Temple SJ, Allan DL, Vance CP, Samac DA (2001) Overexpression of malate dehydrogenase in transgenic alfalfa enhances organic acid synthesis and confers tolerance to aluminum. Plant Physiol. 127: 1836–1844.

338. Menckhoff L, Mielke-Ehret N, Buck F, Vuletić M, Lüthje S (2013) Plasma membrane-associated malate dehydrogenase of maize (*Zea mays* L.) roots: Native versus recombinant protein. J. Proteom. 80: 66–77.

339. Schreier TB, Cléry A, Schläfli M, Galbier F, Stadler M, Demarsy E, Albertini D, Maier BA, Kessler F, Hörtensteiner S, Zeeman SC (2018) Plastidial NAD-dependent malate dehydrogenase: a moonlighting protein involved in early chloroplast development through its interaction with an FtsH12-FtsHi protease complex. Plant Cell 30: 1745–1769.

340. Yıldız S, Okay A, Büyük İ (2021) Defining the roles of PvMDH genes in response to salt stress and detailed characterization of the gene family. J. Plant Biochem. Biotech. 1–4.

341. Pracharoenwattana I, Cornah JE, Smith SM (2007) Arabidopsis peroxisomal malate dehydrogenase functions in β-oxidation but not in the glyoxylate cycle. Plant J. 50: 381–390.

342. Rodriguez RE, Lodeyro A, Poli HO, Zurbriggen M, Peisker M, Palatnik JF, Tognetti VB, Tschiersch H, Hajirezaei MR, Valle EM, Carrillo N (2007) Transgenic tobacco plants overexpressing chloroplastic ferredoxin-NADP (H) reductase display normal rates of photosynthesis and increased tolerance to oxidative stress. Plant Physiol. 143: 639–649.

343. Truernit E, Schmid J, Epple P, Illig J, Sauer N (1996) The sink-specific and stress-regulated Arabidopsis STP4 gene: enhanced expression of a gene encoding a monosaccharide transporter by wounding, elicitors, and pathogen challenge. Plant Cell 8: 2169–2182.

344. Clay NK, Adio AM, Denoux C, Jander G, Ausubel FM (2009) Glucosinolate metabolites required for an *Arabidopsis* innate immune response. Science 323: 95–101.

345. Guo L, Devaiah SP, Narasimhan R, Pan X, Zhang Y, Zhang W, Wang X (2012) Cytosolic glyceraldehyde-3-phosphate dehydrogenases interact with phospholipase Dδ to

transduce hydrogen peroxide signals in the *Arabidopsis* response to stress. Plant Cell 24: 2200–2212.

346. Kim SC, Guo L, Wang X (2020) Nuclear moonlighting of cytosolic glyceraldehyde-3-phosphate dehydrogenase regulates Arabidopsis response to heat stress. Nat. Comm. 11: 1–5.

347. Holtgrefe S, Gohlke J, Starmann J, Druce S, Klocke S, Altmann B, Wojtera J, Lindermayr C, Scheibe R (2008) Regulation of plant cytosolic glyceraldehyde 3-phosphate dehydrogenase isoforms by thiol modifications. Physio. Plant. 133: 211–628.

348. Moreno JC, Rojas BE, Vicente R, Gorka M, Matz T, Chodasiewicz M, Peralta-Ariza JS, Zhang Y, Alseekh S, Childs D, Luzarowski M (2021) Tyr-Asp inhibition of glyceraldehyde 3-phosphate dehydrogenase affects plant redox metabolism. EMBO J. e106800.

349. Nagasaki N, Tomioka R, Maeshima M (2008) A hydrophilic cation-binding protein of *Arabidopsis thaliana*, AtPCaP1, is localized to plasma membrane via N-myristoylation and interacts with calmodulin and the phosphatidylinositol phosphates PtdIns (3, 4, 5) P3 and PtdIns (3, 5) P2. FEBS J. 275: 2267–2282.

350. Nagata C, Miwa C, Tanaka N, Kato M, Suito M, Tsuchihira A, Sato Y, Segami S, Maeshima M (2016) A novel-type phosphatidylinositol phosphate-interactive, Ca-binding protein PCaP1 in *Arabidopsis thaliana*: stable association with plasma membrane and partial involvement in stomata closure. J. Plant Res. 129: 539–550.

351. Giovannoni M, Marti L, Ferrari S, Tanaka-Takada N, Maeshima M, Ott T, De Lorenzo G, Mattei B (2021) The plasma membrane-associated Ca2+-binding protein PCaP1 is required for oligogalacturonide and flagellin-induced priming and immunity. Plant Cell Environ. 44: 3078–3093.

352. Yoon HK, Kim SG, Kim SY, Park CM (2008) Regulation of leaf senescence by NTL9-mediated osmotic stress signaling in Arabidopsis. Molecules & Cells (Springer Science & Business Media BV). 25.

353. Kulich I, Pečenková T, Sekereš J, Smetana O, Fendrych M, Foissner I, Höftberger M, Žárský V (2013) Arabidopsis exocyst subcomplex containing subunit EXO70B1 is involved in autophagy-related transport to the vacuole. Traffic 14: 1155–1165.

354. Seo DH, Ahn MY, Park KY, Kim EY, Kim WT (2016) The N-terminal UND motif of the Arabidopsis U-box E3 ligase PUB18 is critical for the negative regulation of ABA-mediated stomatal movement and determines its ubiquitination specificity for exocyst subunit Exo70B1. Plant Cell 28: 2952–2973.

355. Stegmann M, Anderson RG, Westphal L, Rosahl S, McDowell JM, Trujillo M (2013) The exocyst subunit Exo70B1 is involved in the immune response of *Arabidopsis thaliana* to different pathogens and cell death. Plant Signal. Behav. 8: e27421.

356. Hou H, Fang J, Liang J, Diao Z, Wang W, Yang D, Li S, Tang D (2020) OsExo70B1 positively regulates disease resistance to *Magnaporthe oryzae* in rice. Int. J. Mol. Sci. 21: 7049.

357. Tran LS, Urao T, Qin F, Maruyama K, Kakimoto T, Shinozaki K, Yamaguchi-Shinozaki K (2007) Functional analysis of AHK1/ATHK1 and cytokinin receptor histidine kinases in response to abscisic acid, drought, and salt stress in *Arabidopsis*. Proc. Natl. Acad. Sci. 104: 20623–20628.

358. Desikan R, Horák J, Chaban C, Mira-Rodado V, Witthöft J, Elgass K, Grefen C, Cheung MK, Meixner AJ, Hooley R, Neill SJ (2008) The histidine kinase AHK5 integrates endogenous and environmental signals in *Arabidopsis* guard cells. PLoS One 3: e2491.

359. Pham J, Liu J, Bennett MH, Mansfield JW, Desikan R (2012) Arabidopsis histidine kinase 5 regulates salt sensitivity and resistance against bacterial and fungal infection. New Phytol. 194: 168–180.

360. Hoang XL, Prerostova S, Thu NB, Thao NP, Vankova R, Tran LS (2021) Histidine Kinases: Diverse Functions in Plant Development and Responses to Environmental Conditions. Annu. Rev. Plant Biol. 72: 297–323.

361. Ung H, Moeder W, Yoshioka K (2014) Arabidopsis triphosphate tunnel metalloenzyme2 is a negative regulator of the salicylic acid-mediated feedback amplification loop for defense responses. Plant Physiol. 166: 1009–1021.

362. Hanzawa Y, Imai A, Michael AJ, Komeda Y, Takahashi T (2002) Characterization of the spermidine synthase-related gene family in *Arabidopsis thaliana*. FEBS Lett. 527: 176–180.

363. Gonzalez ME, Marco F, Minguet EG, Carrasco-Sorli P, Blázquez MA, Carbonell J, Ruiz OA, Pieckenstain FL (2011) Perturbation of *spermine synthase* gene expression and transcript profiling provide new insights on the role of the tetraamine spermine in Arabidopsis defense against *Pseudomonas viridiflava*. Plant Physiol. 156: 2266–2277.

364. Tavladoraki P, Rossi MN, Saccuti G, Perez-Amador MA, Polticelli F, Angelini R, Federico R (2006) Heterologous expression and biochemical characterization of a polyamine oxidase from Arabidopsis involved in polyamine back conversion. Plant Physiol. 141: 1519–1532.

365. Angelini R, Tisi A, Rea G, Chen MM, Botta M, Federico R, Cona A (2008) Involvement of polyamine oxidase in wound healing. Plant Physiol. 146: 162–177.

366. Wu J, Liu W, Jahan MS, Shu S, Sun J, Guo S (2021a) Characterization of polyamine oxidase genes in cucumber and roles of CsPAO3 in response to salt stress. Environ. Exp. Bot. 104696.

367. Maeda H, Song W, Sage TL, DellaPenna D (2006) Tocopherols play a crucial role in low-temperature adaptation and phloem loading in *Arabidopsis*. Plant Cell 18: 2710–2732.

368. Sattler SE, Mene-Saffrane L, Farmer EE, Krischke M, Mueller MJ, DellaPenna D (2006) Nonenzymatic lipid peroxidation reprograms gene expression and activates defense markers in *Arabidopsis* tocopherol-deficient mutants. Plant Cell 18: 3706–3720.

369. Achkor H, Díaz M, Fernández MR, Biosca JA, Parés X, Martínez MC (2003) Enhanced formaldehyde detoxification by overexpression of glutathione-dependent formaldehyde dehydrogenase from Arabidopsis. Plant Physiol. 132: 2248–2255.

370. Rizhsky L, Davletova S, Liang H, Mittler R (2004) The Zinc Finger Protein Zat12 Is Required for Cytosolic Ascorbate Peroxidase 1 Expression during Oxidative Stress in *Arabidopsis**[boxs]. J. Biol. Chem. 279: 11736–11743.

371. Vogel JT, Zarka DG, Van Buskirk HA, Fowler SG, Thomashow MF (2005) Roles of the CBF2 and ZAT12 transcription factors in configuring the low temperature transcriptome of Arabidopsis. Plant J. 41: 195–211.

372. Le CT, Brumbarova T, Ivanov R, Stoof C, Weber E, Mohrbacher J, Fink-Straube C, Bauer P (2016) Zinc finger of Arabidopsis thaliana12 (ZAT12) interacts with FER-like iron deficiency-induced transcription factor (FIT) linking iron deficiency and oxidative stress responses. Plant Physiol. 170: 540–557.

373. Guo H, Ecker JR (2003) Plant responses to ethylene gas are mediated by SCFEBF1/EBF2-dependent proteolysis of EIN3 transcription factor. Cell 115: 667–677.

374. Potuschak T, Lechner E, Parmentier Y, Yanagisawa S, Grava S, Koncz C, Genschik P (2003) EIN3-dependent regulation of plant ethylene hormone signaling by two *Arabidopsis* F box proteins: EBF1 and EBF2. Cell 115: 679–689.

375. Zhang L, Li Z, Quan R, Li G, Wang R, Huang R (2011) An AP2 domain-containing gene, ESE1, targeted by the ethylene signaling component EIN3 is important for the salt response in Arabidopsis. Plant Physiol. 157: 854–865.

376. Quan R, Wang J, Yang D, Zhang H, Zhang Z, Huang R (2017) EIN3 and SOS2 synergistically modulate plant salt tolerance. Sci. Rep. 7: 1–1.

377. Feng Y, Xu P, Li B, Li P, Wen X, An F, Gong Y, Xin Y, Zhu Z, Wang Y, Guo H (2017) Ethylene promotes root hair growth through coordinated EIN3/EIL1 and RHD6/RSL1 activity in *Arabidopsis*. Proc. Natl. Acad. Sci. 114: 13834–13839.

378. Huang P, Dong Z, Guo P, Zhang X, Qiu Y, Li B, Wang Y, Guo H (2020) Salicylic acid suppresses apical hook formation via NPR1-mediated repression of EIN3 and EIL1 in Arabidopsis. Plant Cell 32: 612–629.

379. Zhao N, Zhao M, Tian Y, Wang Y, Han C, Fan M, Guo H, Bai MY (2021) Interaction between BZR1 and EIN3 mediates signalling crosstalk between brassinosteroids and ethylene. New Phytol. 232: 2308–2323.

380. Mandaokar A, Browse J (2009) MYB108 acts together with MYB24 to regulate jasmonate-mediated stamen maturation in Arabidopsis. Plant Physiol. 149: 851–862.

381. Xu XF, Wang B, Feng YF, Xue JS, Qian XX, Liu SQ, Zhou J, Yu YH, Yang NY, Xu P, Yang ZN (2019) AUXIN RESPONSE FACTOR17 directly regulates MYB108 for anther dehiscence. Plant Physiol. 181: 645–655.

382. Wu Y, Li T, Cheng Z, Zhao D, Tao J (2021b) R2R3-MYB Transcription factor PlMYB108 confers drought tolerance in herbaceous peony (*Paeonia lactiflora* Pall.). Int. J. Mol. Sci. 22: 11884.

383. Chevalier F, Perazza D, Laporte F, Le Hénanff G, Hornitschek P, Bonneville JM, Herzog M, Vachon G (2008) GeBP and GeBP-like proteins are noncanonical leucine-zipper transcription factors that regulate cytokinin response in Arabidopsis. Plant Physiol. 146: 1142–1154.

384. Huang J, Zhang Q, He Y, Liu W, Xu Y, Liu K, Xian F, Li J, Hu J (2021) Genome-wide identification, expansion mechanism and expression profiling analysis of GLABROUS1 Enhancer-Binding Protein (GeBP) gene family in gramineae crops. Int. J. Mol. Sci. 22: 8758.

385. Lee SC, Lan WZ, Kim BG, Li L, Cheong YH, Pandey GK, Lu G, Buchanan BB, Luan S (2007) A protein phosphorylation/dephosphorylation network regulates a plant potassium cannel. Proc. Natl. Acad. Sci. 104: 15959–15964.

386. Yang Y, Zhang Y, Ding P, Johnson K, Li X, Zhang Y (2012) The ankyrin-repeat transmembrane protein BDA1 functions downstream of the receptor-like protein SNC2 to regulate plant immunity. Plant Physiol. 159: 1857–1865.

387. Yan J, Wang J, Zhang H (2002) An ankyrin repeat-containing protein plays a role in both disease resistance and antioxidation metabolism. Plant J. 29: 193–202.

388. Zhang D, Wan Q, He X, Ning L, Huang Y, Xu Z, Liu J, Shao H (2016) Genome-wide characterization of the ankyrin repeats gene family under salt stress in soybean. Sci. Total Environ. 568: 899–909.

389. Pan X, Xu S, Wu J, Duan Y, Zheng Z, Wang J, Song X, Zhou M (2018) Ankyrin-like protein AnkB interacts with CatB, affects catalase activity, and enhances resistance of *Xanthomonas oryzae* pv. *oryzae* and *Xanthomonas oryzae* pv. *oryzicola* to phenazine-1-carboxylic acid. Appl. Environ. Microbiol. 84: e02145–17.

390. Kolodziej MC, Singla J, Sánchez-Martín J, Zbinden H, Šimková H, Karafiátová M, Doležel J, Gronnier J, Poretti M, Glauser G, Zhu W (2021) A membrane-bound ankyrin repeat protein confers race-specific leaf rust disease resistance in wheat. Nat. Commun. 12: 1–2.

391. Foster J, Kim HU, Nakata PA, Browse J (2012) A previously unknown oxalyl-CoA synthetase is important for oxalate catabolism in *Arabidopsis*. Plant Cell 24: 1217–1229.

392. Foster J, Cheng N, Paris V, Wang L, Wang J, Wang X, Nakata PA (2021) An Arabidopsis oxalyl-CoA decarboxylase, AtOXC, is important for oxalate catabolism in plants. Int. J. Mol. Sci. 22: 3266.

393. Donahue JL, Alford SR, Torabinejad J, Kerwin RE, Nourbakhsh A, Ray WK, Hernick M, Huang X, Lyons BM, Hein PP, Gillaspy GE (2010) The *Arabidopsis thaliana* myo-inositol 1-phosphate synthase1 gene is required for myo-inositol synthesis and suppression of cell death. Plant Cell 22: 888–903.

394. Tena G, Asai T, Chiu WL, Sheen J (2001) Plant mitogen-activated protein kinase signaling cascades. Curr. Opin. Plant Biol. 4: 392–400.

395. Jonak C, Ökrész L, Bögre L, Hirt H (2002) Complexity, cross talk and integration of plant MAP kinase signalling. Curr. Opin. Plant Biol. 5: 415–424.

396. MAPK Group (2002) Mitogen-activated protein kinase cascades in plants: a new nomenclature. Trends Plant Sci. 7: 301–308.

397. Tanoue T, Adachi M, Moriguchi T, Nishida E (2000) A conserved docking motif in MAP kinases common to substrates, activators and regulators. Nat. Cell Biol. 2: 110–116.

398. Mizoguchi T, Irie K. Hirayama T, Hayashida N, Yamaguchi-Shinozaki K, Matsumota K, Shinozaki K (1996) A gene encoding a mitogen-activated protein kinase kinasekinase is induced simultaneously with genes for a mitogen-activated protein kinase and an S6 ribosomal protein kinase by touch, cold, and water stress in Arabidopsis thaliana. Proc. Natl. Acad. Sci. USA 93: 765–769.

399. Zhang S, Klessig DF (1997) Salicylicacidactivates a 48-kD MAP kinase in tobacco. PlantCell 9: 809–824.

400. Zhang S, Klessig DF (1998) The tobacco wounding-activated mitogen-activated protein kinase is encoded by SIPK. Proc. Natl. Acad. Sci. 95: 7225–7230.

401. Romeis T, Piedras P, Zhang S, Klessig DF, Hirt H, Jones J (1999) Rapid Avr9-and Cf-9–dependent activation of MAP kinases in tobacco cell cultures and leaves: Convergence of resistance gene, elicitor, wound, and salicylate responses. Plant Cell 11: 273–287.

402. Munnik T, Ligterink W, Meskiene I, Calderini O, Beyerly J, MusgraveA, Hirt H (1999) Distinct osmo-sensing protein kinase pathways are involved in signalling moderate and severe hyper-osmotic stress. Plant J. 20: 381–388.

403. Cardinale F, Jonak C, Ligterink W, Niehaus K, Boller T, Hirt H (2000) Differentialactivation of fourspecific MAPK pathwaysbydistinctelicitors. J. Biol. Chem. 275: 36734–36740.

404. Seo S, Okamoto M, Seto H, Ishizuka K, Sano H, Ohashi Y (1995) Tobacco MAP kinase: a possible mediator in wound signal transduction pathways. Science 270: 1988–1992.

405. Jonak C, Kiegeri S, Ligterink W, Barker PJ, Huskisson NS, Hirt H (1996) Stress signaling in plants: a mitogen-activatedproteinkinasepathwayisactivatedbycold and drought. Proc. Natl. Acad. Sci. USA 93: 11274–11279.

406. Zhang S, Liu Y, Klessig DF (2000) Multiple levels of tobacco WIPK activation during the induction of cell death by fungal elicitins. Plant J. 23: 339–347.

407. Nakagami H, Pitzschke A, Hirt H (2005) Emerging MAP kinase pathways in plant stress signalling. Trends Plant Sci. 10: 339–346.

408. Suzuki N, Koizumi N, Sano H (2001) Screening of cadmium-responsive genes in *Arabidopsis thaliana* reveals protein denaturation and oxidative stresses to be critical components of cadmium toxicity. Plant Cell Environ. 24: 1177–1188.

409. Liu XM, Kim KE, Kim KC, Nguyen XC, Han HJ, Jung MS, Kim HS, Kim SH, Park HC, Yun DJ, Chung WS (2010) Cadmium activates *Arabidopsis* MPK3 and MPK6 via accumulation of reactive oxygen species. Phytochemistry 71: 614–618.

410. Ichimura K, Mizoguchi T, Yoshida R, Yuasa T, Shinozaki K (2000) Various abiotic stresses rapidly activate *Arabidopsis* MAP kinases ATMPK4 and ATMPK6. Plant J. 24: 655–665.

411. Kiegerl S, Cardinale F, Siligan C, Gross A, Baudouin E, Liwosz A, Eklöf S, Till S, Bögre L, Hirt H, Meskiene I (2000) SIMKK, a mitogen-activated protein kinase (MAPK)

kinase, is a specific activator of the salt stress induced MAPK, SIMK. Plant Cell 12: 2247–2258.

412. Takahashi F, Mizoguchi T, Yoshida R, Ichimura K, Shinozaki K (2011) Calmodulin-dependent activation of MAP kinase for ROS homeostasis in *Arabidopsis*. Mol. Cell 41: 649–660.

413. Kong Q, Qu N, Gao M, Zhang Z, Ding X, Yang F, Li Y, Dong OX, Chen S, Li X, Zhang Y (2012) The MEKK1-MKK1/MKK2-MPK4 kinase cascade negatively regulates immunity mediated by a mitogen-activated protein kinase kinase kinase in *Arabidopsis*. Plant Cell 24: 2225–2236.

414. Su SH, Bush SM, Zaman N, Stecker K, Sussman MR, Krysan P (2013) Deletion of a tandem gene family in Arabidopsis: increased MEKK2 abundance triggers autoimmunity when theMEKK1-MKK1/2-MPK4 signaling cascade is disrupted. Plant Cell 25: 1895–1910.

415. Wang J, Pan C, Wang Y, Ye L, Wu J, Chen L, Zou T, Lu G (2015) Genome-wide identification of MAPK, MAPKK, and MAPKKK gene families and transcriptional profiling analysis during development and stress response in cucumber. BMC Genom. 16: 1–22.

416. Yamada K, Yamaguchi K, Shirakawa T, Nakagami H, Mine A, Ishikawa K, Fujiwara M, Narusaka M, Narusaka Y, Ichimura K, Kobayashi Y (2016) The *Arabidopsis* CERK1-associated kinase PBL27 connects chitin perception to MAPK activation. EMBO J. 35: 2468–2483.

417. Wang C, Wang G, Zhang C, Zhu P, Dai H, Yu N, He Z, Xu L, Wang E (2017) OsCERK1-mediated chitin perception and immune signaling requires receptor-like cytoplasmic kinase 185 to activate an MAPK cascade in rice. Mol. Plant 10: 619–633.

418. Yamada K, Yamaguchi K, Yoshimura S, Terauchi A, Kawasaki T (2017) Conservation of chitin-induced MAPK signaling pathways in rice and *Arabidopsis*. Plant Cell Physiol. 58: 993–1002.

419. Bi G, Zhou Z, Wang W, Li L, Rao S, Wu Y, Zhang X, Menke FL, Chen S, Zhou JM (2018) Receptor-like cytoplasmic kinases directly link diverse pattern recognition

receptors to the activation of mitogen-activated protein kinase cascades in *Arabidopsis*. Plant Cell 30: 1543–1561.

420. Sun T, Nitta Y, Zhang Q, Wu D, Tian H, Lee JS, Zhang Y (2018) Antagonistic interactions between two MAP kinase cascades in plant development and immune signaling. EMBO Rep. 19: e45324.

421. McNeece BT, Sharma K, Lawrence GW, Lawrence KS, Klink VP (2019) The mitogen activated protein kinase (MAPK) gene family functions as a cohort during the *Glycine max* defense response to *Heterodera glycines*. Plant Physiol. Biochem. 137: 25–41.

422. Jammes F, Song C, Shin D, Munemasa S, Takeda K, Gu D, Cho D, Lee S, Giordo R, Sritubtim S, Leonhardt N (2009) MAP kinases MPK9 and MPK12 are preferentially expressed in guard cells and positively regulate ROS-mediated ABA signaling. Proc. Natl. Acad. Sci. 106: 20520–20525.

423. Takahashi F, Yoshida R, Ichimura K, Mizoguchi T, Seo S, Yonezawa M, Maruyama K, Yamaguchi- Shinozaki K, Shinozaki K (2007) The mitogen-activated protein kinase cascade MKK3-MPK6 is an important part of the jasmonate signal transduction pathway in *Arabidopsis*. Plant Cell 19: 805–818.

424. Xu J, Li Y, Wang Y, Liu H, Lei L, Yang H, Liu G, Ren D (2008) Activation of MAPK kinase 9 induces ethylene and camalexin biosynthesis and enhances sensitivity to salt stress in *Arabidopsis*. J. Biol. Chem. 283: 26996–27006.

425. Rasmussen MW, Roux M, Petersen M, Mundy J (2012) MAP kinase cascades in *Arabidopsis* innate immunity. Front. Plant Sci. 3: 169.

426. Alonso JM, Stepanova AN, Leisse TJ, Kim CJ, Chen H, Shinn P, Stevenson DK, Zimmerman J, Barajas P, Cheuk R, Gadrinab C, Heller C, Jeske A, Koesema E, Meyers CC, Parker H, Prednis L, Ansari Y, Choy N, Deen H, Geralt M, Hazari N, Hom E, Karnes M, Mulholland C, Ndubaku R, Schmidt I, Guzman P, Anguilar-Henonin L, Schmid M, Weigel D, Carter DE, Marchand T, RisseeuwE, Brogden D, Zeko A, Crosby WL, Berry CC, Ecker JR (2003). Genome-wide insertional mutagenesis of *Arabidopsis thaliana*. Science 301: 653–657.

427. Meyer AJ, Fricker MD (2002) Control of demand-driven biosynthesis of glutathione in green *Arabidopsis* suspension culture cells. Plant Physiol. 130: 1927–1937.

428. Lindermayr C, Sell S, Müller B, Leister D, Durner, J (2010). Redox regulation of the NPR1-TGA1 system of *Arabidopsis thaliana* by nitric oxide. Plant Cell 22: 2894–2907.

429. Lebrun-Garcia A, Ouaked F, Chiltz A, Pugin A (1998) Activation of MAPK homologues by elicitors in tobacco cells. Plant J. 15: 773–781.

430. Tillemans V, Dispa L, Remacle C, Collinge M, Motte P (2005) Functional distribution and dynamics of *Arabidopsis* SR splicing factors in living plant cells. Plant J. 41: 567–582.

431. Bradford, MM (1976) A rapid and sensitive method for the quantitation of microgram quantities of protein utilizing the principle of protein-dye binding. Anal. Biochem. 72: 248–254.

432. Clough SJ, Bent AF (1998) Floral dip: a simplified method for *Agrobacterium*-mediated transformation of *Arabidopsis thalian*a. Plant J. 16: 735–743.

433. Yoo SD, Cho YH, Sheen J (2007) *Arabidopsis* mesophyll protoplasts: a versatile cell system for transient gene expression analysis. Nat. Protoc. 2: 1565–1572.

434. Singh A, Ram H, Abbas N, Chattopadhyay S (2012) Molecular interactions of GBF1 with HY5 and HYH proteins during light-mediated seedling development in *Arabidopsis thaliana*. J. Biol. Chem. 287: 25995–26009.

435. Dong X, Mindrinos M, Davis KR, Ausubel FM (1991) Induction of Arabidopsis defense genes by virulent and avirulent Pseudomonas syringae strains and by a cloned avirulence gene. Plant Cell 3: 61–72.

436. Chow CN, Zheng HQ, Wu NY, Chien CH, Huang HD, Lee TY, Chiang-Hseih YF, Hou PF, Yang TY, Chang WC (2015) PlantPAN 2.0: an update of plant promoter analysis navigator for reconstructing transcriptional regulatory networks in plants. Nucleic Acids Res. 44: D1154–D1160.

437. Kumar D, Chattopadhyay S (2018) Glutathione modulates the expression of heat shock proteins via the transcription factors BZIP10 and MYB21 in *Arabidopsis*. J. Exp. Bot. 69: 3729–3743.

438. Velikova V, Yordanov I, Edreva A (2000) Oxidative stress and some antioxidant systems in acid rain-treated bean plants: protective role of exogenous polyamines. Plant Sci.151: 59–66.

439. Daudi A, O'Brien JA (2012) Detection of Hydrogen Peroxide by DAB Staining in *Arabidopsis* Leaves. Bio-protocol 2: e263.

440. Lichtenthaler HK (1987) Chlorophylls and carotenoids: pigments of photosynthetic biomembranes. Methods Enzymol. 148: 350–382.

441. Bates LS, Waldren RP, Teare ID (1973) Rapid determination of free proline for water-stress studies. Plant Soil 39: 205–207.

442. Hodges DM, DeLong JM, Forney CF, Prange RK (1999) Improving the thiobarbituric acid-reactive-substances assay for estimating lipid peroxidation in plant tissues containing anthocyanin and other interfering compounds. Planta 207: 604–611.

443. Bohnert HJ, Sheveleva E (1998) Plant stress adaptations-making metabolism move. Curr. Opin. Plant Biol. 1: 267–274.

444. Asai T, Tena G, Plotnikova J, Willmann MR, Chiu WL, Gomez-Gomez L, Boller T, Ausubel FM, Sheen J (2002) MAP kinase signalling cascade in *Arabidopsis* innate immunity. Nature 415: 977–983.

445. Pérez-Salamó I, Papdi C, Rigó G, Zsigmond L, Vilela B, Lumbreras V, Nagy I, Horváth B, Domoki M, Darula Z, MedzihradszkyK, Bögre L, Koncz C, SzabadosL (2014) The heat shock factor A4A confers salt tolerance and is regulated by oxidative stress and the mitogen-activated protein kinases MPK3 and MPK6. Plant Physiol. 65: 319–334.

446. Yokawa K, Kagenishi T, Baluška F (2013) Root photomorphogenesis in laboratory-maintained *Arabidopsis* seedlings. Trends Plant Sci. 18: 117–119.

447. Mattoo AK, Upadhyay RK, Rudrabhatla S (2015) Abiotic stress in crops: Candidate genes, osmolytes, polyamines, and biotechnological intervention. In: Pandey G (eds.) *Elucidation of abiotic stress signaling in plants*. Springer, New York, USA, pp. 415–437.

448. Meyer AJ (2008) The integration of glutathione homeostasis and redox signaling. J. Plant Physiol. 165: 1390–1403.

449. Pitzschke A (2015) Modes of MAPK substrate recognition and control. Trends Plant Sci. 20: 49–55.

450. Wang H, Avci U, Nakashima J, Hahn MG, Chen F, Dixon RA (2010b) Mutation of WRKY transcription factors initiates pith secondary wall formation and increases stem biomass in dicotyledonous plants. Proc. Natl. Acad. Sci. 107: 22338–22343.

451. Chakraborty J, Ghosh P, Sen S, Das S (2018) Epigenetic and transcriptional control of chickpea WRKY40 promoter activity under *Fusarium* stress and its heterologous expression in *Arabidopsis* leads to enhanced resistance against bacterial pathogen. Plant Sci. 276: 250–267.

452. Taj GO, Sharma SU, Gaur VS, Kumar AN (2011) Prediction of downstream interaction of transcription factors with MAPK3 in *Arabidopsis thaliana* using protein sequence information. Int. J. Bioinfo. Res. 3: 167–177.

453. Pathak RK, Giri P, Taj G, Kumar A (2013) Molecular modeling and docking approach to predict the potential interacting partners involved in various biological processes of MAPK with downstream WRKY transcription factor family in *Arabidopsis thaliana*. Int. J. Comp. Bioinfo. In Silico Model. 2: 262–268.

LIST OF PUBLICATIONS (Till August 2022)

1. **Boro P**, Sultana A, Mandal K, Chattopadhyay S (2022) Interplay between glutathione and mitogen-activated protein kinase 3 via transcription factor WRKY40 under combined osmotic and cold stress in Arabidopsis. **Journal of Plant Physiology** 271: 153664.
2. Mandal K, **Boro P**, Chattopadhyay S (2021) Micro-RNA based gene regulation: A potential way for crop improvements. **Plant Gene** 27: 100312.
3. Sultana A, **Boro P**, Mandal K, Chattopadhyay S (2020) AAL-toxin induced stress in *Arabidopsis thaliana* is alleviated through GSH-mediated salicylic acid and ethylene pathways. **Plant Cell, Tissue and Organ Culture (PCTOC)** 141: 299-314.
4. **Boro P**, Sultana A, Mandal K, Chattopadhyay S (2018) Transcriptomic changes under stress conditions with special reference to glutathione contents. **The Nucleus** 61: 241-252.

Manuscripts under consideration

1. Datta R, Mandal K, **Boro P**, Sultana A, Chattopadyay S. Glutathione imparts stress tolerance against *Alternaria brassicicola* infection via miRNA mediated gene regulation. **Plant Signaling & Behaviour** (communicated).
2. **Boro P** and Chattopadyay S. Crosstalk between MAPKs and GSH under stress: A critical review. **Journal of Biosciences** (accepted).

LIST OF PROCEEDINGS (Till August 2022)

1. National Symposium on "**Frontiers in Plant Science Research"** held on 10th June, 2022 organized by **ARCHANA SHARMA FOUNDATION OF CALCUTTA** in collaboration with **DEPARTMENT OF BOTANY, UNIVERSITY OF CALCUTTA**.
2. International symposium on **ADVANCES IN PLANT BIOTECHNOLOGY AND NUTRITIONAL SECURITY** held from 28th to 30th April, 2022 organized by **PLANT TISSUE CULTURE ASSOCIATION (INDIA)**.
3. National virtual conference on **GENOMICS TO PHENOMICS: A NEW HORIZON IN PLANT SCIENCE RESEARCH** held from 28th February to 1st March, 2021 organized by **DEPARTMENT OF BOTANY, UNIVERSITY OF CALCUTTA**.